Fabrizio Nicolosi

Giuseppe Paduano

AIRCRAFT PRELIMINARY DESIGN APPLICATIONS

ADAS 1.0

Aircraft Design and Analysis Software

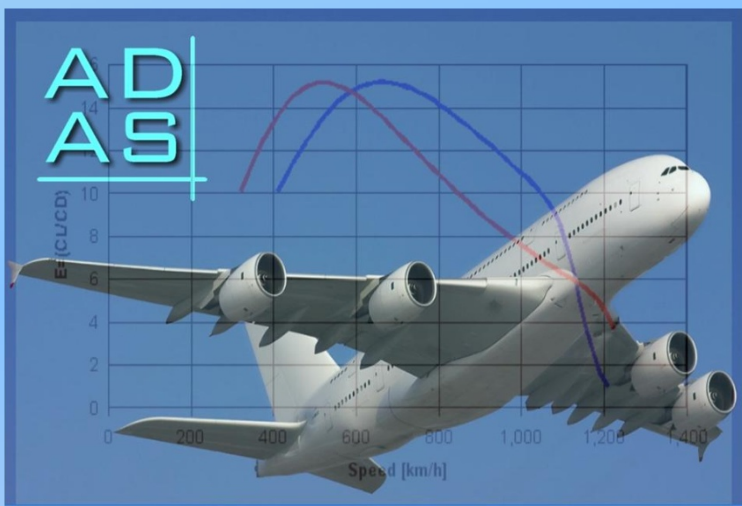

2011

Index

1. **Chapter I**

THE AIRCRAFTS DESIGN

1.1 - THE BORN OF AN AIRCRAFT DESIGN

The aircraft design is a is a complex process, articulated in many different stages spread over time and related between variously.

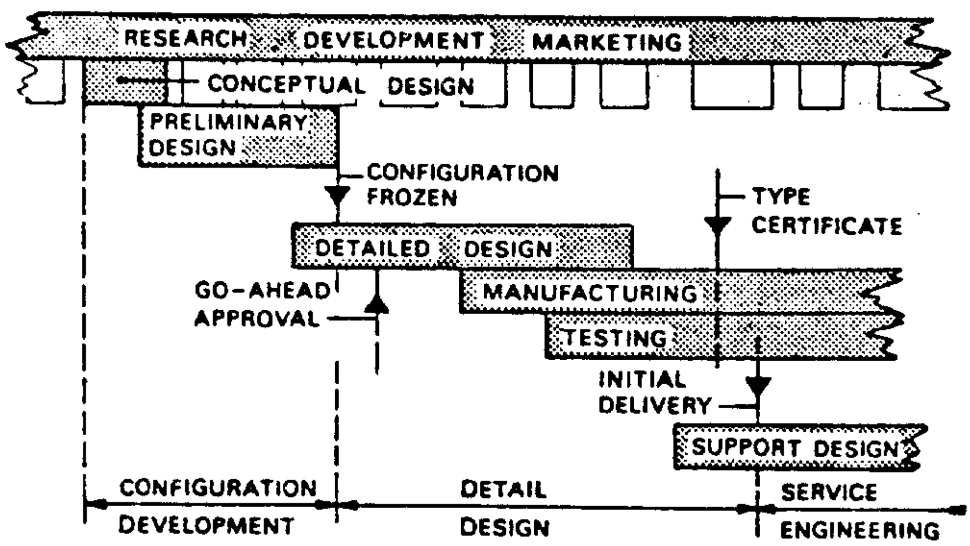

Figure 1. 1 – Development of Aircraft Design phases

The preliminary design is intended as an objective determination of the main geometric parameters, aerodynamic, structural, propulsion, stability and control characteristics useful to the initial definition of the new project, starting from the knowledge of the mission specifics.

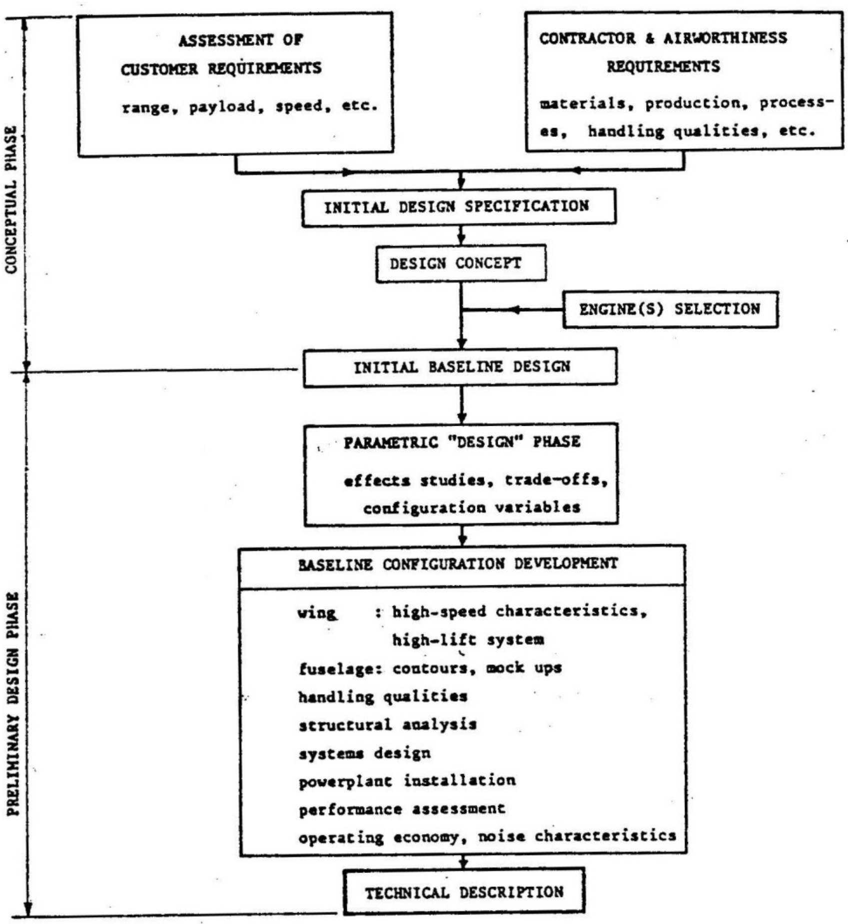

Figure 1. 2 – Diagram of the conceptual phases and preliminary sizing of a transport aircraft in high subsonic.

A mission specification or design specification can be drawn with different way depending on the aircraft type. For example, it can be the idea of a single designer that, in case of small companies, is at knowledgeof the guidelines of the market needs and he know the commercial potential of the product that is about to build.
Different is the case of the medium-big companies that are aimed to make an aircraft with bigger sizing and with bigger economic impact. In this case, in fact, the mission specification is the product of a complex process consultation, done in respect of the different entity needs.
Who take part to drafting of the document is: the representation of the design department; the potential client; the company that build the engines, to give the information on the available techniques and productive of new solutions or of existent products; the certifying body to organize a workgroup that can follow the realization of the new aircraft from the start at the end; at list the delegation of the "political-business world", inevitably present for economically relevant project, with the duty to guide the choices of the whole workgroup to the right directions.
At list, there is the case of military design. The mission specification is generally drawn from the state government authorities and from the military technical body.
So, the definition of mission specification is the base for the aeronautic design.
When the start requirements have been set, become necessary the choice of the base configuration of the new aircraft and the next activation of the analysis flux of the preliminary design, whose aim to verify that the chosen solution can satisfy the instruction of the project specification.
The results come from the development of this phase of the project and affect decisively the future life of the implementation process.

An accurate analysis of the obtained conclusions and the accordance of the product characteristics with the market needs can determine the continuation or the ending of the design activity.
From the above is immediately understand the importance of this document to characterize deeply the product that is about to be built and to give the guideline of its design.
It is the data base for the work of preliminary sizing that represent the target of this study.

1.2 - THE MISSION SPECIFICATION.

The data given in the mission specification are many and can be different as the case. Typically it is defined through a limited number of parameters, most notably for the preliminary sizing, the flight range, the number of passengers or the payload, and the takeoff and landing distance. This quantities do a particular influence on the choice of the wing area and maximum thrust or power required, as shown more detailed in the next chapter.
Below an indications list is drawn that it can find in the mission specification.

A) Flight Performance
   1) Takeoff: takeoff distance, balanced takeoff distance.
   2) Landing: landing distance.
   3) Climb: climb rate, gradient, rate and gradient from regulations, time to climb.
   4) Service ceiling: absolute in symmetric flight, in maneuver.
   5) Cruise: Speed and altitude, maximum cruise speed and altitude.
   6) Range: range with maximum payload, range without payload.
   7) Endurance.
   8) Maximum roll speed; maximum turn speed and radius.
   9) Time to descent between two altitude.
   10) Stall speed.

B) Weight: maximum takeoff weight, maximum landing weight.

C) Loads: payload, position.

D) Systems and standard equipment; safety regulation.

E) Engines: propeller, turbopropeller, jet, turbofan; number of engines, positions, developer.

F) Status: military, civil, state.

G) Type: passenger, goods, mixed, bombardier, fighter, interceptor etc.

H) Use: tactic, strategic, school, line, charter, commuter, etc.

I) Costs: direct operating costs, purchase cost.

J) Certification.

K) Design filosophy: operative life, fail-safe, use of new technologies, fatigue test, etc.

For example there are shown below two case of mission specification, mainly used for preliminary sizing and for the evaluation of the main flight performance, so they are free of all costs and/or management indications resulting more important in the organization phase of the production.
The aircraft that have been taken in example are transport jets, *Airbus A320* and *Boeing 737-700*.

Figure 1. 3 – *Airbus A320*.

Figure 1. 4 – *Boeing B737-700*.

Mission Specification For A Jet Transport

Payload:	150 Passengers at 175 lbs each and 30 lbs of baggage each.
Crew:	Two pilots and three cabin attendants at 175 lbs each and 30 lbs baggage each.
Range:	1,500 nm, followed by 1 hour loiter, followed by a 100 nm flight to alternate.
Altitude:	35,000 ft (for the design range).
Cruise Speed:	M = 0.82 at 35,000 ft.
Climb:	Direct climb to 35,000 ft. at max. W_{TO} is desired.
Take-off and Landing:	Take-off fieldlength, 7,500 ft. at S.L. Landing fieldlength, 5,000 ft. at S.L. Landing performance at $W_L = 0.85W_{TO}$.
Powerplants:	Two turbofans.
Pressurization:	5,000 ft. cabin at 35,000 ft.
Certification Base:	FAR 25

Mission Profile:

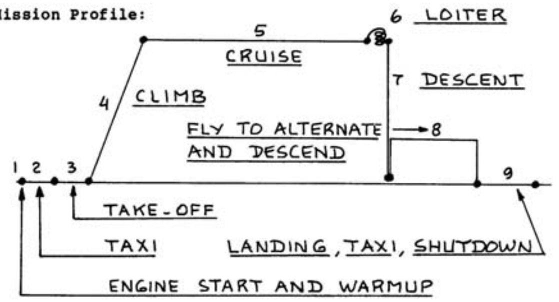

Figure 1. 5 –Mission specification for a transport jet.

Table 1. 1 –Comparison of data from mission specification of the Airbus A320 and Boeing B737-700.

	Specification	***Airbus A-320***	***Boeing B737-700***
Number of passengers	150	150	149
Number of crew	2 + 3 cabincrew	2	2
Range [km]	2780	5000 with reserve	5700 with reserve
Cruise altitude [m]	10700	10700	12500
Cruise speed [km/h]	915	900 max	880
Climb requirement	Climb to 10668 at MTOW		
Takeoff ditance [m]	2290	2300	2500
Landing distance [m]	1520	1470	1500
Engines	2 turbofan	2 turbofan	2 turbofan
Certification	FAR 25	FAR 25	FAR 25

2. **Chapter II**

THE SOFTWARE ADAS 1.0

2.1 – THE DEVELOPMENT OF ADAS

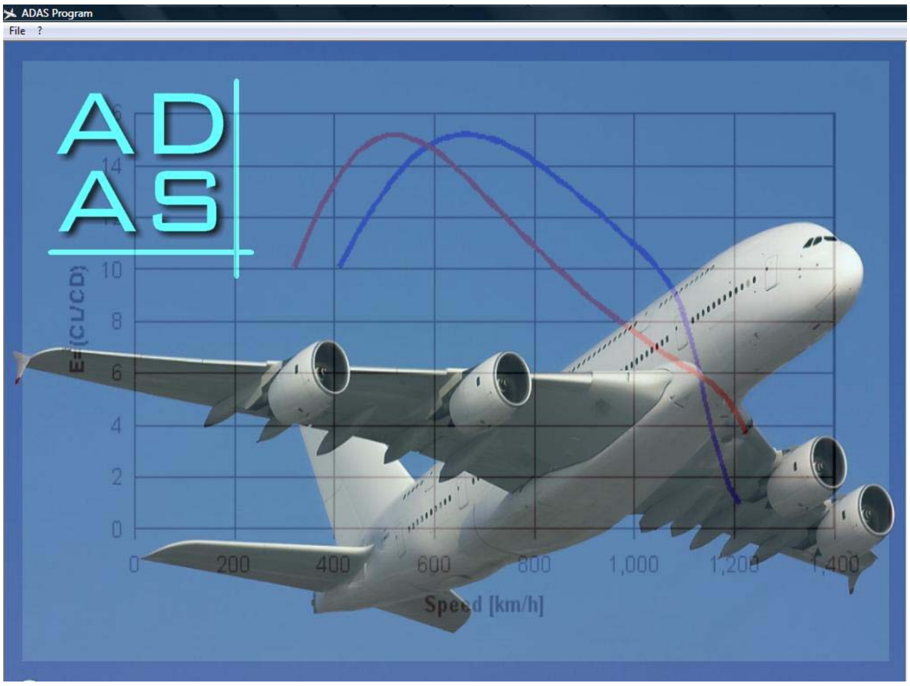

Figure 2. 1 – ADAS Main Screen.

The purpose of the software ADAS, Aircraft Design and Analysis Software, is to provide to the user an tool simply and effective, that is useful for the development of a set of procedure used for the determination of the main characteristic of an aircraft design in its embryonic stage.
Of the many phases in which aircraft design is divided, for the use of the software ADAS is interested the so called "Preliminary Design", understood as its conceptual definition that have as target the determination of the main geometrics, aerodynamics, structural, propulsive, stability and control parameters useful at the definition of the characteristics of the new project, starting from the knowledge of the Mission Specification.
The realization of this work is suggested from the opportunity to give to aerospace engineering students a tool through familiarize with the calculation methodology and with the intricate influence that different design parameters have mutually with varying efficiency degree.
ADAS, also, aims as an useful application for a brief evaluation of a wide range of and aircraft characteristics in the phase of ideation or already exists.
The user in ADAS have at disposition a list of modules to which can easily enter from the Main Menu. Each modules is dedicated to the development of a particular aspect of design; the user have the possibility to use them following a ordered path, in the scope of a complete preliminary design, or individually, for some modules, for the simply performing of calculation relatives of single

design aspects. Plus, in almost all the software's windows it can be called external applications for the conversion units, for ISA data and to open a simply calculator.
In addition to numerous calculation and methodology aspects, ADAS is however an user friendly software, for the frequent use of diagram, for the possibility of the user to refresh or modify a data sets used for the calculation, and also, for the possibility to export data and results obtained as in graphic way as numerical way in appropriate files (.txt and .bmp).
The software is implemented in *Visual Basic 6*. The GUI (Graphical user interface) and the code are generated in the *Microsoft Visual Studio 6*environment.
ADAS can work on any computer having the *Microsoft Windows OS*.

2.2 – THE STRUCTURE OF THE SOFTWARE

The software consists of seventeen modules, of which eleven are for calculation, as shown in the Main Menù below.

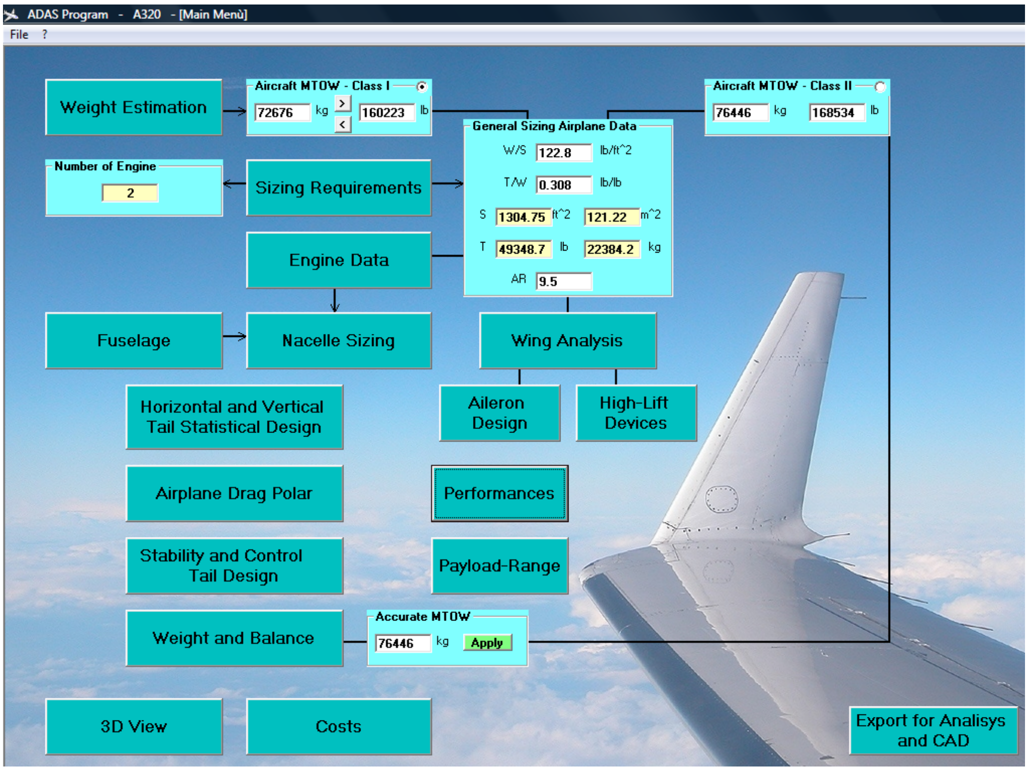

Figure 2. 2 – ADAS Main Menù.

The flow chart below show briefly the use of all independent modules, some of its, as red arrow underline, can used only if a several module is done before.

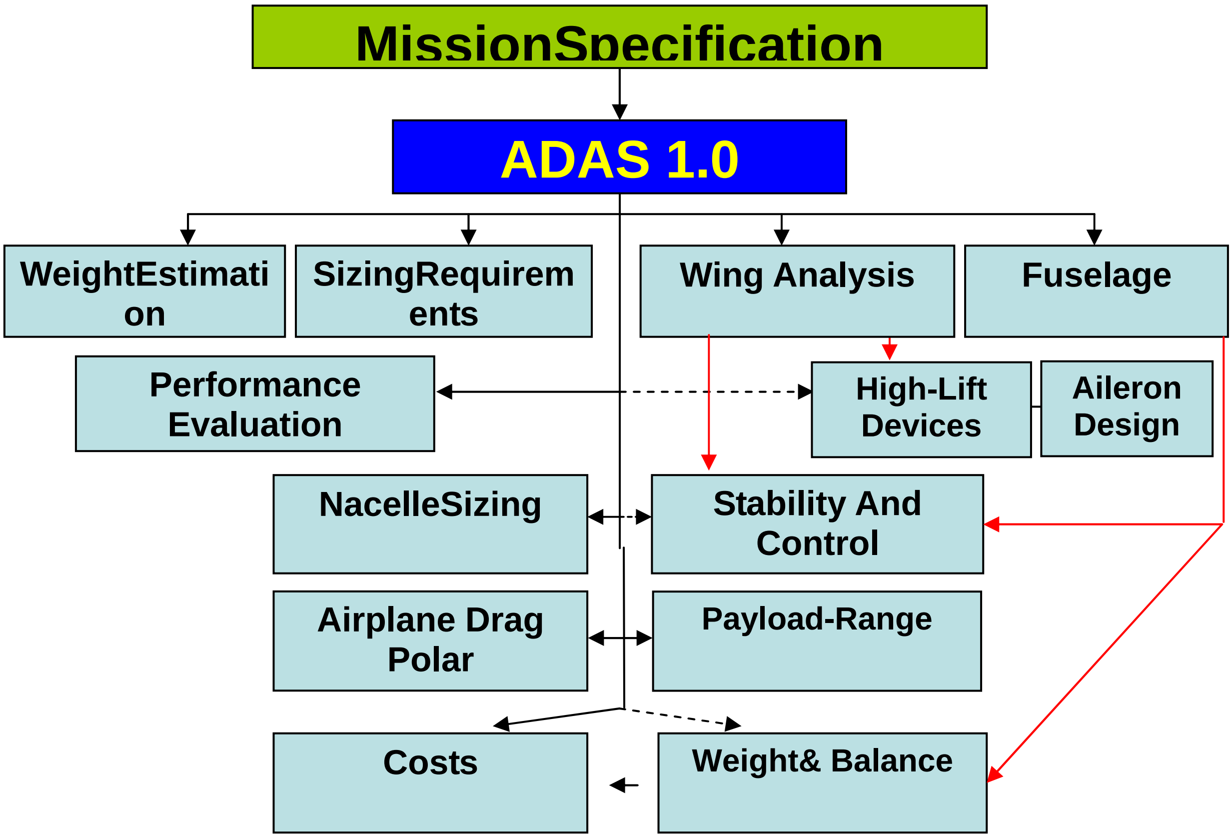

Instead the flow chart below show the full path for a complete aircraft design. With red arrows now is represented the recommended loop for the design.

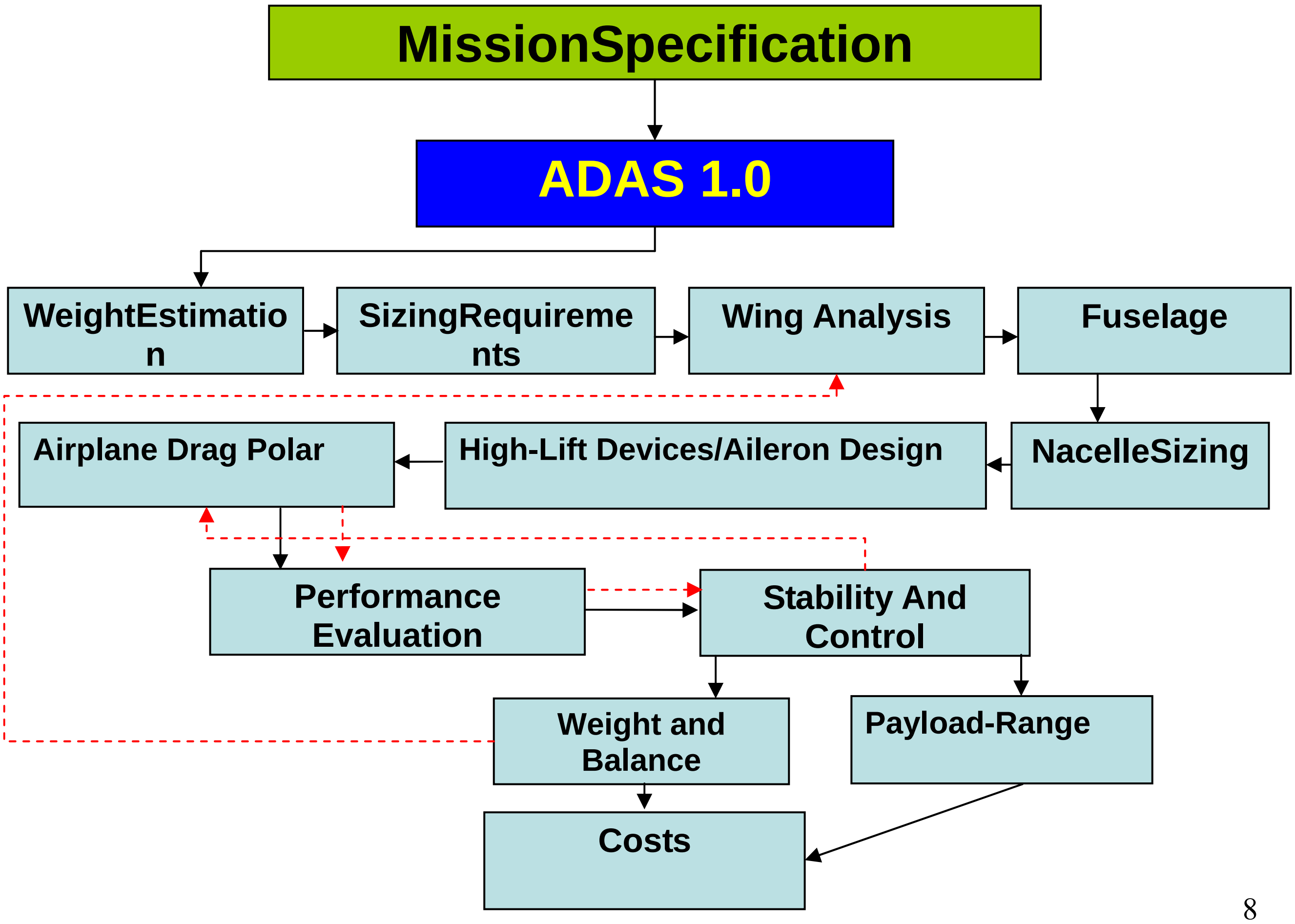

Below is given a brief description of each modules, postponing the detailed analysis for next Chapter.

- ***Weight Estimation*** – this module is dedicated to the preliminary evaluation of the maximum takeoff weight, of the empty weight and of the required fuel for the mission, starting from data given in the mission specification. The method used is statistical or so called "first class estimation".

- ***Sizing Requirements*** – this module is concerned for the determination of the aircraft design point and so for the estimation of wing surface, wing span or aspect ratio, of the maximum takeoff thrust or power and of maximum value of lift coefficient in clean configuration. The calculation procedure is based on statistical data and on requirements imposed from the aeronautic regulations.

- ***Wing Analysis*** – this module allows to the user to obtain detailed information of the functioning and of the wing geometry, as the lift curve, load distribution, structural stress, stall path, chord distribution along the wing span and the characteristics of the airfoils. It is based on various methodologies, characterized by different accuracy degree, and it use two external software for detailed calculation, Multhopp method and Weissenger method.

- ***Fuselage*** – With this module it's possible starting by the maximum payload required by the specification, to size the fuselage, as for geometry, in order to obtain the best layout possible for the disposition of seat in the passenger cabin, as for aerodynamic, studying the best combination of wing-fuselage, and evaluating the effects of this choice on the performance of the complete aircraft from the calculation of the shift of the aerodynamic centre "Xac" through the so called "Strip Method". The module allow also to evaluate from the semi empirical methods the same results, in order to choose the best value for design.

- ***Nacelle Sizing*** – In this module is given to the user the possibility of design the nacelles. This throughthe calculation of the nacelle sizing from the value of maximum thrust or power available. This dimensions can be modified for any needs. As in the fuselage here it possible to calculate the effect of the nacelles on the performance. Again with the Strip Method.

- ***High-lift Devices*** – after the wing analysis it's possible to proceed to the High lift devices design. These are divided in Flap and Slat, respectively Trailing Edge devices and Leading Edge devices. Giving in input the geometric data, devices type and deflection the variation of lift, drag and moment coefficient will be obtained by semi empirical method. This results can be saved as takeoff or landing condition.

- ***Aileron Design*** – after the choice of geometry of the flaps it possible to place after them the aileron. In this module is possible giving the aileron geometry, and some other data, to obtain the roll performances of the aircraft. This is obtained by "strip method" or semi empirical method. After this, the user can evaluate the turn performances giving some engine and aerodynamic data.

- ***Airplane drag polar***–after the sizing of all aircraft components, thid module allow the user to calculate the airplane drag polar, obtaining the results needed to the evaluation of the aircraft performance, and understand the goodness of the work done.

- ***Performance Evaluation*** – this module is useful for the evaluation of an aircraft performances from a list of data gave in input by the user related to weight, geometry, aerodynamic, and propulsive system.

- ***Stability and Control*** - This module is divided in four part:

  - ***Horizontal Tail Design***:this module allow to design the horizontal tail through two "critical" conditions of equilibrium for the aircraft.
  - ***Vertical Tail Design***: this module allow to design the vertical tail through the critical condition of engine failure during takeoff and with maximum backward barycenter, and lateral gust.
  - ***Longitudinal Stability and Control***: after the horizontal tail design in this module is possible to analyze the longitudinal stability and control of the complete airplane.
  - ***Lateral Stability (Dihedral Effect)***: after the horizontal and vertical tail design is possible to calculate the roll derivatives due to lateral gust, and so the effect of the dihedral angle.

- ***Weight and Balance*** – this module must be done at the end of all aircraft sizing, in fact, here it's possible to evaluate the weight of the aircraft with more accuracy, this is called also "class II estimation" and use semi empirical methods. After this the user can evaluate the exact position of CG and it's shift with payload position with the classical loading loops, in this way the user can eventually change the position of some part, wing, nacelle etc.

- ***Payload-Range*** – in this module the user, with the knowledge of the aircraft weight data and the parasite drag coefficient, can evaluate the range of the aircraft with the number of passenger at a condition chosen by the user. The calculation is done assuming constant CL and speed.

- ***Costs*** – this module at list can estimate with some input data, the Direct Operating Cost, the Indirect Operating Cost, and Total Operating Cost of an aircraft. The methodology used is the AEA Association of European Airlines methodology of 2003 for cost estimation, and updated with the actual dollar purchasing power of the dollar (2011).

3. **Chapter III**

ADAS MODULES METHODOLOGY

3.1 – WEIGHT ESTIMATION

3.1.1 -Introduction

The first step done for a process of preliminary design is to define the aircraft weight and the minimum fuel required for a specific mission that is characterized by information present in the mission specification. This analysis is done through semi empirical methodology, based on statistical data.
The method allow to determine the fuel weight, the empty weight and the maximum takeoff weight, it is based on the definition of the aircraft's mission profile and on the usage of a series of plots and statistical relations that describes the trend of the empty weight with the maximum takeoff weight, for different aircraft category.

3.1.2 - The Semi empirical Methodology

The maximum takeoff weight W_{TO} can be defined with the sum of the operative empty weight W_{OE}, fuel weight W_F and payload W_{PL}.

$$W_{TO} = W_{OE} + W_F + W_{PL} \qquad \textbf{(3. 1)}$$

The operative empty weight can be described as the sum of the empty weight W_E, that is the sum of the structural empty weight and fixed equipment weight, then of the fuel weight and non-consumable oil W_{tfo} and the crew weight.

$$W_{OE} = W_E + W_{tfo} + W_{crew} \qquad \textbf{(3. 2)}$$

So by the equations (3.1) and (3.2) we have the maximum takeoff weight.

$$W_{TO} = W_E + W_{tfo} + W_{crew} + W_F + W_{PL} \qquad \textbf{(3. 3)}$$

The calculation procedure for the W_{TO} and W_E is based on the search of the two condition to impose. The first is statistical, depending on the class of the aircraft and on factors associated with technology innovation as the use of non-conventional materials or solutions that allow to have high payload capacity. It is represented by the follow equation.

$$\log_{10} W_{TO} = a + b \cdot \log_{10} W_E , \qquad \textbf{(3. 4)}$$

Where the coefficients *a* and *b* are obtained through the smoothing of existing aircraft data. As example two diagrams in logarithmic scale are shown where the empty weight as a function of maximum takeoff weight for jet and propeller aircraft.
In this diagrams the line of best fitting are drawn and them represent graphically the equation (3.4)

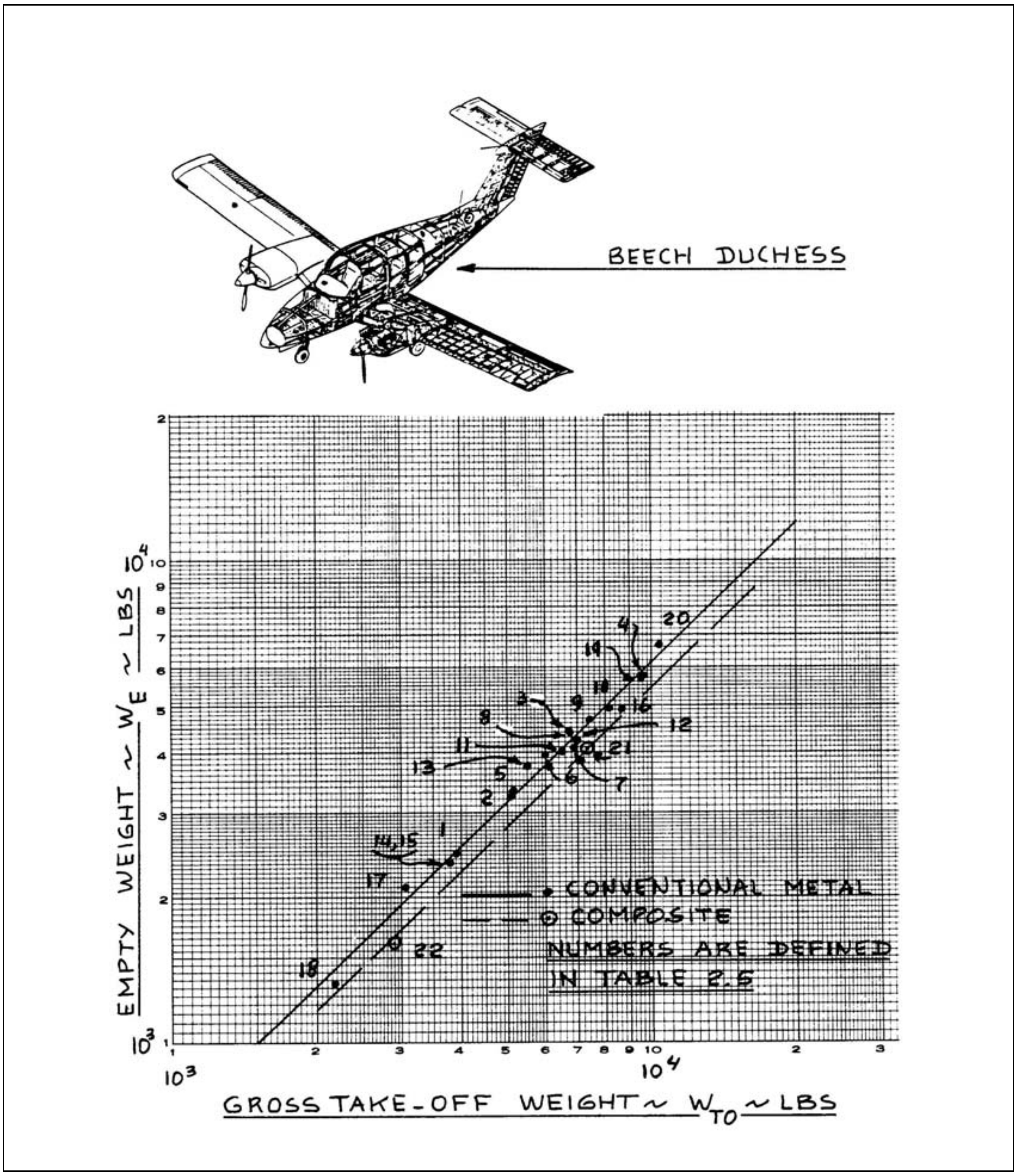

Figure 3. 1 – Diagram of empty weight as a function of maximum takeoff weight for the class of twin engine propeller.

Twin Engine Propeller - $\log_{10} W_{TO} = 0.0966 + 1.0298 \cdot \log_{10} W_E$ **(3. 5)**

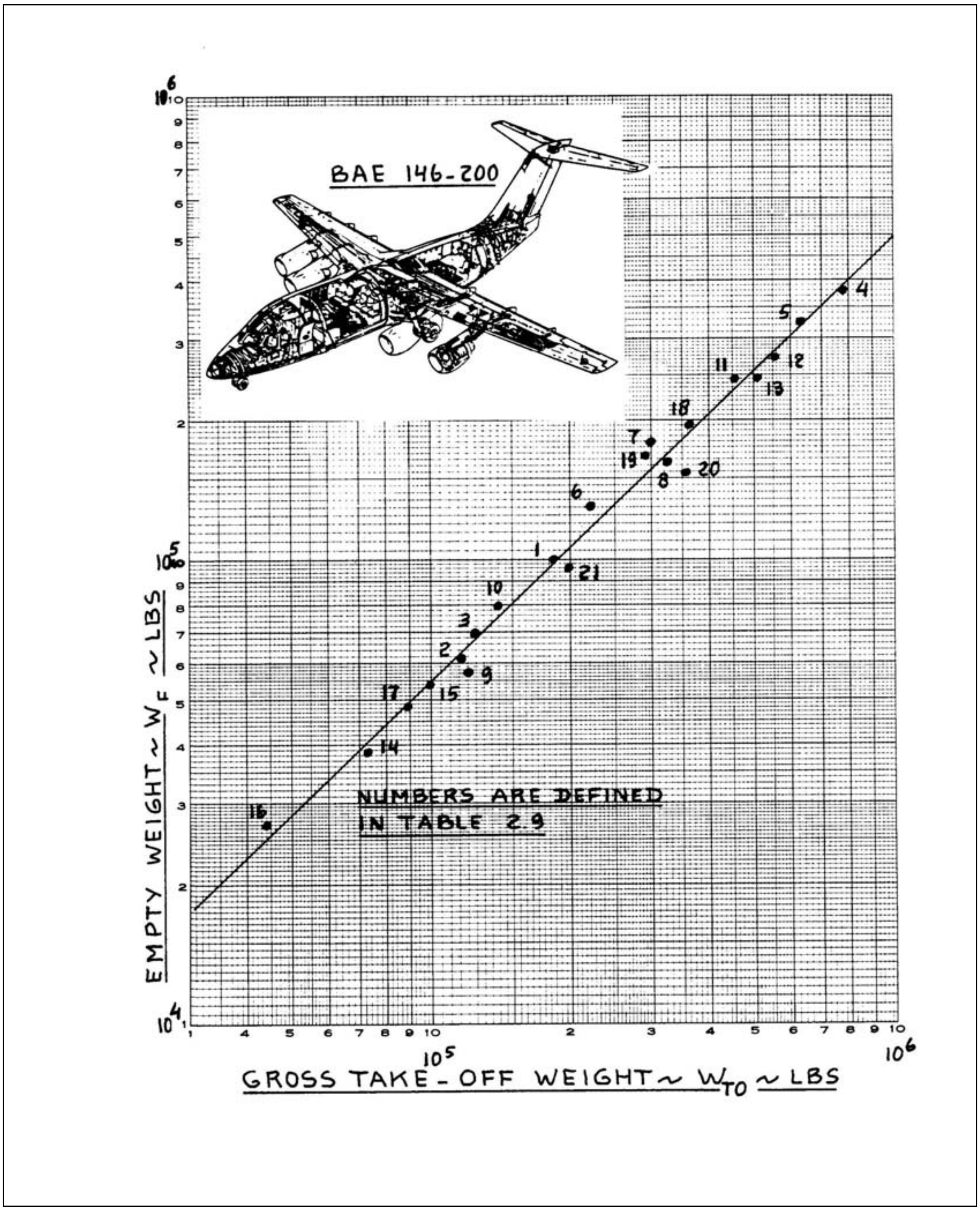

Figure 3. 2–Diagram of empty weight as a function of maximum takeoff weight for the class of Transport Jets.

Transport Jet - $\log_{10} W_{TO} = 0.0833 + 1.0383 \cdot \log_{10} W_E$ **(3. 6)**

In the next pages is shown the tables used as the source for the above diagram.

Table 2.5 Weight Data for Twin Engine Propeller Driven Airplanes

No.	Type	Gross Take-off Weight, W_{TO} (lbs)	Empty Weight, W_E(lbs)	Maximum Landing Weight, W_{Land} (lbs)	Max. Internal Fuel Weight, W_{MIF}(lbs)
	BEECH				
1	Duchess 76	3,900	2,466	3,900	587
2	Baron 95-B55	5,100	3,236	5,100	587
3	Duke B60	6,775	4,423	6,775	834
4	King Air C90 (TBP)	9,650	5,765	9,168	2,515
	CESSNA				
5	Crusader T303	5,150	3,305	5,000	898
6	340A	5,990	3,948	5,990	1,192
7	402C Businessliner	6,850	4,077	6,850	1,250
8	414A Chancellor	6,750	4,368	6,750	1,250
9	421 Golden Eagle	7,450	4,668	7,450	1,250
10	Conquest I (TBP)	8,200	4,915	8,000	2,443
	PIPER				
11	Navajo	6,500	4,003	6,500	1,127
12	Chieftain	7,000	4,221	7,000	1,127
13	Aerostar 600A	5,500	3,737	5,500	1,018
14	Seminole PA-44-180	3,800	2,354	3,800	646
15	Seminole PA-44-180T	3,800	2,430	3,800	646
16	Cheyenne I (TBP)	8,700	4,910	8,700	2,017
17	Wing Derringer D-1	3,050	2,100	2,900	511
18	Partenavia P66C-160	2,183	1,322	2,183	251
19	Piaggio P166-DL3 (TBP)	9,480	5,732	8,377	1,850
20	Gulf-Am 840A (TBP)	10,325	6,629	10,325	2,784
21	Learfan 2100 (TBP)	7,350*	4,100	7,000	1,572
22	Rutan 40 Defiant	2,900*	1,610	2,900	528

* 21 and 22 are composite built airplanes

Figure 3. 3 – Data table of the aircrafts represented in the diagram of figure 3.1.

Table 2.9 Weight Data for Transport Jets

No.	Type	Gross Take-off Weight, W_{TO} (lbs)	Empty Weight*, W_E(lbs)	Maximum Landing Weight, W_{Land} (lbs)	Max. Internal Fuel Weight, W_{MIF}(lbs)
	BOEING				
1	727-200	184,800	100,000	154,500	52,990
2	737-200	115,500	61,630	103,000	39,104
3	737-300	124,500	69,930	114,000	35,108
4	747-200B	775,000	380,000	564,000	343,279
5	747-SP	630,000	325,000	450,000	329,851
6	757-200	220,000	130,420	198,000	73,229
7	767-200	300,000	179,082	270,000	109,385
	McDONNELL-DOUGLAS				
8	DC8-Super 71	325,000	162,700	240,000	156,733
9	DC9-30	121,000	57,190	110,000	24,117
10	DC9-80	140,000	79,757	128,000	37,852
11	DC10-10	455,000	244,903	363,500	142,135
12	DC10-40	555,000	271,062	403,000	239,075
13	Lockheed L1011-500	510,000	245,500	368,000	155,982
14	Fokker F28-4000	73,000	38,683	69,500	16,842
15	Rombac-111-560	99,650	53,762	87,000	24,549
16	VFW-Fokker 614	44,000	26,850	44,000	10,928
17	BAe 146-200	89,500	48,500	77,500	22,324
	AIRBUS				
18	A300-B4-200	363,760	195,109	295,420	195,109
19	A310-202	291,000	168,910	261,250	94,798
20	Ilyushin-Il-62M	357,150	153,000	231,500	183,700
21	Tupolev-154	198,416	95,900	176,370	73,085

* W_E here means typical airline operating weight empty, W_{OE}

Figure 3. 4–Data table of the aircrafts represented in the diagram of figure 3.2.

For the aircraft of other class the follow information can be used.

Table 2.15 Regression Line Constants A and B of Equation

Airplane Type	A	B
1. Homebuilts		
Pers. fun and transportation	0.3411	0.9519
Scaled Fighters	0.5542	0.8654
Composites	0.8222	0.8050
2. Single Engine Propeller Driven	-0.1440	1.1162
3. Twin Engine Propeller Driven	0.0966	1.0298
Composites	0.1130	1.0403
4. Agricultural	-0.4398	1.1946
5. Business Jets	0.2678	0.9979
6. Regional TBP	0.3774	0.9647
7. Transport Jets	0.0833	1.0383
8. Military Trainers		
Jets	0.6632	0.8640
Turboprops	-1.4041	1.4660
Turboprops without No.2	0.1677	0.9978
Piston/Props	0.5627	0.8761
9. Fighters		
Jets(+ ext.load)	0.5091	0.9505
Jets(clean)	0.1362	1.0116
Turboprops(+ ext.load)	0.2705	0.9830
10. Mil. Patrol, Bomb and Transport		
Jets	-0.2009	1.1037
Turboprops	-0.4179	1.1446
11. Flying Boats, Amphibious and Float Airplanes	0.1703	1.0083
12. Supersonic Cruise	0.4221	0.9876

$$W_E = \text{invlog}_{10}\{(\log_{10} W_{TO} - A)/B\}$$

Figure 3. 5 – Table of the coefficients A and B useful for the equation (3.4).

The second condition is given from the information contained in the mission specification and with the follow method.

The W_{PL} and the W_{crew} can be obtained by the knowledge of number of passenger and the crew, by the average weight of the generic passenger and baggage, and from cargo weight.

The fuel weight and the trapped oil W_{tfo} can be assigned as a percentage of the maximum takeoff weight W_{tfo}/W_{TO} . Tipically a value of 0.5% is assigned.

So the fuel onboard is given by the sum of the used fuel and a reserve ratio.

$W_F = W_{Fused} + W_{Freserve}$ **(3. 7)**

The weight of reserve fuel can be express by the percentage of the fuel used ($M_{res} = W_{Rreserve}/W_{Fused}$), for example 25% for light propeller aircraft.

The value of W_{Fused} can be obtained by the fuel fraction method, based on the definition of the aircraft mission profile.

The mission profile is a series of phases, each listed below:

- Engine start and warmup
- Taxi
- Takeoff
- Climb
- Cruise
- Loiter

- Descet
- Alternate (transfer to alternate airport)
- Landing

Each one is characterized by a value of fraction between the weight of the aircraft in that phase and the starting weight, equal to final weight plus the fuel used.

$$\frac{W_{j+1}}{W_j} \quad \textbf{(3. 8)}$$

This value is obtained through statistical data charts. For the cruise phase, loiter or transfer to alternate airport, the fraction can be calculated using the Breguet formulas for the estimation of the range and the endurance.

$$\text{Propeller aircraft} \begin{cases} \text{Range } R = 375 \cdot \dfrac{\eta_p}{c_p} \cdot \dfrac{L}{D} \cdot \ln\left(\dfrac{W_f}{W_i}\right) \\ \\ \text{Endurance } En = 375 \cdot \dfrac{1}{V} \cdot \dfrac{\eta_p}{c_p} \cdot \dfrac{L}{D} \cdot \ln\left(\dfrac{W_f}{W_i}\right) \end{cases} \quad \textbf{(3. 9)}$$

$$\text{Jet aircraft} \begin{cases} \text{Range } R = \dfrac{V}{c_j} \cdot \dfrac{L}{D} \cdot \ln\left(\dfrac{W_f}{W_i}\right) \\ \\ \text{Endurance } En = \dfrac{1}{c_j} \cdot \dfrac{L}{D} \cdot \ln\left(\dfrac{W_f}{W_i}\right) \end{cases} \quad \textbf{(3. 10)}$$

Where c_p is the specific consumption of propeller aircraft, η_p is the propeller efficiency, c_j is the specific consumption for jet aircraft. The weight fraction can be simply obtained inverting the above equations.
The whole fuel fraction of the mission M_{ff}, given by the fraction of the weight at the end and at the start of the mission is calculated by the following formula.

$$M_{ff} = \frac{W_1}{W_{TO}} \cdot \frac{W_2}{W_3} \cdot \frac{W_3}{W_4} \cdot \ldots \cdot \frac{W_{n-1}}{W_{n-2}} \cdot \frac{W_n}{W_{n-1}} = \frac{W_n}{W_{TO}} \quad \textbf{(3. 11)}$$

So the used fuel is expressed by a function of maximum takeoff weight, as shown below.

$$W_{Fused} = W_{TO} - W_{fin} = (1 - M_{ff}) \cdot W_{TO} \quad \textbf{(3. 12)}$$

The overall fuel weight is so calculated as a function of the W_{TO} .

$$W_F = (1 + M_{res}) \cdot (1 - M_{ff}) \cdot W_{TO} \quad \textbf{(3. 13)}$$

By substituting of (3.12) in the (3.3) and taking out the W_E , the formula (3.14) is obtained.

$$W_E = W_{TO} \cdot \left[1 - (1 + M_{res}) \cdot (1 - M_{ff}) - M_{tfo}\right] - (W_{PL} + W_{crew}) = W_{TO} \cdot c - d \,. \qquad \textbf{(3. 14)}$$

Where the value c and $d$are expressed as follow.

$$c = \left[1 - (1 + M_{res}) \cdot (1 - M_{ff}) - M_{tfo}\right]$$

(3. 15)

$$d = W_{PL} + W_{crew}$$

The equation (3.14)represent so the second condition.
The value of the empty weight and the maximum takeoff weight can be obtained by the resolution of the following system of two non-linear equationin two unknowns.

$$\begin{cases} W_E = W_{TO} \cdot c - d \\ W_E = inv\log_{10}\left[\dfrac{\log_{10} W_{TO} - a}{b}\right] \end{cases} \qquad \textbf{(3. 16)}$$

It can be solved by an iteration method, ADAS use the “bisection method”. Graphically the solution represent the intersection of two curve, as shown in figure 3.1.

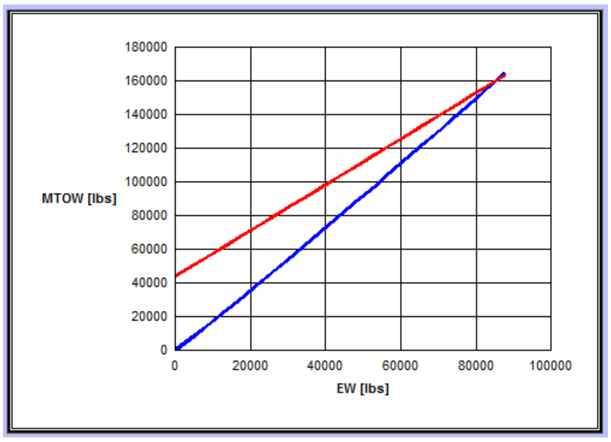

Figure 3.1 – example of graphic solution of the system (3.16)

3.2 – SIZING REQUIREMENTS

3.2.1 - Introduction

The aircraft design is made in the respect of a number requirements that involve different flight phases. The product have to guarantee specific performance for range and endurance, stall speed, take off length, landing length, maneuverability, cruise speed or maximum speed, climb speed and climb time at an given altitude. This characteristic depend on a number of design parameters, as wing surface, wing span or aspect ratio, takeoff thrust or power and maximum lift coefficient in clean configuration, takeoff configuration and landing configuration.
The methodology used here is semi empirical and allow to find a series of possible value for wing loading and fraction between takeoff thrust and weight, for jet aircraft, or weight and takeoff power for propeller aircraft.

3.2.2 - The methodology for the determination of Design Point

The Design Point is a representative point of the aircraft in a diagram that have on vertical axis the value of T/W or W/P, and on horizontal axis the wing loading W/S. It can't be determined univocal but it can be chosen by the designer in a range of value limited by representative curves of desired performances. Each requirement impose limitations, that may be more or less incisive depending on the assigned value. The requirements taken into account are:

- Stall speed
- Takeoff distance
- Landing distance
- Climb performances
- Cruise speed or maximum speed

3.2.3 The Stall speed limitation

Some mission specifics require that the stall speed have not to exceed minimum values. In particular, for the aircraft subjects at FAR 23 certification have not to exceed the 61 knots of stall speed. While the aircraft subjects at FAR 25 certification aren't limited, so this part is until for them.
The designer can choose to respect this limitation with or without the use of high lift devices, or with different value of maximum takeoff lift coefficient.
At equal value of altitude and stall speed, different value of maximum lift coefficients involves different limitation for the determination of the design point. They are represented by vertical lines that move themselves on the right of the plot as grow the $C_{L\max}$ value, as seen by the following formula.

$$\left(\frac{W}{T}\right)_{TO} = V_s^2 \cdot \frac{\rho}{2} \cdot C_{L\max\text{-L}} \quad \textbf{(3.2.1)}$$

Increasing value of stall speed, with constant altitude and $C_{L\max}$, the lines moves on the right. at last with growing of altitude, with constant stall speed and $C_{L\max}$, the lines moves on the left, to lesser value of wing loading.

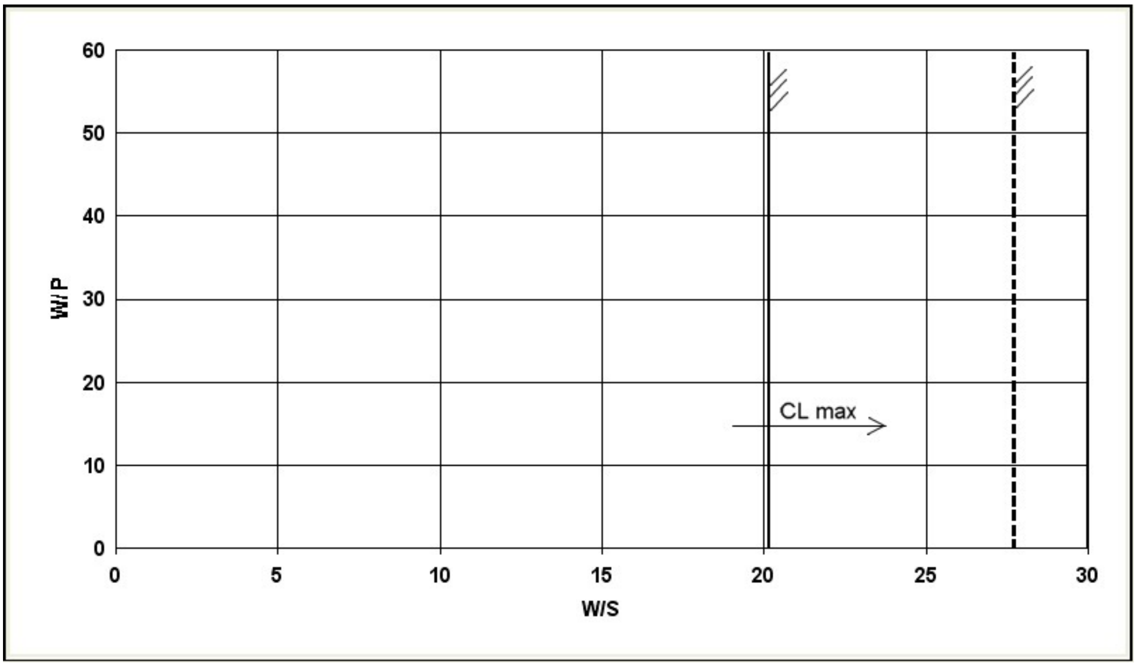

Figure 3. 1 – Stall speed requirements: the lines are at same altitude and same stall speed with different value of maximum lift coefficent.

3.2.4 - Takeoff requirements.

The takeoff requirements are assigned with total takeofflength or takeoff ground length in the case of aircraft certified with FAR 23 regulation, and with takeoff field length for aircraft certified with FAR 25 regulation. In the assumption that the thrust given by the engine is symmetric respect the middle plan of the aircraft and parallel to the ground, the equilibrium of the longitudinal force can be expressed with the equation 3.2.2.

$$\frac{W}{g}\cdot\frac{dV}{dt} = T - D - \mu_r \cdot (W - L) \quad \textbf{(3.2.2)}$$

The inertial force on the first member is balanced by the sum of thrust available *T*, aerodynamic drag *D* and the friction, μ_r is the rolling friction coefficient.From the equation (3.2.2) is possible to obtain the following formula.

$$S_g = \frac{\left(\frac{V_{LOFF}}{V_{STO}}\right)^2 \cdot \left(\frac{W}{S}\right)}{g \cdot \sigma \cdot C_{L\max TO} \cdot \left[\frac{T}{W}\right]_{V=0.7V_{LOFF}}} \quad \textbf{(3.2.1)}$$

Where V_{LOFF} is the speed at liftoff and V_{STO} is the stall speed at takeoff, σ is the density ratio.

This is valid in the assumption of:

- Constant C_L
- Constant net longitudinal force
- Thrust available is much greater than the total braking force, given by the sum of drag and friction

In case of aircraft certified with FAR 23 regulation, exist a statistical relationship, see figure 3.5, that binds the ground length and T/W or W/P, W/S, $C_{L\,\max\,\mathrm{TO}}$ and σ, appearing in (3.3.3), through a takeoff parameter called TOP_{23}.

$$S_{TO\ \mathrm{Ground}} = 4.9 \cdot TOP_{23} + 0.009 \cdot TOP_{23}^2 \quad \textbf{(3.2.2)}$$

The ground lenght is linked with the total takeoff length with another semiempirical law.

$$S_{TO} = 1.66 \cdot S_{TO\ \mathrm{Ground}} \quad \textbf{(3.2.3)}$$

So the relationship (3.3.3) the TOP_{23} is given by.

$$TOP_{23} = \frac{\left(\frac{W}{S}\right)_{TO} \cdot \left(\frac{W}{P}\right)_{TO}}{\sigma \cdot C_{L\,\max\text{ - TO}}} \quad \text{or} \quad TOP_{23} = \frac{\left(\frac{W}{S}\right)_{TO} \cdot \left(\frac{T}{P}\right)_{TO}}{\sigma \cdot C_{L\,\max\text{ - TO}} \cdot \left(\frac{T}{W}\right)_{TO}} \quad \textbf{(3.2.4)}$$

So assigning a value of takeoff length or ground length and determined the value of TOP_{23}, is established a relationship between the wing loading and $(T/W)_{TO}$ or $(W/P)_{TO}$.The value $(T/P)_{TO}$ is given by the user.

Likewise, in the case of aircrafts certified with FAR 25 regulation exist a statistical relationship, see figure 3.6, that binds the takeoff field length with T/W or W/P, W/S, $C_{L\,\max\,\mathrm{TO}}$ and σ, through the takeoff parameter called TOP_{25}.

$$S_{TO\ \text{Field Length}} = 37.5 \cdot TOP_{25} \quad \textbf{(3.2.5)}$$

This parameter is defined, for jets and propeller, as follow.

$$TOP_{25} = \frac{\left(\frac{W}{S}\right)_{TO}}{\sigma \cdot C_{L\,\max\text{ - TO}} \cdot \left(\frac{T}{W}\right)_{TO}} \quad \text{or} \quad TOP_{25} = \frac{\left(\frac{W}{S}\right)_{TO} \cdot \left(\frac{W}{P}\right)_{TO}}{\sigma \cdot C_{L\,\max\text{ - TO}} \cdot \left(\frac{T}{P}\right)_{TO}} \quad \textbf{(3.2.6)}$$

So assigning a value of takeoff length or ground length and determined the value of TOP_{23}, is established a relationship between the wing loading and $(T/W)_{TO}$ or $(W/P)_{TO}$. The value $(T/P)_{TO}$ is given by the user.

In both cases is possible see how higher value of wing loading or altitude involve a growth of the takeoff distance, while higher value of maximum takeoff lift coefficient or takeoff thrust or power cause a reduction of the takeoff distance. So for the choice of the design point, as for propeller aircraft as for jet aircraft, higher value of $C_{L\max \mathrm{TO}}$ involves lesser restrictive curve, while lesser value of takeoff distance involves the opposite effect.

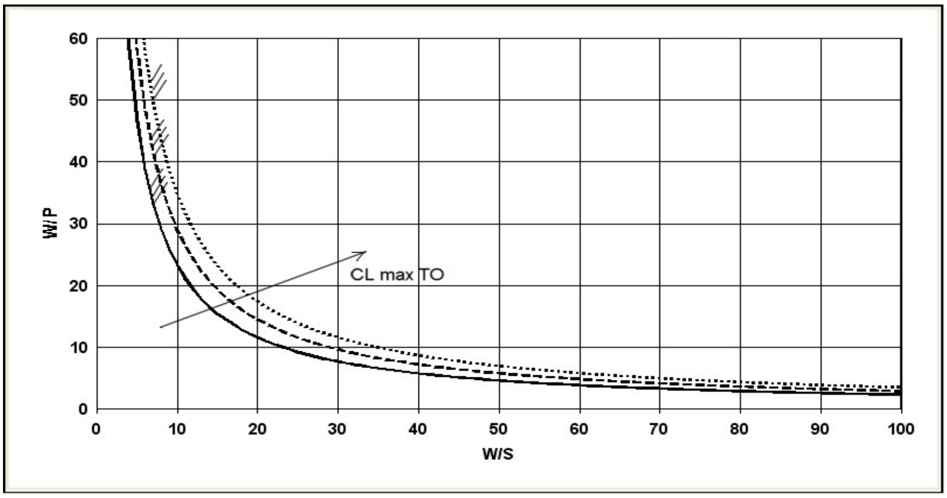

Figure 3. 2 – Takeoff limitation for propeller aircraft.

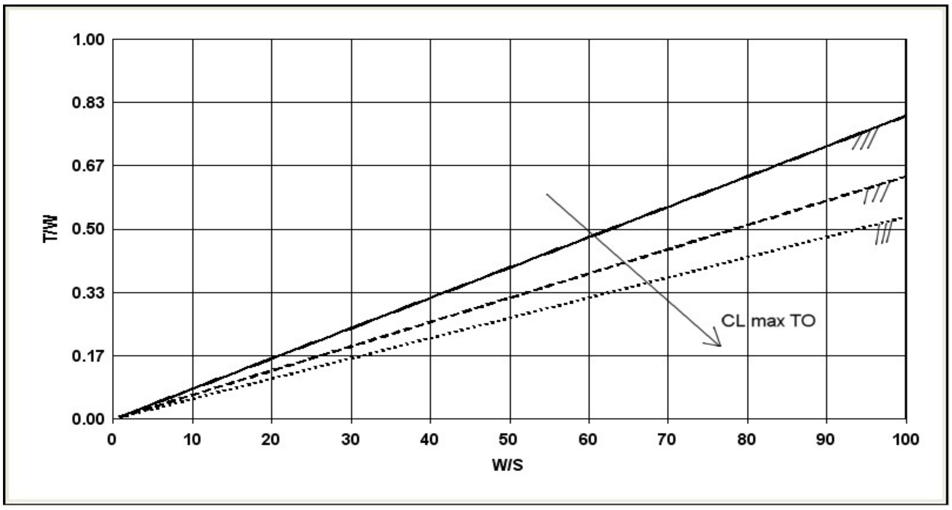

Figure 3.3–Takeoff limitation for jet aircraft.

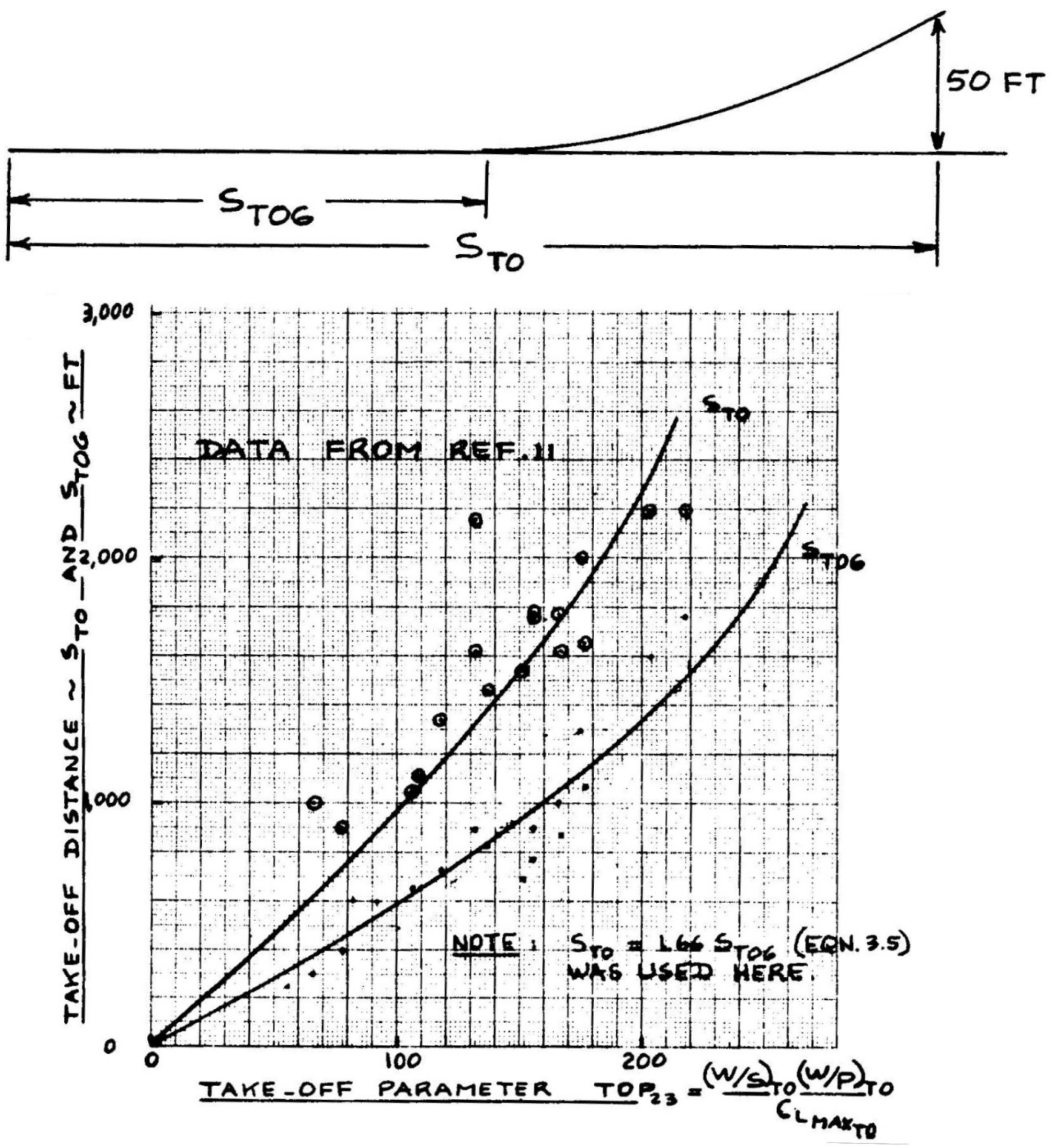

Figure 3. 4 – Diagram of semi empirical relationship for FAR23.

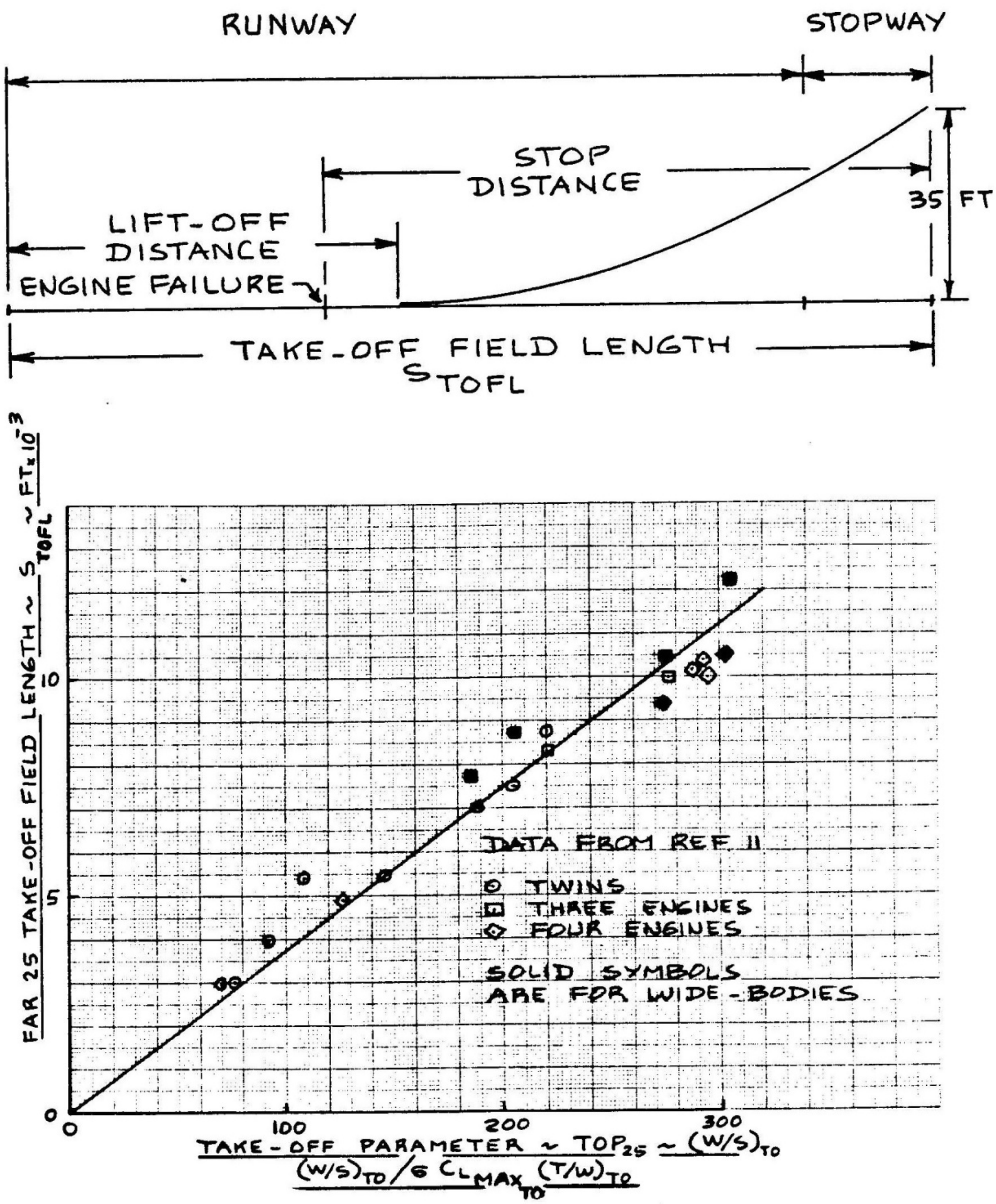

Figure 3. 5–Diagram of semi empirical relationship for FAR25.

3.2.5 - Landing requirements

The landing specifications are assigned, as total landing length or ground length, in the case of aircraft certified with FAR 23 regulation, as a landing field length for FAR 25.In the assumption that the thrust given by the engine is symmetric respect the middle plan of the aircraft and parallel to the ground, the equilibrium of the longitudinal force can be expressed with the equation 3.2.9.

$$\frac{W}{g}\cdot\frac{dV}{dt} = -T_{reverse} - D - \mu_r \cdot (W - L) \quad \textbf{(3.2.7)}$$

The inertial force at the first member is balanced by the sum of the reverse thrust, if available, $T_{reverse}$, Drag D and friction coefficient.
From the (3.2.9) is possible obtain the relationship between the landing length and stall speed in landing configuration. (in this equation instead of touchdown speed V_{TD} is shown the V_{SL} that is proportional through a factor k_{TD}).

$$S_g = \frac{W\cdot k_{TD}^2\cdot V_{SL}^2}{2\cdot g}\cdot\left[\frac{1}{T_{reverse} + D + \mu_r\cdot(W-L)}\right]_{V=0.7V_{TD}} \quad \textbf{(3.2.8)}$$

This is valid in the assumption of:

- Constant C_L
- Constant net longitudinal force
- Thrust available is much greater than the total braking force, given by the sum of drag and friction

In case of aircraft certified with FAR 23 regulation, exist a statistical relationship, see figure 3.8, that binds the ground length to the stall speed.

$$S_{L\ \mathrm{Ground}} = 0.265\cdot V_{\mathrm{SL}}^2 \quad \textbf{(3.2.9)}$$

And the ground length is binds with the total landing length with another semi empirical law.

$$S_L = 0.5136\cdot S_{L\ Ground} \quad \textbf{(3.2.10)}$$

In case of aircraft certified with FAR 25, the statistical relationship(see the figure 3.9) that binds the landing field length and stall speed is the following.

$$S_{L\ \mathrm{Field\,Length}} = 0.507\cdot V_{SL}^2 . \quad \textbf{(3.2.11)}$$

The V_{SL} is linked with wing loading, altitude and maximum lift coefficient through the equation of the equilibriumat the normal translation.

$$V_{SL} = \sqrt{\frac{2\cdot W_L}{\rho\cdot S\cdot C_{L\max L}}} \quad \textbf{(3.2.12)}$$

Assuming so the weight fraction between landing and takeoff is possible obtain the representative equation of this limitation. Is clear that also here the propulsive characteristics don't exert significant influence.
As in case of propeller aircraft as in case of jet aircraft, the representative curve are vertical lines, that move to right with the grown of maximum lift coefficient in landing configuration. An increasing of the assumed landing distance show an enlargement of the "good space" for the choice of the design point.

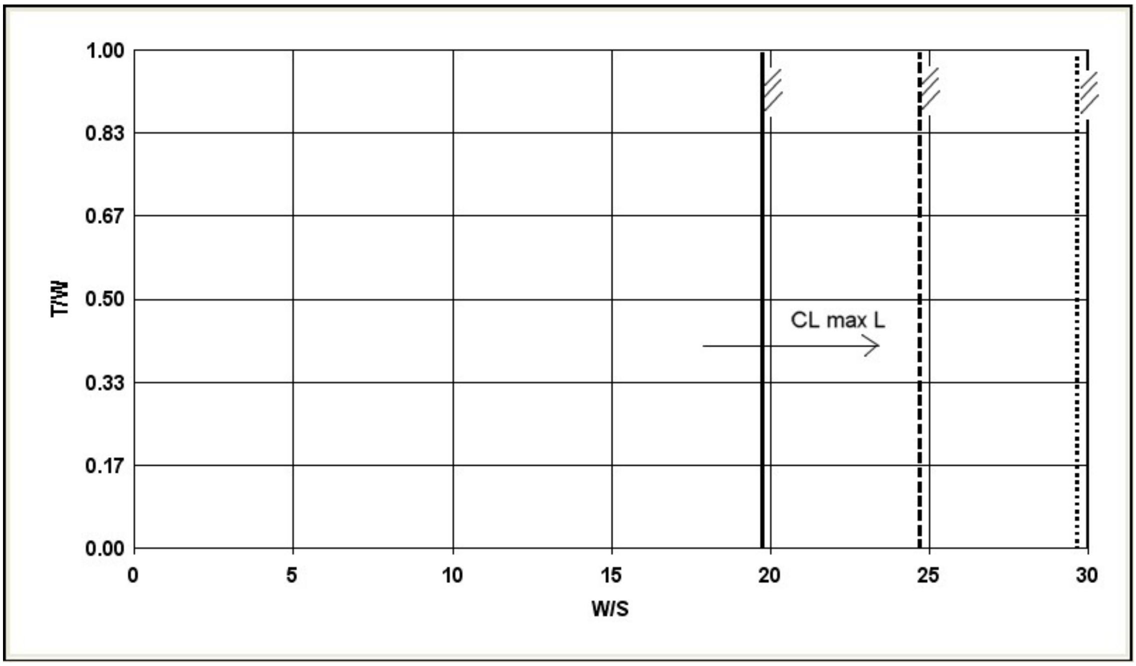

Figure 3. 6–Landing limitation for jet aircraft .

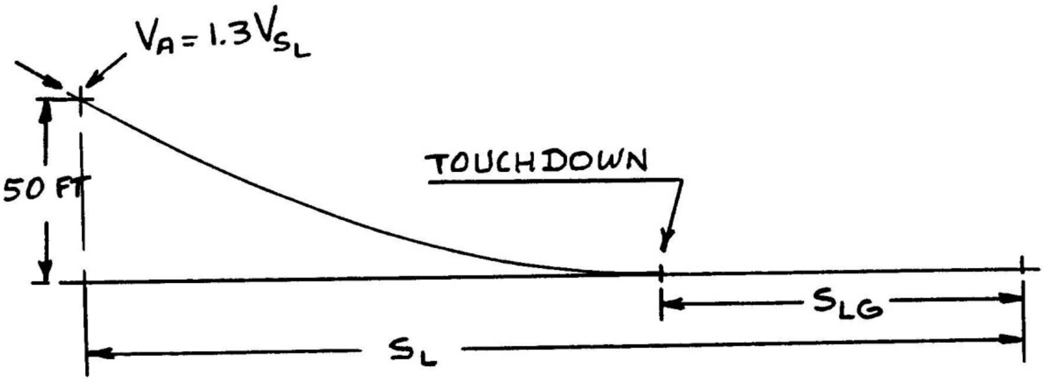

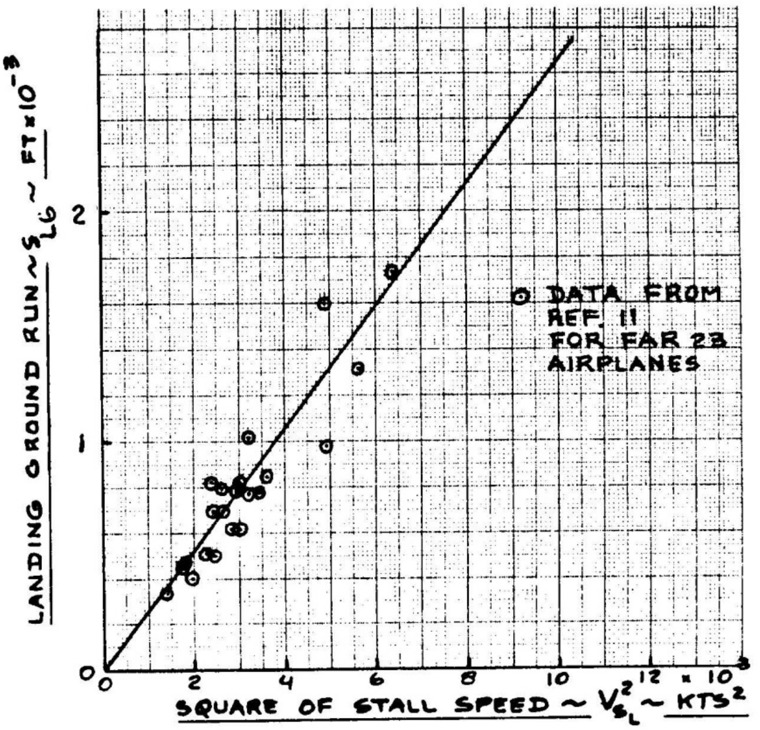

Figura 3. 7–Diagram of the semi empiric relationship for FAR23.

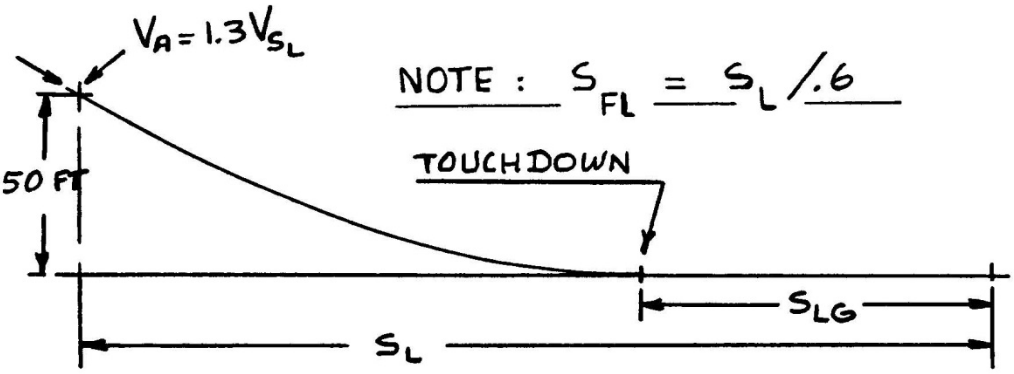

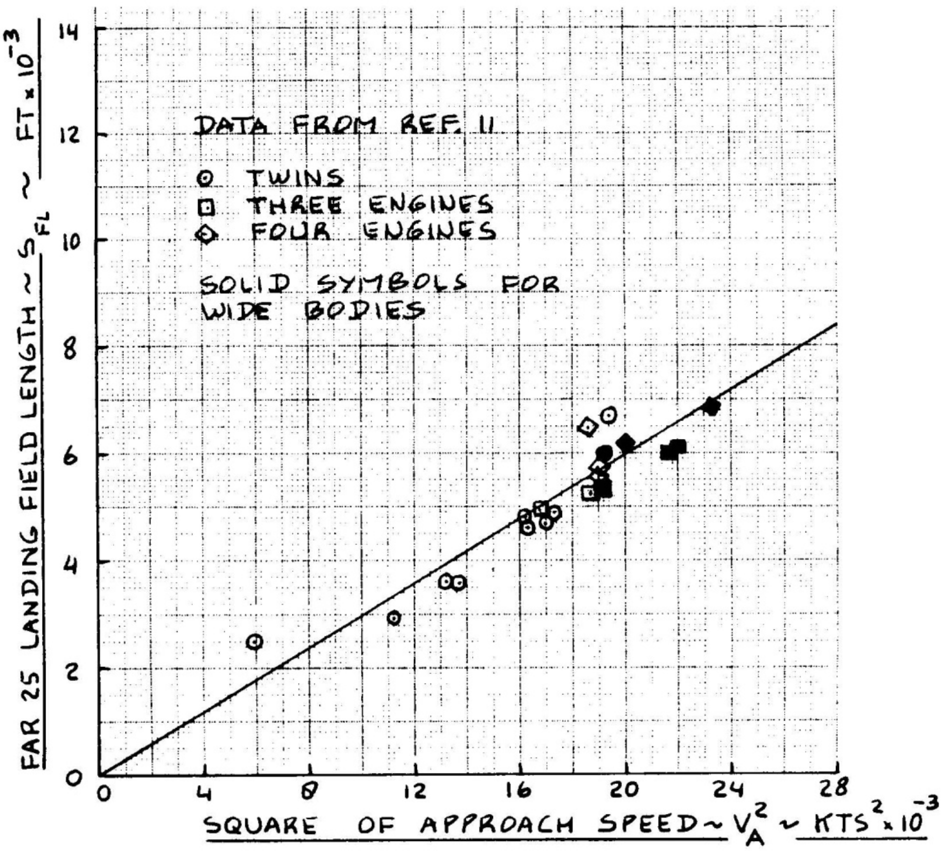

Figure 3. 8–Diagram of semi empirical relationship for FAR 25.

3.2.6 - Climb Requirements

The search of climb characteristics needs the determination of preliminary drag polar, in various flight condition. Actually for the analysis of preliminary sizing, the absence of data relatives to aerodynamic behavior of the aircraft denies a realistic and fine definition of drag polar. So is opportune to use an analytic model based on following equation.

$$C_D = C_{D0} + \frac{C_L^2}{\pi \cdot AR \cdot e} \quad \textbf{(3.2.13)}$$

A first evaluation of the required parameters in the equation (3.2.15) for the different flight configuration, can be done starting from the knowledge of the information of similar aircraft of the same category, so through a semi empirical methodology.
The parasite drag coefficient in clean configuration C_{D0} can be evaluated as the fraction between the parasite area *f* and wing surface *S*.

$$C_{D0} = \frac{f}{S} \quad \textbf{(3.2.14)}$$

The parasite area is linked to friction coefficient C_f, to the wet area and maximum takeoff weight from a statistical relationship, the coefficients change with the aircraft category, the diagram are reported in figure 3.11 and 3.14 for twin engine propeller and transport jet.
The wing surface is evaluated assuming a plausible value of wing loading W_{TO}/S seeing the similar aircraft. (ADAS suggest this value after the choice of category).
Another design parameter is the aspect ratio AR .

$$AR = \frac{b^2}{S} \quad \textbf{(3.2.15)}$$

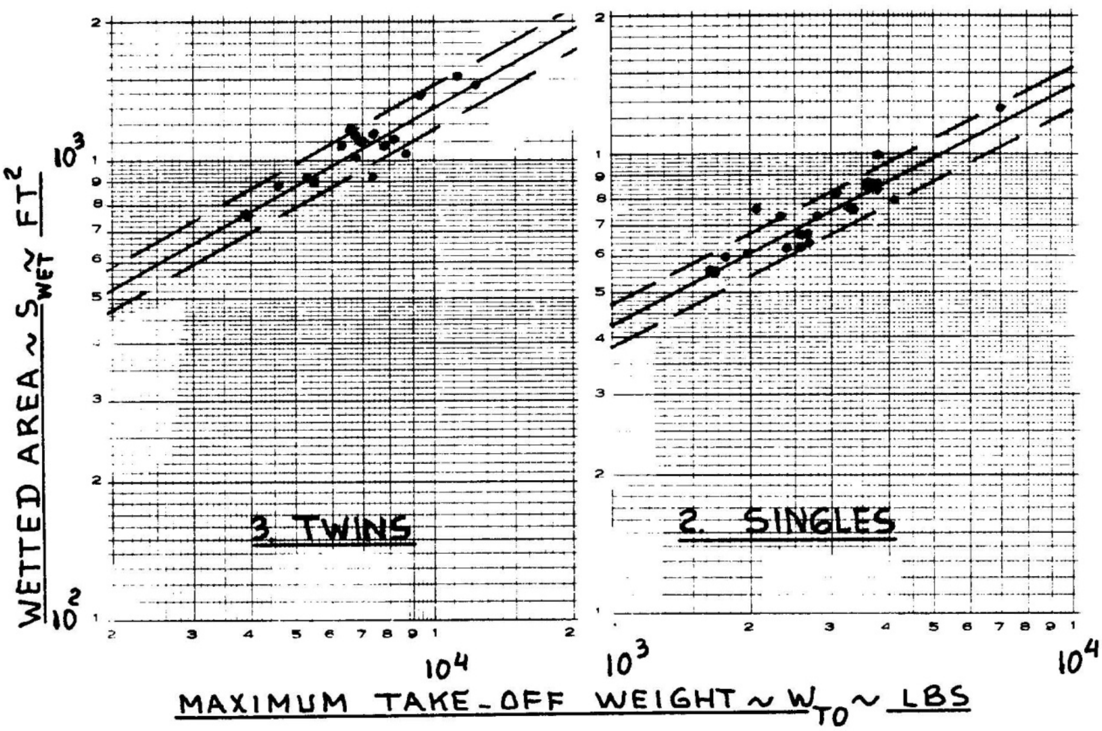

Figure 3. 9 – Diagram of statistical relationship that link the wet area with maximum takeoff weight for propeller aircraft.

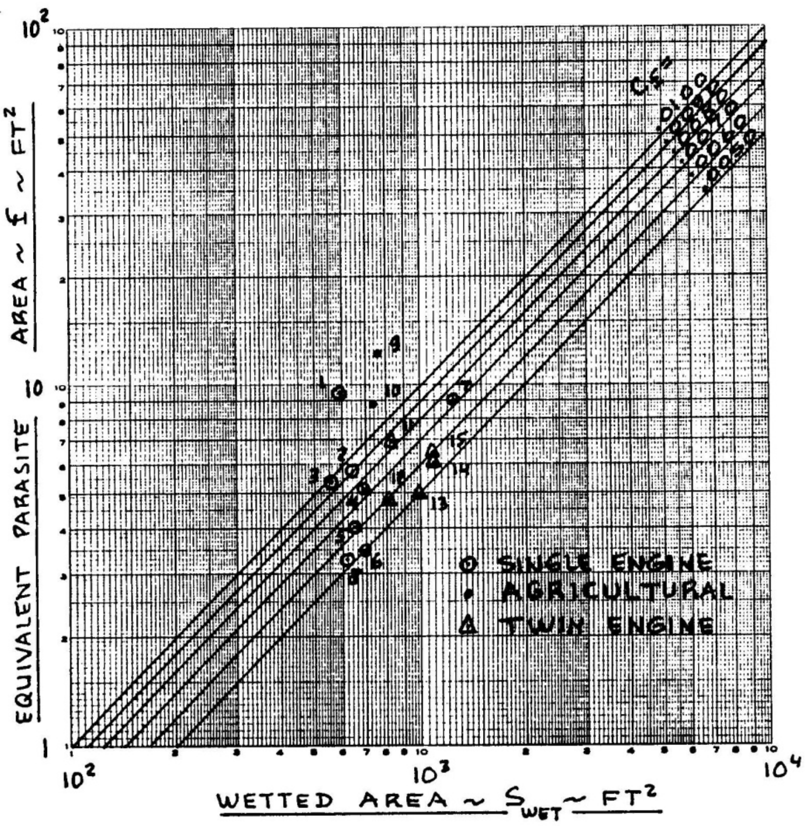

Figure 3. 10 – Diagram of statistical relationship that link the parasite area with wet area.

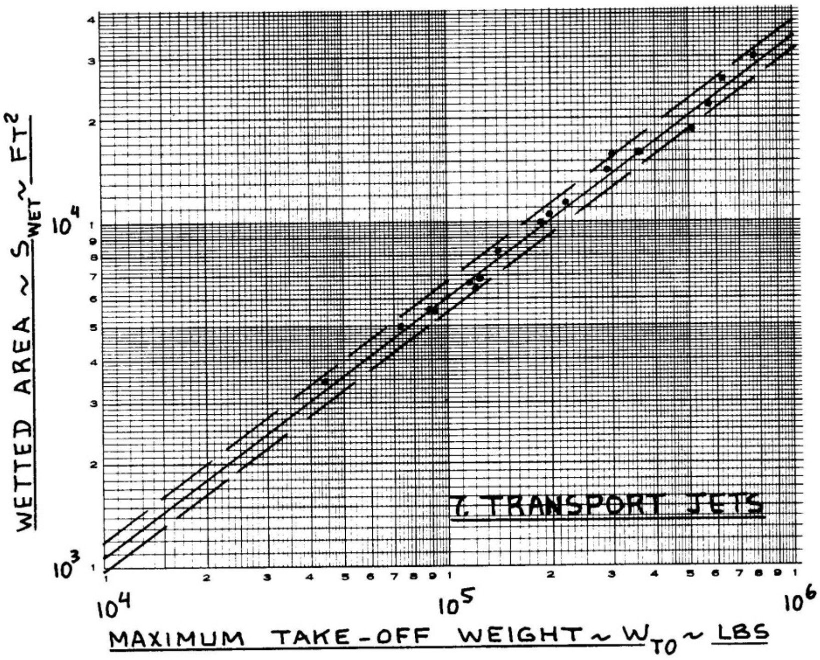

Figure 3. 11–Diagram of the statistical relationship between wet area and maximum takeoff weight for transport jet.

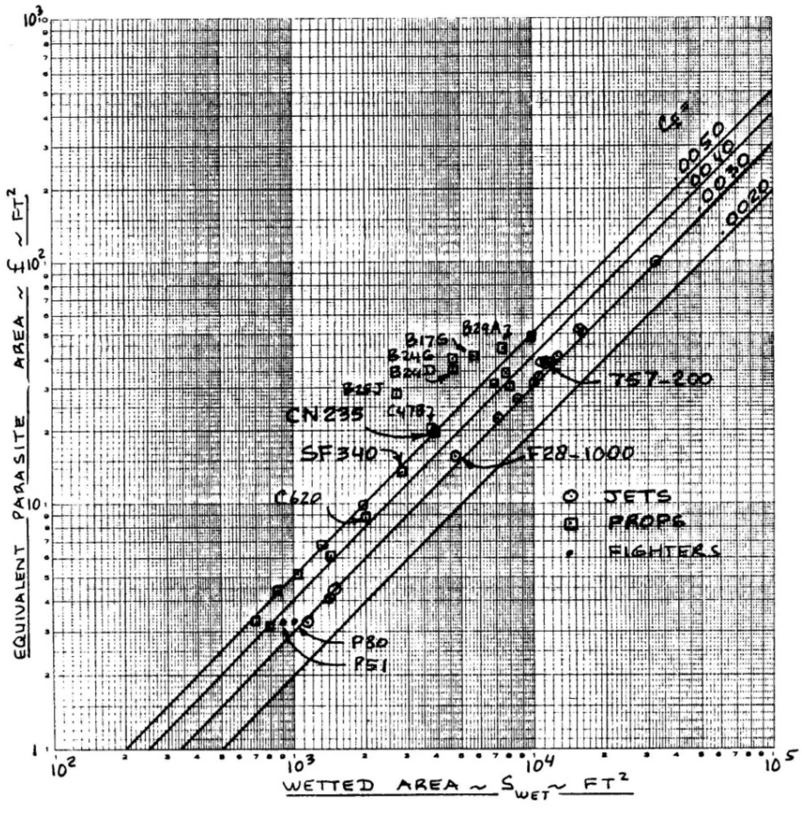

Figure 3.12–Diagram of the statistical relationship betweeen parasite area and wet area.

For the choice of AR is important know that for higher value of aspect ratio involves a reduction of the induced drag, causing so a better general performances but also the requirement to grow the structural weight and so the operative empty weight.
At constant value of maximum takeoff weight, so, an higher value of AR involves a reduction of payload or boarded fuel and then the maximum range.
In the case of bigger aircraft, the choice of the aspect ratio can be decided by business needs, connected with the compatibility of the aircraft with most existent airport structures.
The value of Oswald factor e in clean configuration, takeoff and landing configurations and the value of increment of the parasite drag coefficient ΔC_{D0} in takeoff and landing configurations, must be chosen in typical interval of the aircraft category.

From the drag polar is possible so to proceed with the requirements imposed by the FAR23 and FAR 25. This is characterized by minimum value of rate to climb RC and climb gradient $CGR = RC/V = \sin\vartheta$ in various flight conditions.

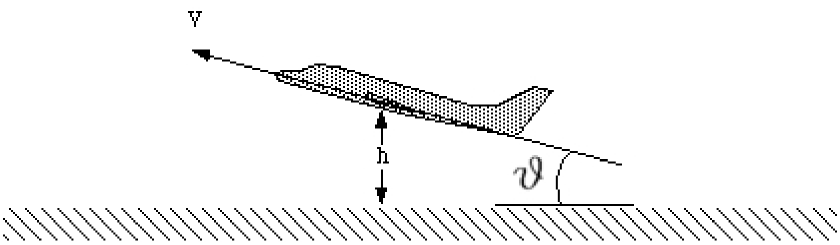

Figure 3. 13 – Climb phase

In the case of FAR 23 regulation, it's given the following restrictions:

1. FAR23.65 – $RC \geq 300\,fpm$ assuming
   a. AEO –All Engine Operative
   b. Gear up
   c. High lift devices in Takeoff condition
   d. Maximum thrust or powercontinous
   e. Sea level

2. FAR23.65 - $CGR \geq 1/12$ rad assuming
   a. AEO - All Engine Operative
   b. Gear up
   c. High lift devices in Takeoff condition
   d. Maximum thrust or powercontinous
   e. Sea level

3. FAR23.67 - $RC \geq 0.027 \cdot V_S\ fpm$ assuming
   a. OEI – One Engine Inoperative
   b. Best high lift devices position
   c. Maximum takeoff thrust or power on operative engine
   d. altitude5000 ft

4. FAR23.77 - $CGR \geq 1/30$ rad assuming
    a. AEO - All Engine Operative
    b. Gear down
    c. High lift devices in landing condition
    d. Maximum takeoff thrust or power
    e. Sea level

For the FAR 25 instead:

1. FAR25.111 – $CGR \geq 0.012$ rad for twin engine,
   $CGR \geq 0.015$ rad for threeengine,
   $CGR \geq 0.017$ rad for fourengine, assuming
    a. OEI - One Engine Inoperative
    b. Gear up
    c. High lift devices in Takeoff condition
    d. $V = 1.2 \cdot V_{STO}$
    e. Maximum takeoff thrust or power
    f. Ground Effect

2. FAR25.121 – $CGR \geq 0.000$ rad for twin engine,
   $CGR \geq 0.003$ rad forthreeengine,
   $CGR \geq 0.005$ rad for fourengine, assuming
    a. OEI - One Engine Inoperative
    b. Gear down
    c. High lift devices in Takeoff condition
    d. $V_{LOFF} < V < 1.2 \cdot V_{STO}$
    e. Maximum takeoff thrust or power
    f. Ground Effect

3. FAR25.121 – $CGR \geq 0.024$ rad for twin engine,
   $CGR \geq 0.027$ rad for threeengine,
   $CGR \geq 0.030$ rad for fourengine, assuming
    a. OEI - One Engine Inoperative
    b. Gear up
    c. High lift devices in Takeoff condition
    d. $V = 1.2 \cdot V_{STO}$
    e. Maximum takeoff thrust or power

4. FAR25.121 – $CGR \geq 0.012$ rad for twin engine,
   $CGR \geq 0.015$ rad for threeengine,
   $CGR \geq 0.017$ rad for fourengine, assuming
    a. OEI - One Engine Inoperative
    b. Gear up
    c. High lift devices up
    d. $V = 1.25 \cdot V_S$
    e. Max continuous thrust or power

FAR25.119 – $CGR \geq 0.032$ rad assuming

a. AEO – All Engine Operative
b. Gear down
c. High lift devices in landing condition
d. $V = 1.3 \cdot V_{SL}$
e. Maximum landingweight

5. FAR25.121 – $CGR \geq 0.021$ rad for twin engine
$CGR \geq 0.024$ rad for threeengine,
$CGR \geq 0.027$ rad for fourengine, assuming

a. OEI - One Engine Inoperative
b. Gear down
c. High lift devices in approach condition
d. $V = 1.5 \cdot V_A$
e. Maximum takeoff thrust or power
f. Maximum landingweight

Higher rate of climb and climb angle with constant altitude and every other condition give more limiting condition for the choice of the design point, as in the case of propeller aircraft as for transport jet.

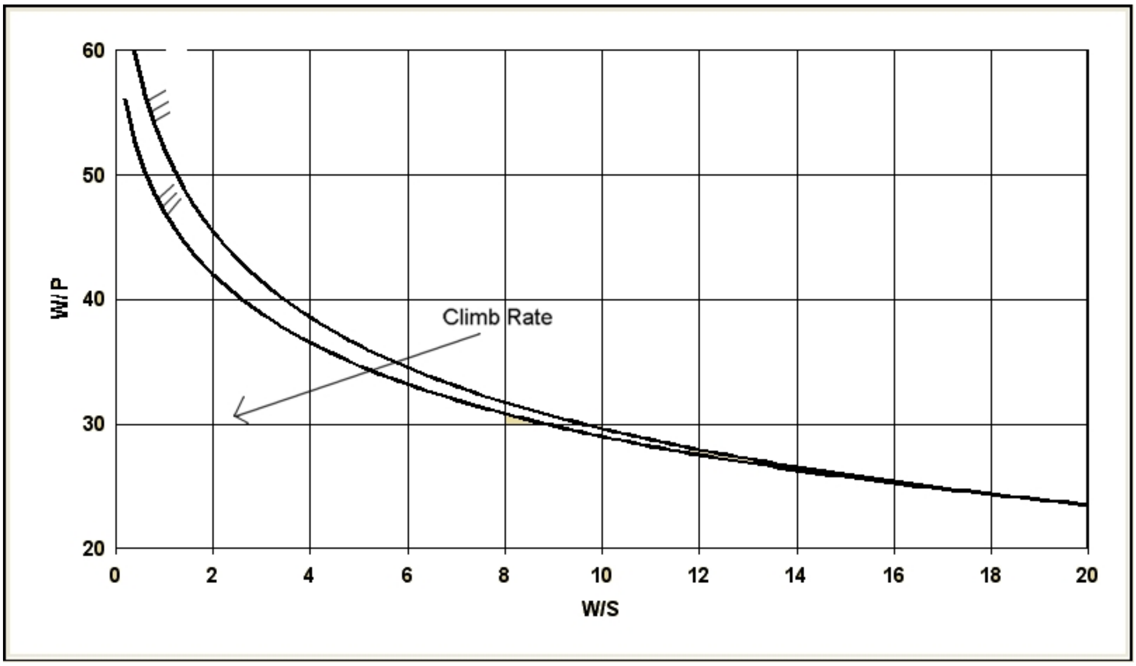

Figura 3. 14 – Climb Requirements for a propeller aircraft.

3.2.7 - Dimensionamento in base ai requisiti di crociera.

The mission specification can give information about the averagecruise speed or, sometimes, about the maximum speed of the new aircraft. In the first case, the parameter is generally referred on a condition of engine with throttle setting between 75% and 80%, while in the second case it is referred on the maximum continuative thrust or power.
The equilibrium equation for a levelled flight, can be expressed as follow.

$$\begin{cases} W = \frac{1}{2} \cdot \rho \cdot V^2 \cdot S \cdot C_L \\ T = \frac{1}{2} \cdot \rho \cdot V^2 \cdot S \cdot C_D \end{cases} \quad \textbf{(3.2.16)}$$

The drag coefficient can be considered as the sum of parasite drag and induced drag.

$$C_D = C_{D0} + C_{Di} \quad \textbf{(3.2.17)}$$

In cruise condition or maximum speed, the incidence is very small, and characterized by low value of lift coefficients and induced drag, so this contribution can be estimated approximately as 10% of the parasite drag.

$$C_D \approx 1.1 \cdot C_{D0}. \quad \textbf{(3.2.18)}$$

substituing the (3.2.20) in the second equation of the system (3.2.18) then the speed can be obtained as follow.

$$V = \sqrt{\frac{2 \cdot T}{\rho \cdot S \cdot 1.1 \cdot C_{D0}}} = \sqrt{\frac{1.82}{\rho_0}} \cdot \sqrt{\frac{T}{W}} \cdot \sqrt{\frac{W}{S}} \cdot \sqrt{\frac{1}{\sigma}} \cdot \sqrt{\frac{1}{C_{D0}}} \quad \textbf{(3.2.19)}$$

Or for propeller aircraft in function of power.

$$V = \sqrt[3]{\frac{1.82}{\rho_0}} \cdot \sqrt[3]{\frac{P}{W}} \cdot \sqrt[3]{\frac{W}{S}} \cdot \sqrt[3]{\frac{1}{\sigma}} \cdot \sqrt[3]{\frac{1}{C_{D0}}} \quad \textbf{(3.2.20)}$$

From the last formulas it’s clear how the cruise speed or maximum speed are dependent on a series of parameters the resume the aircraft characteristics: wing loading, fraction between thrust and weight or weight and power, the altitude and drag coefficient.
On this consideration is possible introduce the power index, that includes in all the parameters listed above and is obtained by a statistical relationship with cruise speed or maximum speed for propeller driven aircraft.

$$I_P = \sqrt[3]{\frac{(W/S)}{\sigma \cdot (W/P)}} \quad \textbf{(3.2.21)}$$

Reporting in a diagram $V - I_p$ the data of similar aircraft is possible to deduce a statistical law between speed and power index.

The same method can be used for evaluate the relationship between power index and propeller efficiency and parasite drag coefficient, as shown in the figure 3.16

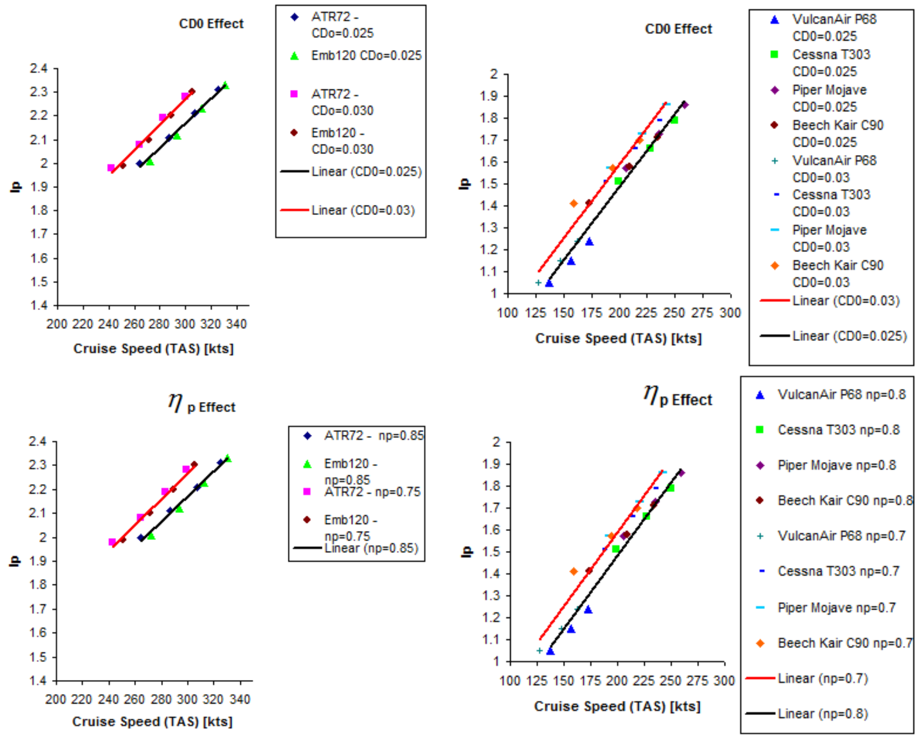

Figura 4. 15 – Index power trend shifts with different parasite drag coefficient and propeller efficiency.

To obtain an useful relationship for the plot $(W/P)_{TO} - (W/S)_{TO}$ is necessary to change the condition expressed in the (3.2.23) with a takeoff condition.

$$I_P = \sqrt[3]{\frac{1}{\sigma}} \cdot \sqrt[3]{\left(\frac{W_{cond}}{S}\right) \cdot \left(\frac{W_{TO}}{W_{cond}}\right)} \cdot \sqrt[3]{\left(\frac{P_{cond}}{W_{cond}}\right) \cdot \left(\frac{W_{cond}}{W_{TO}}\right) \cdot \left(\frac{P_{TO}}{P_{cond}}\right) \cdot \left(\frac{P_{cond}}{P_{TO}}\right)} \quad \textbf{(3.2.22)}$$

$$\left(\frac{W_{TO}}{P_{TO}}\right) = \frac{1}{\sigma \cdot I_p^3} \cdot \left(\frac{W_{TO}}{S}\right) \cdot \left(\frac{P_{cond}}{P_{TO}}\right) \quad \textbf{(3.2.23)}$$

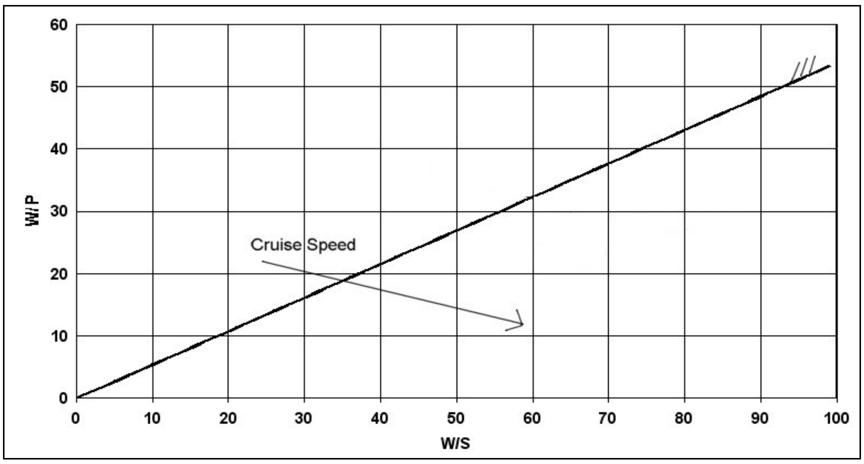

Figure 3. 17 – Cruise limitation for propeller driven aircraft.

For jet driven aircraft, instead, starting from (3.2.18) is obtained the following relationship between $(T/W)_{TO}$ and $(W/S)_{TO}$.

$$\left(\frac{T}{W}\right)_{cond} = C_{D0_{comp}} \cdot q \cdot \left(\frac{S}{W}\right)_{cond} + \frac{1}{q \cdot \pi \cdot AR \cdot e} \cdot \left(\frac{W}{S}\right)_{cond} \quad \textbf{(3. 26)}$$

Where q is the dynamic pressure. At the value of parasite drag is added now also the compressibility contribution, that can be estimated by the figure 3.18.

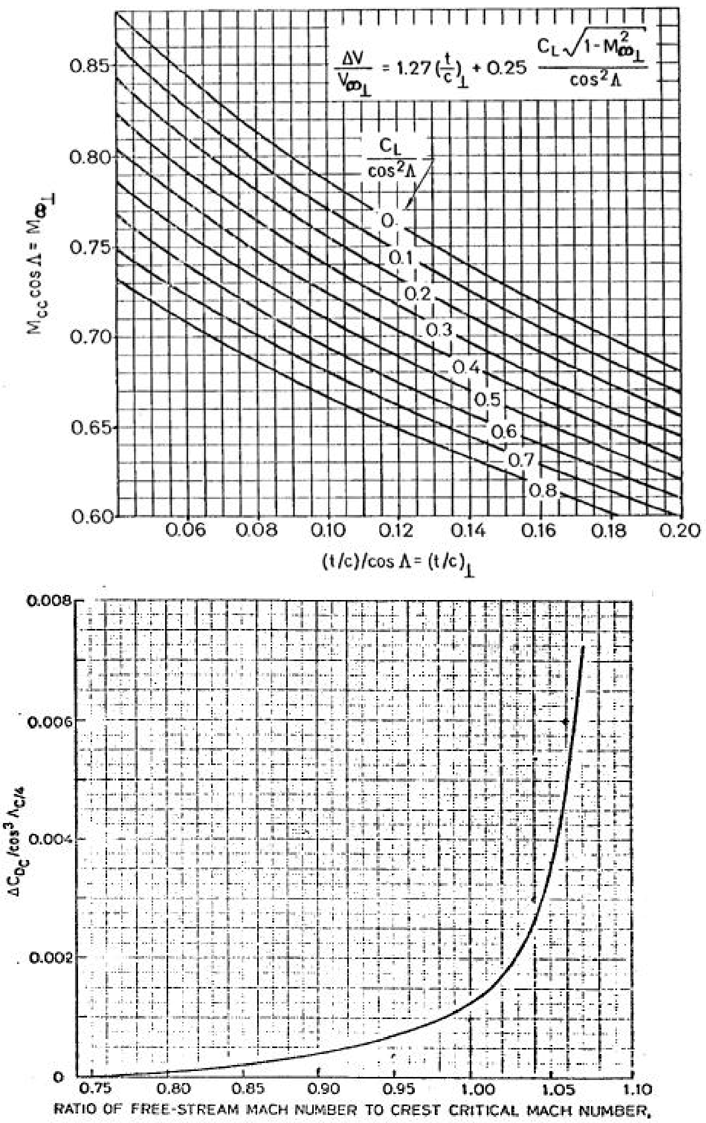

Figure 3. 18 – Compressiblity effect on parasite drag.

The wing loading is at denominator of the contribution due to parasite drag, while it is at numerator for the contribution due to induced drag. So at lower value of $(W/S)_{cond}$ there is a superiority of viscous term on the induced, and vice versa.
Also here we have to obtain an equation for the plot $(T/W)_{TO} - (W/S)_{TO}$. The W_{cond}/W_{TO} depend on aircraft type, for example a transport jet as the Airbus A380 can have a mean value of 0.8, while for an executive it can be unitary.
So processing the (3.2.26)we can obtain the following equation.

$$\left(\frac{T}{W}\right)_{TO} = \left[C_{D0} \cdot q \cdot \left(\frac{S}{W_{TO}}\right) \cdot \left(\frac{W_{TO}}{W_{cond}}\right) + \frac{1}{q \cdot \pi \cdot AR \cdot e} \cdot \left(\frac{W_{TO}}{S}\right) \cdot \left(\frac{W_{cond}}{W_{TO}}\right)\right] \cdot \left(\frac{T_{TO}}{T_{cond}}\right) \cdot \left(\frac{W_{cond}}{W_{TO}}\right) \quad \textbf{(4.27)}$$

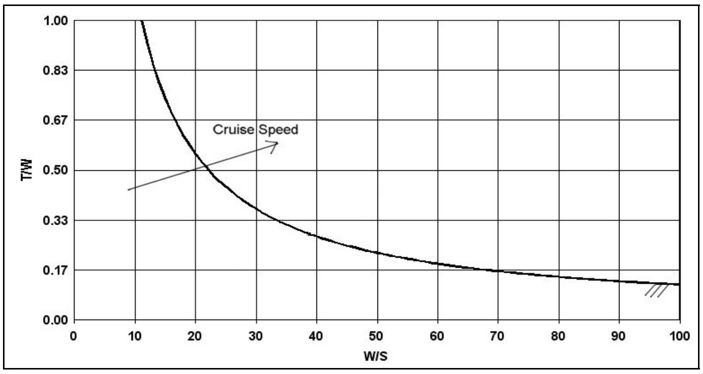

Figure 3. 19–Cruise limitation.

3.2.8 - Research of the design point.

After all is possible to see the range of value good for the choice of the design point. In the following figure are drawn examples of plot useful for the research of the design point. The first is for propeller driven the other is for jet driven. The allowed zone have the white background.

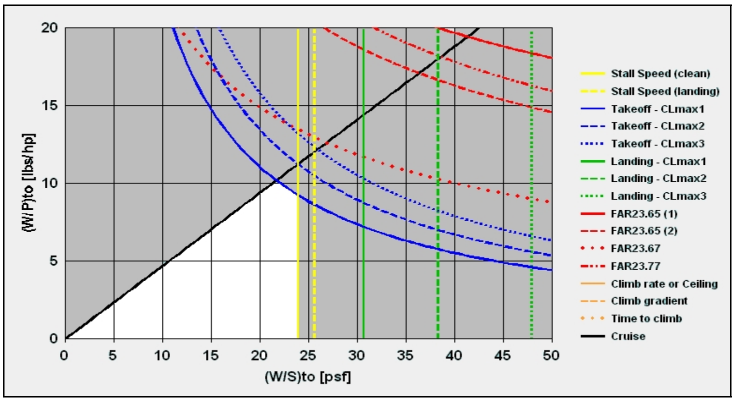

Figure 3. 20 – Chart used for the choice of the design point, for propeller aircraft.

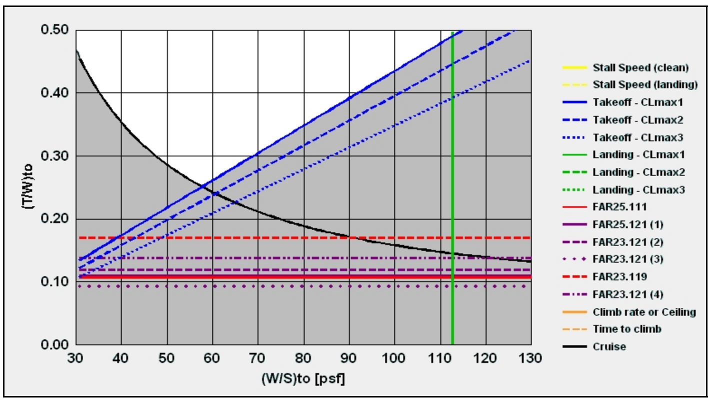

Figure 3. 21–Chart used for the choice of the design point, for transport jets.

3.3 - WING ANALYSIS

3.3.1 - Introduction

The preliminary analysis of the weight estimation and the design point allow to do the preliminary design of the geometric, aerodynamic and structural characteristics of the wing, with the purpose to determine its contribution on the drag polar of the complete aircraft. The analysis of the wing can be done with two different approach, one semi empirical and the other withpanel methods as Multhopp or Vortex lattice, for the determination of the load distribution on the wing span.

3.3.2 - The methodology for wing analysis

An important help for the wing design can be the calculation of the value of crest critical Mach number and the drag divergence Mach number. In fact through that is possible verify if the wing characteristics satisfy the buffet barrier needs and the stall condition. By the information of wing surface, aircraft weight, altitude, flight Mach number, mean thickness, sweep angle and airfoils type, it's possible to evaluate the M_{cc} and M_{div} through the following figure and formula (3.3.1).

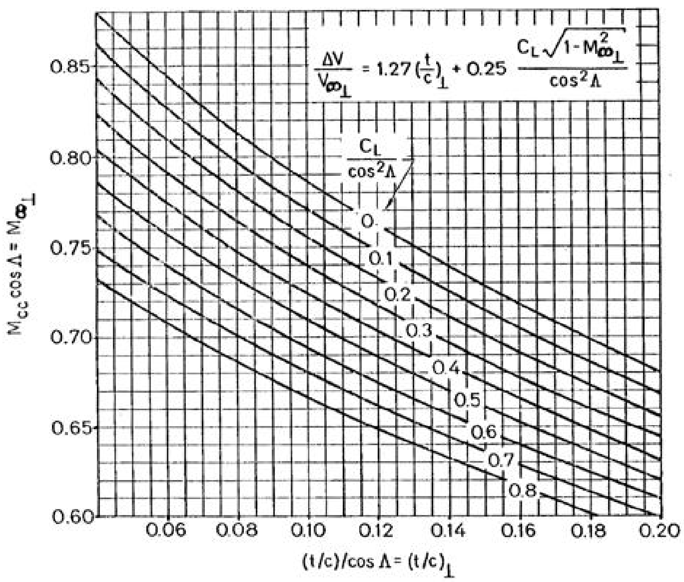

Figure 3. 22 –Chart used for the evaluation of Crest Critical Mach number

$$M_{DD} = M_{cc} \cdot \left[1.02 + 0.08 \cdot \left(1 - \cos\Lambda_{\frac{c}{4}}\right)\right] \quad \textbf{(3.3.1)}$$

It's possible then to draw a diagram where the results are shown through the following procedure: a value of lift coefficient C_L is fixed, then M_{cc} is evaluated by the figure 3.22, then it's possible to calculate the maximum lift coefficient by the Prandtl and Glauert rule.

$$C_{L\,\max\,\mathrm{M}\neq 0} = \frac{C_{L\,\max\,\mathrm{M}=0}}{\sqrt{1-M^2}} \quad \textbf{(3.3.2)}$$

So comparing the $C_{L\,\max\,\mathrm{M}\neq 0}$ with chosen C_L, is established which between stall condition and buffet is the most critical, if $C_L > C_{L\,\max\,\mathrm{M}\neq 0}$ then the critical condition is the stall, if $C_L < C_{L\,\max\,\mathrm{M}\neq 0}$ then the critical condition is the buffet.

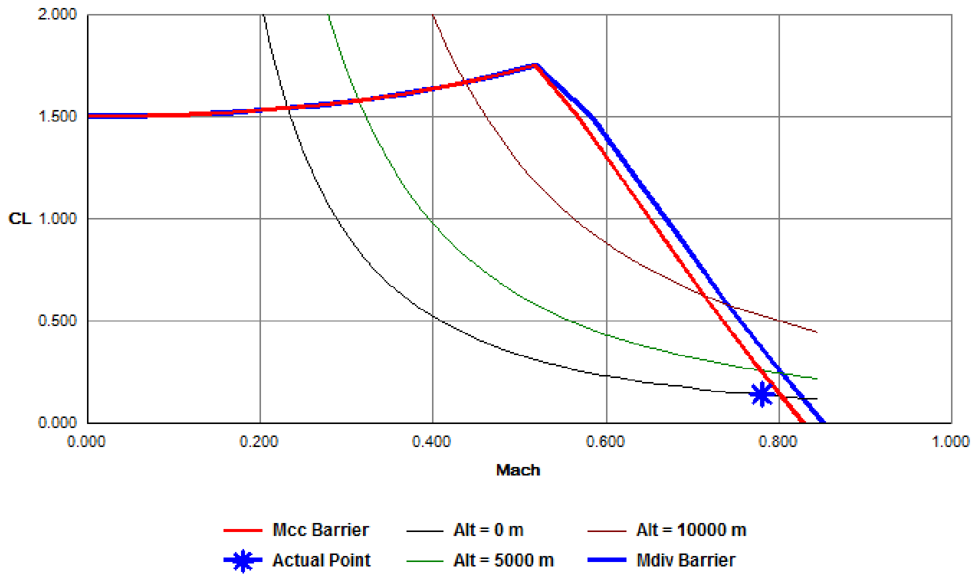

Figure 3. 23 –Example of chart used for the evaluation of critical condition.

3.3.3 - The semiempiricalestimation

The semi empirical analysis start from the choice of geometry of the wing, this can be given choosing the wing sections characteristics, position, dimensions, aerodynamics. So the results are obtained as follow.

Wing Surface. The wing surface is calculated from the sections data as sum of trapezes, it represent the reference surface for the execution of all calculations.

Aspect Ratio. The aspect ratio is evaluated as the classical formula (3.2.17) from the chosen geometry.

Taper ratio. The taper ratio is calculated as the ratio assigned external chord and root chord.

Maximum mean thickness. All the parameters used to describe the airfoils, it's used to determine the characteristics of the mean airfoil of the wing. These are calculated through the influence area of the airfoils as shown in figure 3.24.

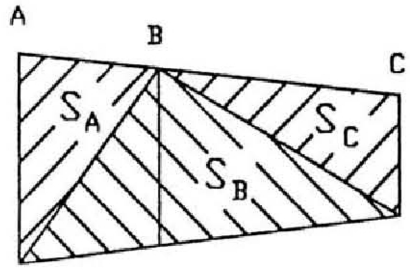

Figure 3. 24 – Influence area of the sections for finite wing.

Then is possible to calculate the coefficients.

$$K_i = \frac{2 \cdot S_i}{S} \quad \textbf{(3.3.3)}$$

The mean parameters can be obtained from the (3.3.4).

$$\bar{x} = x_1 \cdot K_1 + x_2 \cdot K_2 + ... + x_n \cdot K_n \quad \textbf{(3.3.4)}$$

So the mean thicknes of the wing is evaluated by this method, and so also the other mean parameters.

Mean geometric chord. The mean geometric chord is calculated by the ratio between the wing surface and wing span.

Mean aerodynamic chord and its position. The mean aerodynamic chord and its position on the semi-wing are estimated by the classical definitions.

$$MAC = \frac{2}{S} \cdot \int_0^{\frac{b}{2}} c^2(y) \cdot dy$$

$$x_{MAC} = \frac{2}{S} \cdot \int_0^{\frac{b}{2}} x_{l.e.}(y) \cdot c(y) \cdot dy \quad \textbf{(3.3. 5)}$$

$$y_{MAC} = \frac{2}{S} \cdot \int_0^{\frac{b}{2}} y \cdot c(y) \cdot dy$$

Equivalent Wing. From the real wing is possible to define an equivalent straight–tapered wing, that have the same surface, same span and same external chord, but different root chord and sweep angle. It’s possible to define the following relationship.

$$\begin{cases} c_{root\ \mathrm{equiv}} = \dfrac{\dfrac{S_{net}}{0.5\cdot b\cdot(1-\eta_{root})} - 2\cdot c_{tip}}{0.5\cdot b\cdot(1-\eta_{root})}\cdot 0.5\cdot b\cdot\eta_{root} + \dfrac{S_{net}}{0.5\cdot b\cdot(1-\eta_{root})} - c_{tip} \\ S_{net} = \sum_{i=1}^{n-1}\left[0.5\cdot b\cdot(\eta_{i+1}-\eta_i)\cdot(c_{i+1}-c_i)\right] \\ \Lambda_{LE\ \mathrm{equiv}} = atn\left[\dfrac{b(x_{l.e.\,\mathrm{tip}} - x_{l.e.\,\mathrm{root}})(1-\eta_{root}) - 0.5b\sum_{i=1}^{n-1}(x_{l.e.\,\mathrm{i}} + x_{l.e.\,\mathrm{i+1}} - 2\cdot x_{l.e.\,\mathrm{root}})(\eta_{i+1}-\eta_i)}{0.5\cdot b\cdot(1-\eta_{root})^2}\right] \end{cases} \quad \textbf{(3.3.6)}$$

Also for the equivalent wing can be calculated the mean geometric chord and the mean aerodynamic chord.

The last linear value of lift coefficient C_L^*. It's calculated with the same method of mean thickness.

Zero lift angle. The $\alpha_{Z.L.}$ of the finite wing is calculated through the use of figure 3.25 and from the knowledge of the zero lift angles and the geometric twist of the airfoils. So the angle between the asymptotic flow and the root chord so to have the zero lift on the airfoil in position η is given by (3.3.7).

$\alpha_{Cl=0}(\eta) = \alpha_{z.l.}(\eta) - \varepsilon(\eta)$ **(3.3.7)**

The aerodynamc twist of the section η can be defined as the relative pitch between the zero lift direction of the airfoil and the root airfoil.

$\varepsilon_a(\eta) = \alpha_{Cl=0}(\eta_{root}) - \alpha_{Cl=0}(\eta)$ **(3.3.8)**

Imposing the equality below.

$$2\cdot\int_0^1 \varepsilon_a(\eta)\cdot c(\eta)\cdot C_{l\alpha}(\eta)\cdot d\eta = \varepsilon_{a.e.}\cdot c(\eta_{tip})\cdot \overline{C}_{l\alpha}\cdot\frac{b}{2}, \quad \textbf{(3.3.9)}$$

The following formula is obtained.

$$\varepsilon_{a.e.} = \frac{2\cdot\int_0^1 \varepsilon_a(\eta)\cdot c(\eta)\cdot C_{l\alpha}(\eta)\cdot d\eta}{c(\eta_{tip})\cdot\overline{C}_{l\alpha}\cdot\dfrac{b}{2}}. \quad \textbf{(3.3.10)}$$

At the end estimating the j factor from the figure 3.25 as a function of taper ratio and aspect ratio of the equivalent wing, it's possible to obtain the zero lift angle.

$\alpha_{Z.L.} = \alpha_{Cl=0}(\eta_{root}) + j \cdot \varepsilon_{a.e.}$ **(3.3. 11)**

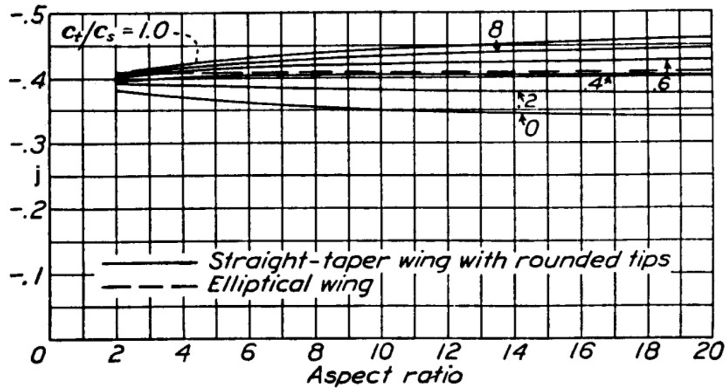

Figure 3. 25 – Diagram for the evaluation of factor j.

Maximum wing lift coefficient. The $C_{L\max\ w}$ is calculated from the knowledge of equivalent wing sweep angle and mean value of $\Delta y/c$ and $C_{l\max}$ of the airfoils, through the diagram in figure 3.26. this figure is valid strictly for high value of taper ratio without twist and for Mach number lower than 0.2.

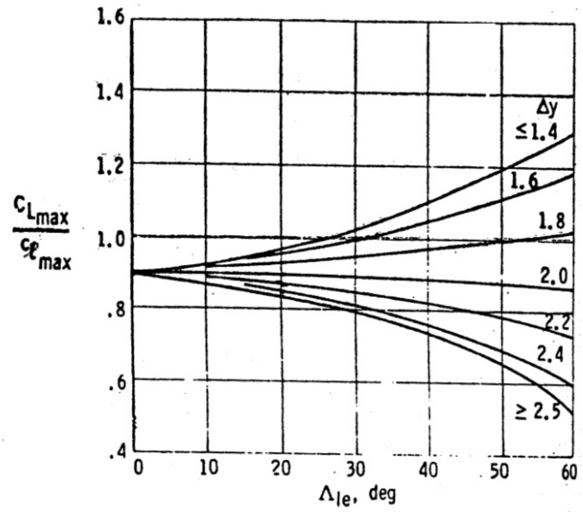

Figure 3. 26– Diagram useful for the calculation of $C_{L\max\ w}$ **.**

Lift coefficient curve slope. The $C_{L\alpha}$ of the finite wing can be evaluated by any of the following formulas, with some assumption.

Abbott: straight wing, high AR , incompressible:

$$C_{L\alpha} = f_a \cdot \frac{\overline{C}_{l\alpha} \cdot \frac{b}{p}}{1 + \left[\frac{57.3 \cdot \overline{C}_{l\alpha}}{\pi \cdot AR \cdot \frac{p}{b}} \right]} \quad \textbf{(3.3. 12)}$$

Roskam: swept wing, compressible and subsonic:

$$C_{L\alpha} = \frac{2 \cdot \pi \cdot AR}{2 + \sqrt{\frac{4 \cdot \pi^2 \cdot AR^2 \cdot \left(1 - M^2\right)^2}{\overline{C}_{l\alpha}^2 \cdot \left(1 - M^2\right)^2} \cdot \left(1 + \frac{\tan^2 \Lambda_{\frac{c}{2}}}{\left(1 - M^2\right)^2}\right) + 4}} \quad \textbf{(3.3. 13)}$$

Anderson:straight wing, high AR , incompressible:

$$C_{L\alpha} = \frac{1}{57.3} \cdot \frac{\overline{C}_{l\alpha}}{1 + \frac{\overline{C}_{l\alpha}}{0.95 \cdot \pi \cdot AR}} \quad \textbf{(3.3. 14)}$$

Anderson: straight wing, high AR , compressible and subsonic:

$$C_{L\alpha} = \frac{1}{57.3} \cdot \frac{\overline{C}_{l\alpha}}{\sqrt{1 - M^2} + \frac{\overline{C}_{l\alpha}}{0.95 \cdot \pi \cdot AR}} \quad \textbf{(3.3. 15)}$$

Anderson: straight wing, high AR , compressible and supersonic:

$$C_{L\alpha} = \frac{1}{57.3} \cdot \frac{4}{\sqrt{M^2 - 1}} \quad \textbf{(3.3. 16)}$$

Anderson: straight wing, low AR , incompressible:

$$C_{L\alpha} = \frac{1}{57.3} \cdot \frac{\overline{C}_{l\alpha}}{\sqrt{1 + \left[\frac{\overline{C}_{l\alpha}}{\pi \cdot AR}\right]^2} + \frac{\overline{C}_{l\alpha}}{\pi \cdot AR}} \quad \textbf{(3.3. 17)}$$

Anderson: straight wing, low AR, compressible and subsonic:

$$C_{L\alpha} = \frac{1}{57.3} \cdot \frac{\overline{C}_{l\alpha}}{\sqrt{1 - M^2 + \left[\frac{\overline{C}_{l\alpha}}{\pi \cdot AR}\right]^2} + \frac{\overline{C}_{l\alpha}}{\pi \cdot AR}} \quad \textbf{(3.3. 18)}$$

Anderson: straight wing, low AR, compressible and supersonic:

$$C_{L\alpha} = \frac{1}{57.3} \cdot \frac{4}{\sqrt{M^2 - 1}} \cdot \left(1 - \frac{1}{2 \cdot AR \cdot \sqrt{M^2 - 1}}\right) \quad \textbf{(3.3. 19)}$$

Anderson: swept wing, incompressible:

$$C_{L\alpha} = \frac{1}{57.3} \cdot \frac{\overline{C}_{l\alpha} \cdot \cos\Lambda_{\frac{c}{2}}}{\sqrt{1 + \left[\frac{\overline{C}_{l\alpha} \cdot \cos\Lambda_{\frac{c}{2}}}{\pi \cdot AR}\right]^2} + \frac{\overline{C}_{l\alpha} \cdot \cos\Lambda_{\frac{c}{2}}}{\pi \cdot AR}} \quad \textbf{(3.3. 20)}$$

Anderson: swept wing, compressible and subsonic:

$$C_{L\alpha} = \frac{1}{57.3} \cdot \frac{\overline{C}_{l\alpha} \cdot \cos\Lambda_{\frac{c}{2}}}{\sqrt{1 - M^2 \cdot \cos^2\Lambda_{\frac{c}{2}} + \left[\frac{\overline{C}_{l\alpha} \cdot \cos\Lambda_{\frac{c}{2}}}{\pi \cdot AR}\right]^2} + \frac{\overline{C}_{l\alpha} \cdot \cos\Lambda_{\frac{c}{2}}}{\pi \cdot AR}} \quad \textbf{(3.3. 21)}$$

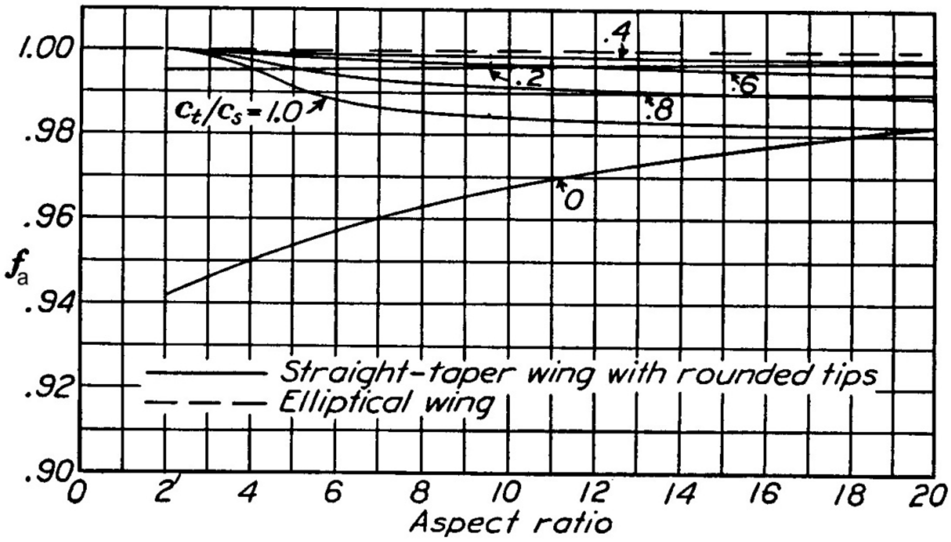

Figure 3. 27 – Diagram useful for the evaluation of *fa*.

Angle of attack of the maximum lift coefficent. To calculate $\alpha_{CL\max\ W}$ it's used the followin procedure: first it's evaluated the angle of attack at maximum lift coefficent through the linear trend of the lift line, then it's added to this angle the increment evaluated by the diagram in figure 3.28,this is valid strictly for wing with high taper ratio without twist, with unique airfoil type and Mach number included between 0.2 and 0.6.

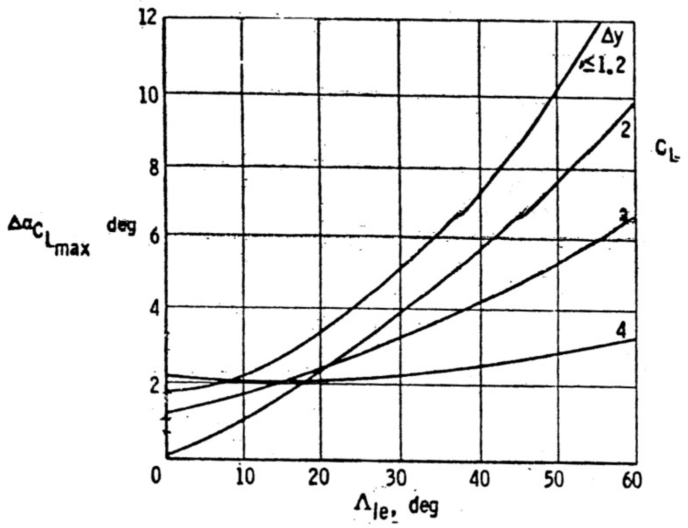

Figure 3. 28 – diagram useful for evaluation of $\alpha_{CL\max\ W}$.

Angle of attack of C_L^*. The angle α_W^* is calculated dividing the value of C_L^* for $C_{L\alpha}$.

Wing lift curve. The function $C_L = f(\alpha)$ is obtained from the union of two curve. The straight lift line from $\alpha_{Z.L.}$ to α_W^* and a third degree polynomial that is obtained imposing the passage through the point (α_W^*, C_L^*) and $(\alpha_{CL\max W}, C_{L\max W})$ with the conditions $\frac{dC_L}{d\alpha}(\alpha_W^*) = C_{L\alpha}$ and $\frac{dC_L}{d\alpha}(\alpha_{CL\max W}) = 0$.

The effect of the presence of the fuselage can be evaluated by the figure 3.29 knowing the value of the ratio between fuselage and wing span.

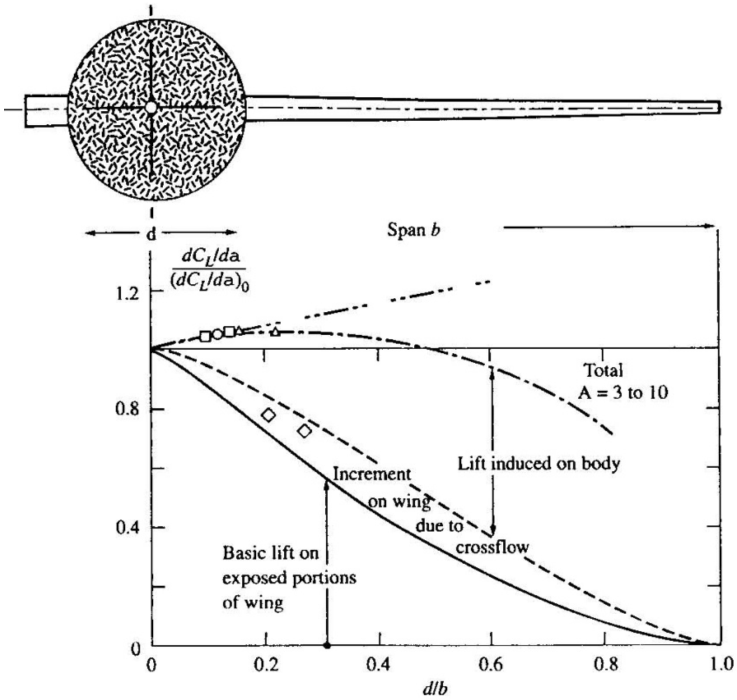

Figura 3.29 – Diagram useful for the determination to the correction factor due to fuselage interference.

Induced drag curve. The function $C_{Di} = f(\alpha)$ is evaluated through the follow formula.

$$C_{Di} = \frac{C_L^2}{\pi \cdot AR \cdot u} + v \cdot C_L \cdot \varepsilon_{a.e.} \cdot \overline{C}_{l\alpha} + \left(\varepsilon_{a.e.} \cdot \overline{C}_{l\alpha}\right)^2 \cdot w \quad \textbf{(3.3.22)}$$

Also here the effect of the presence of the fuselage can be evaluated by the figure 3.30 knowing the value of the ratio between fuselage and wing span, and founding the value of correction factor *s*.

$$C_{Di} = \frac{C_L^2}{\pi \cdot AR \cdot u \cdot s} + v \cdot C_L \cdot \varepsilon_{a.e.} \cdot \overline{C}_{l\alpha} + \left(\varepsilon_{a.e.} \cdot \overline{C}_{l\alpha}\right)^2 \cdot w \quad \textbf{(3.3. 23)}$$

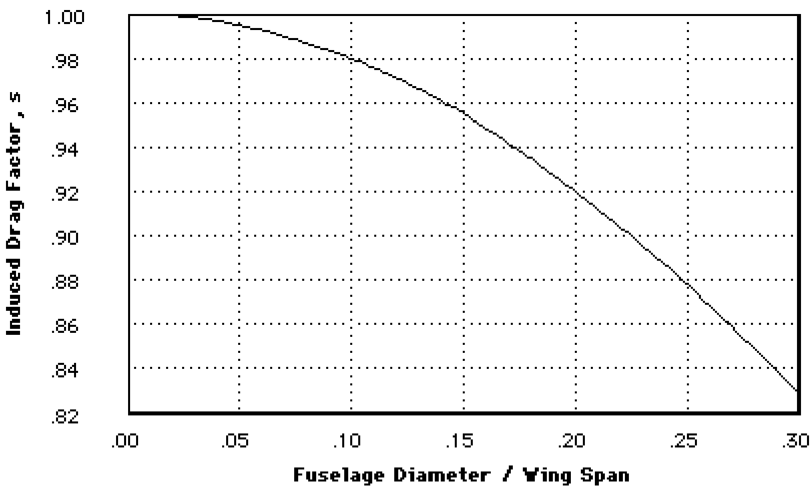

Figure3.30 – s factor.

The value of the factors *u*, *v* and *w*can be founded from the figures in 3.31.

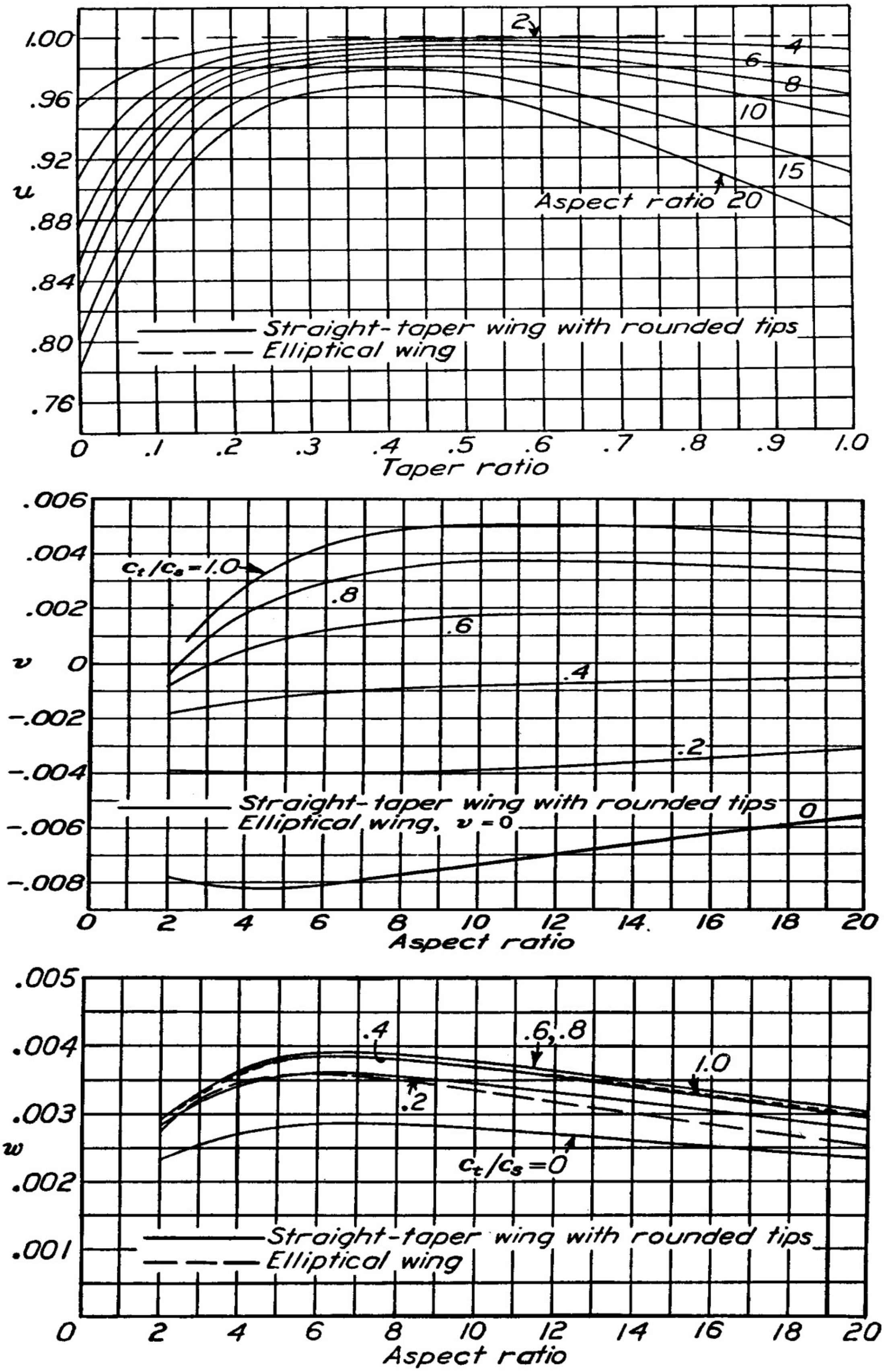

Figure 3. 31 –Diagram useful for the evaluation of u,v and w.

Wing Drag. From the drag polar $C_l = f(C_d)$ of all the airfoils with a trend of drag coefficient as follow.

$$C_d = C_{d\,\min} + k \cdot \left(C_l - C_{l\ id} \right)^2 \textbf{ (3.3.24)}$$

Where the required value are briefly resumed in the figure 3.32.

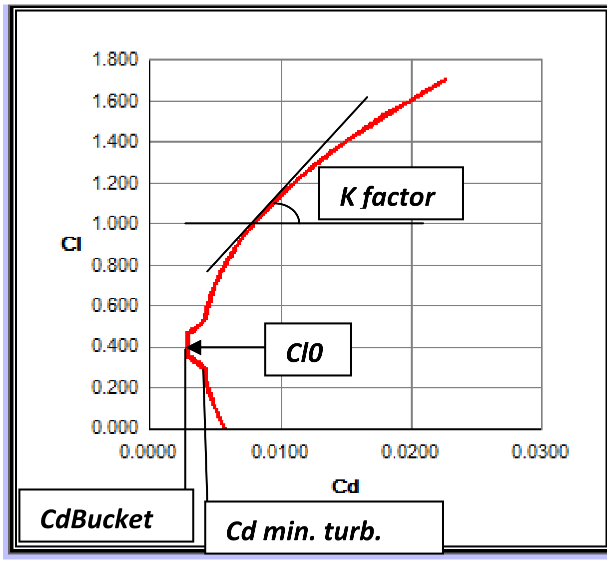

Figure 3. 32 – example of airfoil drag polar.

The drag polar of the mean airfoil can be evaluated with the methodology, described before, of *k* coefficients.

$$\overline{C}_d(C_l) = C_{d1} \cdot K_1 + C_{d2} \cdot K_2 + \ldots + C_{dn} \cdot K_n \textbf{ (3.3.25)}$$

The contribution of the wing for a value of lift coefficient C_L, can be evaluated from the drag polar of the mean airfoil, assuming that the bi-dimensional lift coefficientacross thespan is equal to C_L of the wing.This is so a very approximated method but good for a preliminary semi empirical analysis.

3.4 - FUSELAGE

3.4.1 - Introduction

The fuselage have the function to accommodate the cockpit, payload and if it's needed the engine. It must link the wing with the stabilization and control system of the tail. The first approach to the fuselage design is what allow to obtain the shape and external dimension of the body of the fuselage, starting from the definition of the internal spaces of its (*internal layout*).
Shape and dimensions of the fuselage vary according to the aircraft category . the most used cross section in the civil airplanes are the follows.

- Rectangularsection
- Ovalized section
- Circular
- Circular lobes section

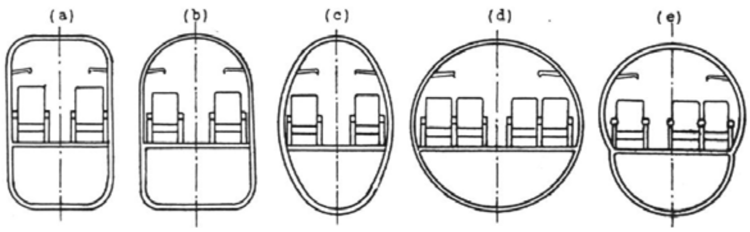

Figura 3.33 – Fuselage sections.

From lateral view the shape of the fuselage can be the following:

- Streamline shape, for high speed aircraft
- Streamline shape with curvilinear axis
- Circularlobes
- "Caribou" shape
- High penetration shape and long cilindric section, the most used.

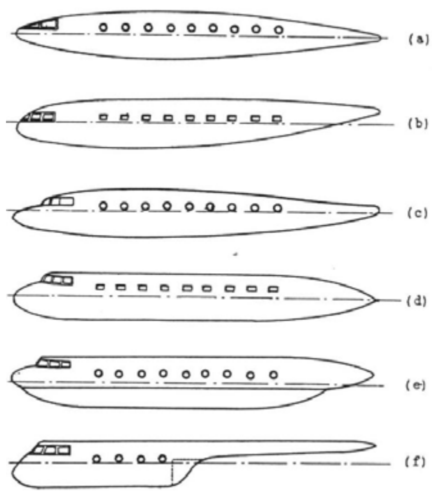

Figura 3.34 – Some Fuselageshape.

3.4.2 - Basic PassengerCabin layout

It's good often to start the fuselage design from the characteristics of the cross section. This must have a circular shape, and the choice have two reasons.

- To Reduce the possibility of separation at small angle of attack or sideslip.
- To assure the correct behavior of the structure for the internal pressure loads.

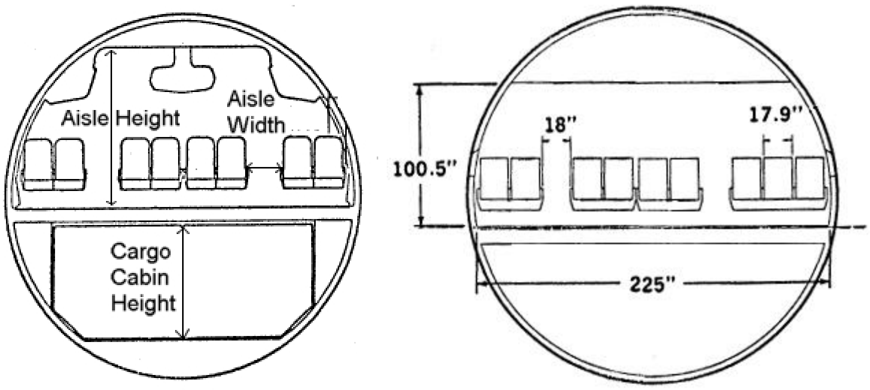

Figure 3.34 – Typical dimensions for the fuselage cross section for transport aircraft.

To choose what geometry to use, it's required the payload. The disposition of the passengers or of the cargo affects directly on the fuselage diameter. For the passenger is useful see the FAR about this argument, that give the limit measures for the best accommodation of the passengers.

Typical passenger compartment data			
	First Class	Economy	High density/small aircraft
Aisle width (cm)	51-71	46-51	>30
Aisle Height (cm)	>193	>193	>152

Class	Seat width (mm)	Seat width (in)
Charter	400–420	16–17
Economy	475–525	19–21
Business	575–625	23–25
First	625–700	25–28

(For reference a public service bus seat is approximately 425 mm [17 in] wide.)

Figure 3.35 – Typical passenger compartment data.

3.4.3 - Fuselage layout

The fuselage is divided in three principal part:

- **Nose** – initial part of the fuselage including the nose cone and cockpit
- **Cabin** – The passenger cabin is the central part and it's almost a constant section
- **Tailcone**– the ending part of the fuselage, usually have an angle that allow to takeoff without touch the ground, the so called "*Upsweep*".

The fundamental parameters for a correct fuselage design are the maximum equivalent diameter and the fuselage length.

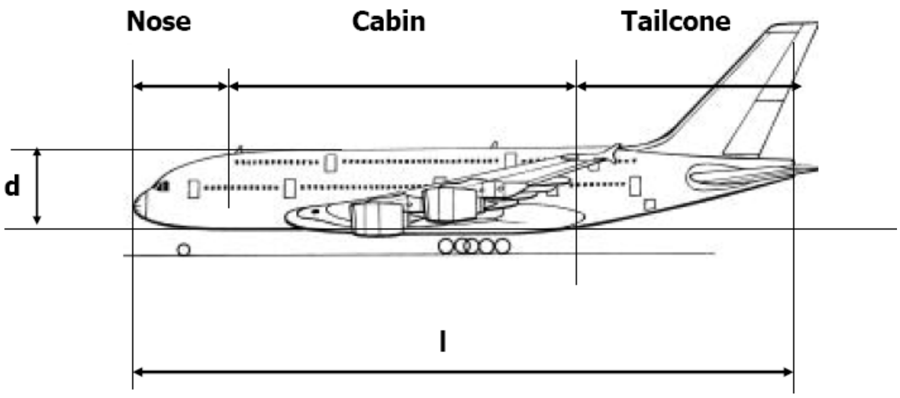

Figure 3.36 – Fuselage principal part.

This part can be approximated so with two method. The first is to use two polynomials for the nose and the tailcone that have as principal condition to cross through three selected point (A,B,C in the figure 3.37) and two null derivatives where the nose and tailcone meet the cabin (in B,C).

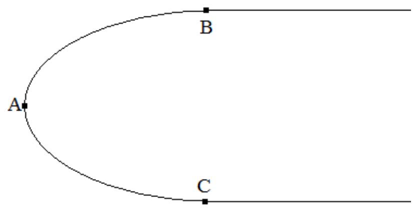

Figure 3.36 – Sketch of a nose described by three points A,B,C.

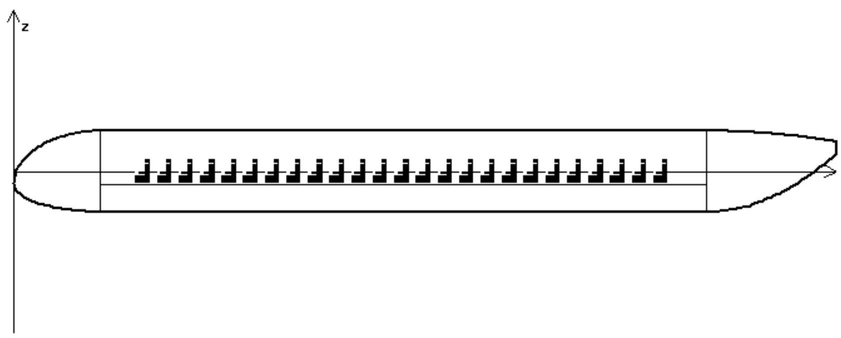

Figure 3.37 – Example of fuselage layout with three part method.

The second method that ignore the internal layout, is also called "*coniclofting*", this method allow to modeling the fuselage more precisely respect the first method, and allow to better follow the flow, if possible. The lofting methods consist to define the mathematical function that allow to model the cross sections with continuous curve. The used functions are the classic equations of the conic that are very simple and assure a variability of the cross sections shape.
The conic are described by the equation (3.4.1):

$$Ax^2 + Bxy + Cy^2 + Dx + Ey + F = 0 \quad \textbf{(3.4.1)}$$

They are generated by the intersection of the right cone with circular section with a plan, its relative position gives the following conic:

- Perpendicular plan respect the cone symmetry axis → CIRCLE
- Inclined plan respect the cone symmetry axis → ELLIPSE
- Parallel plan respect the generating line→ PARABOLA
- Parallel plan respect the rotation axis → HYPERBOLA

Below an example of the cutting.

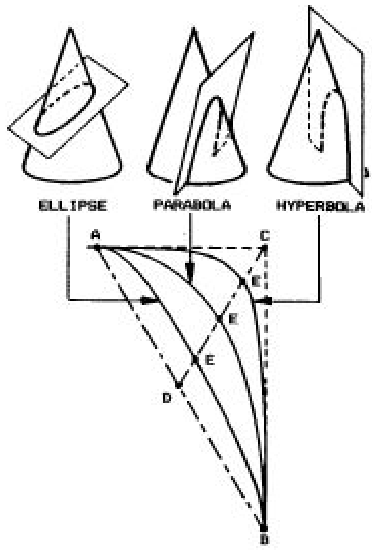

Figure 3.38 –conic types .

To build the generic conic, knowing the starting and ending point, called A and B in figure 3.39, and the angle of tangency.

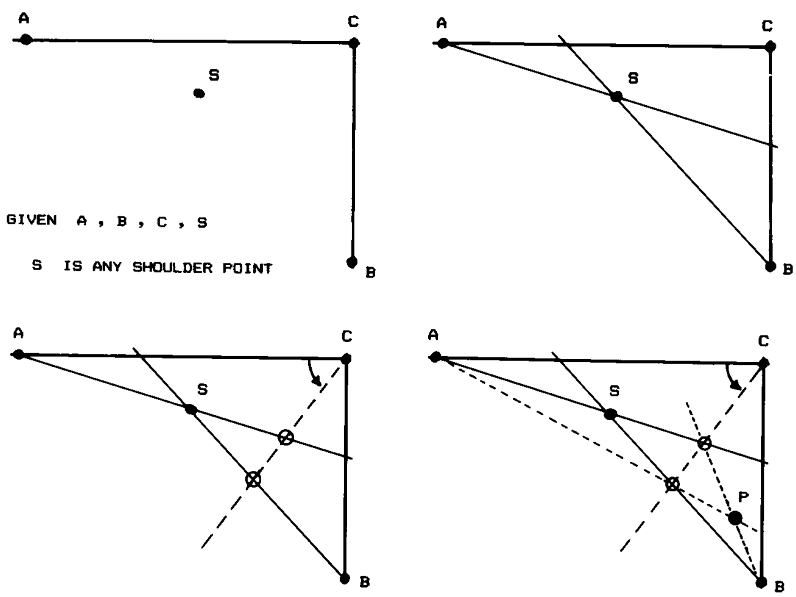

Figure 3.39 –Conic layout .

In the figure 3.39 is shown the intersection between the tangents in A and B, called C, and with S is called the generic shoulder point that give the conical shape.
To have this points it's possible to proceed like this: it's drawn a semi right that have the origin in C, inclined of an arbitrary angle respect the segment AC, it will identify two intersection with segments AS and BS. The intersection of the two semi right having origin in A and B and crossing through the above defined points identify point P, belonging to the conic.
The variation of the inclination angle of the semi right that have the origin in C will increase the number of points.

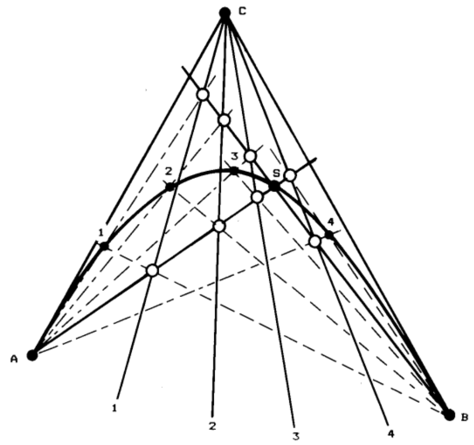

Figure 3.40 –Conic layout example.

With an enough number of points it's possible have the desired conic.
This method can be used for the fuselage layout merging the points A,B,C and S of all the cross sections with a continuous longitudinal curve also called "longitudinal control lines".

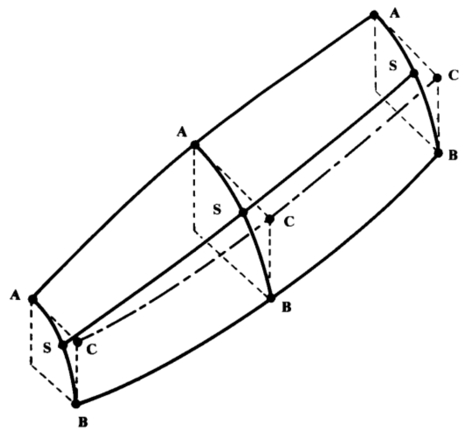

Figure 3.41 –Longitudinal control lines.

So It's possible have a number of control cross sections where is possible to vary the layout as required, moving the point S as desired.

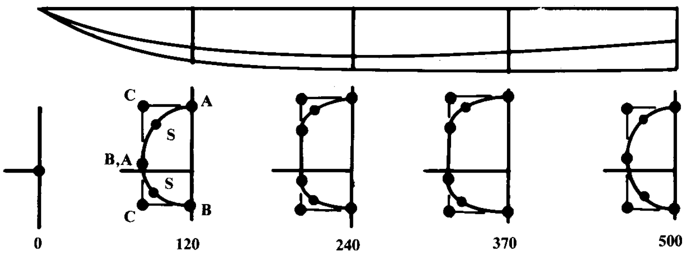

Figure 3.42 –Example of fuselage lofting.

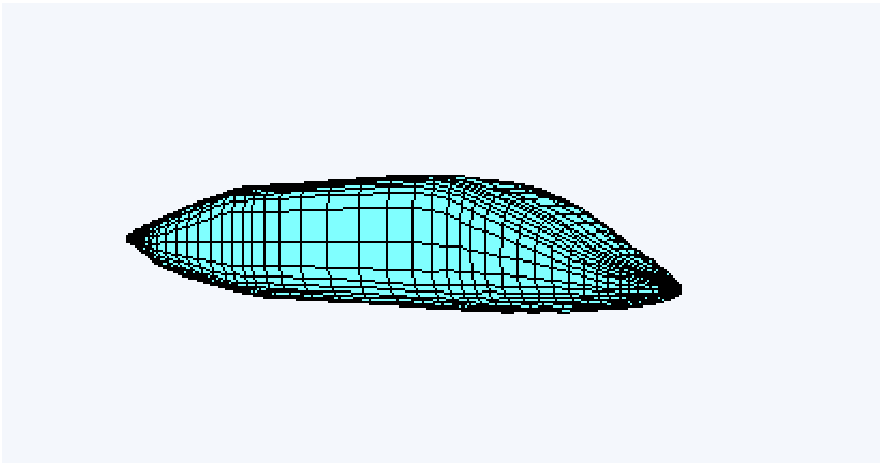

Figure 3.43 –Example of fuselage layout with method of conic lofting.

3.4.4 - Fuselage Analysis – Moment Coefficient

The fuselage analysis is important to know the contribution of the fuselage on the aerodynamic drag and moment, for the second one this is possible through the strip method or so called "Munk Method" in the form developed by Multhopp.
The moment coefficient of the fuselage, for what, since it is a pure couple, is not necessary specify the pole, assuming the linearity, is represented by the following equation in function of the angle of attack.

$$C_m^{fus} = C_{m0}^{fus} + C_{m\alpha}^{fus} \cdot \alpha_{body} \qquad (3.4.2)$$

Each term in the equation (3.4.2) can be calculated by the Multhopp method, the two coefficients "$\boldsymbol{C_{m0}}$" and "$\boldsymbol{C_{m\alpha}}$" can be obtained from the following equations.

$$C_{m0}^{fus} = \frac{K_2 - K_1}{36.5 \cdot S \cdot MAC} \cdot \int_o^{l_F} W_F^2 \cdot \left(\alpha_{0L}^{w} + i_{cl}^{Fus}\right) \cdot dx$$

$$C_{m\alpha}^{fus} = \frac{1}{36.5 \cdot S \cdot MAC} \cdot \left\{ \int_0^{l_{F1}} W_F^2 \cdot \left[\left(\frac{\partial \varepsilon_u}{\partial \alpha} \right)_1 + 1 \right] \cdot dx_1 + \int_0^{l_{F2}} W_F^2 \cdot \left[\left(\frac{\partial \varepsilon_u}{\partial \alpha} \right)_2 + 1 \right] \cdot dx_2 \right\} \qquad (3.4.3)$$

Instead of the integrals it's possible to substitute them with summations.

$$C_{m\alpha}^{fus} = \frac{1}{36.5 \cdot S \cdot CMA} \cdot \left\{ \sum_{j=1}^{n1} W_{Fj}^2 \cdot \left[\left(\frac{\partial \varepsilon_u}{\partial \alpha} \right)_1 + 1 \right] \cdot \Delta x_1 + \sum_{j=1}^{n2} W_{Fj}^2 \cdot \left[\left(\frac{\partial \varepsilon_u}{\partial \alpha} \right)_2 + 1 \right] \cdot \Delta x_2 \right\} \quad \textbf{(3.4.4)}$$

$$C_{m0}^{fus} = \frac{K_2 - K_1}{36.5 \cdot S \cdot CMA} \cdot \sum_{j=1}^{n} W_{Fj}^2 \cdot \left(\alpha_{0L}^{w} + i_{cl}^{Fus} \right) \cdot \Delta x \quad \textbf{(3.4.5)}$$

For "C_{m0}" the fuselage must be divided for all its length, in equal parts, regardless of the wing position.

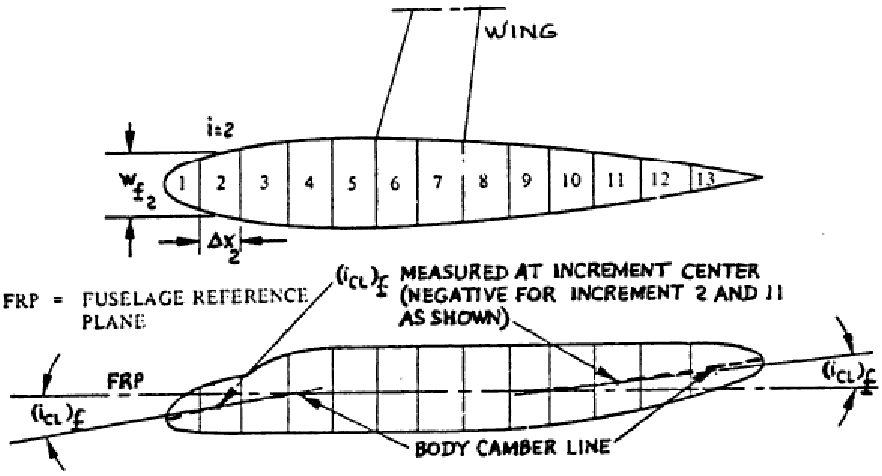

Figure 3.44 –Fuselage strips for the determination of Cm_0.

For "$C_{m\alpha}$" instead is necessary consider of the position of the wing, in particular for the strips before the wing, it's used the subscript "1" in the first summation, while for the strips after the wing, it's used the subscript "2" in the summation.

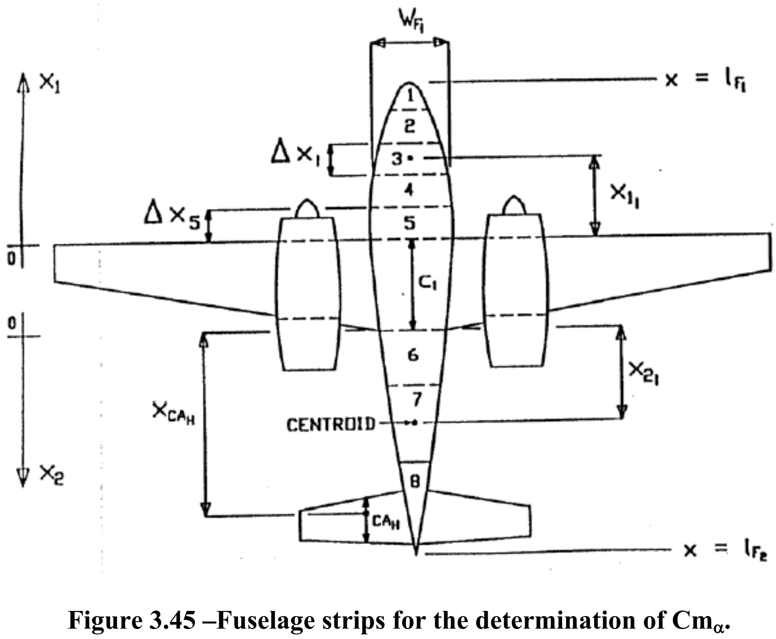

Figure 3.45 –Fuselage strips for the determination of Cm_α.

The parameters in the equation (3.4.5) and (3.4.6) are:

- $K_2 - K_1$ – This correction factor is dependent on the value of the fineness ratio l_f/d_f and is evaluated by the following figure.

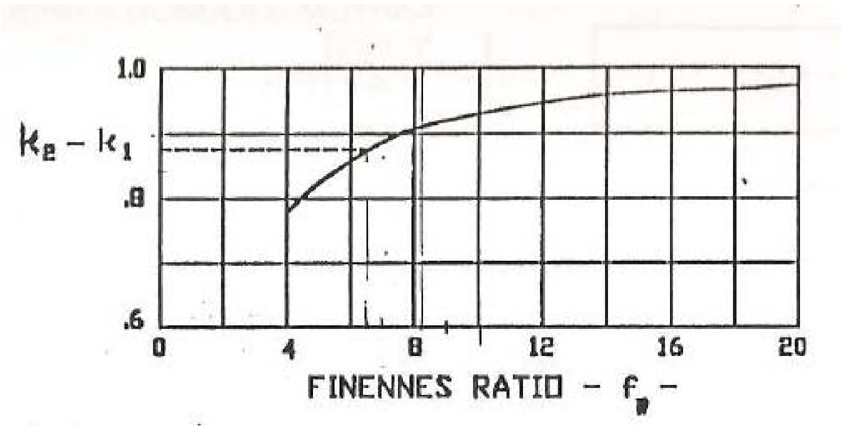

Figure 3.46 –$K_2 - K_1$ correction factor in function of fineness ratio.

- Sw – reference wing surface.
- MAC – mean aerodynamic chord.
- W_{Fj} – the j-th fuselage sectionwidth
- α_{0Lw} – the zero lift angle of the wing, referred to the construction line of the fuselage
- i_{clfus} – incidence angle of the mean line of the fuselage corresponding with the j-th section respect the construction line of the fuselage.
- Δx_j – the length of the j-th part of the fuselage.
- $\left(\frac{\partial \varepsilon_u}{\partial \alpha}\right)_1$ - upwash at the sections before the wing. It's calculated by the following formula.

$$\left(\frac{\partial \varepsilon_u}{\partial \alpha}\right)_1 = \left(\overline{\frac{\partial \varepsilon_u}{\partial \alpha}}\right) \cdot \frac{C_{L\alpha}^{w}}{0.0785} \qquad \textbf{(3.4.6)}$$

Where the $C_{L\alpha}$ is the lift coefficient of the wing and $\left(\overline{\frac{\partial \varepsilon_u}{\partial \alpha}}\right)$ is the derivative that can be evaluated by the uses of the following figures 3.46 and 3.47, where the first figure it's used for evaluate the value of the strip close to the wing, while the second it's used for the other strips in front of the wing.

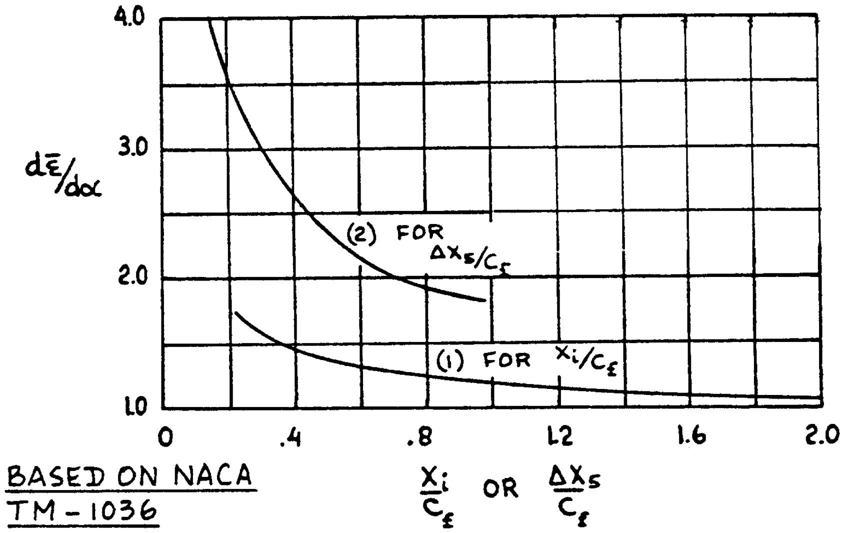

Figure 3.47 –K_2 – K_1correction factor in function of fineness ratio.

- $\left(\frac{\partial \varepsilon_u}{\partial \alpha}\right)_2$ - downwash calculated for each section rear the wing it can be calculated by the following formula:

$$\left(\frac{\partial \varepsilon_u}{\partial \alpha}\right)_2 = \left[\frac{x_2}{l_{F2}} \cdot \left(1 - \overline{\frac{\partial \varepsilon}{\partial \alpha}}\right)\right] \qquad \textbf{(3.4.7)}$$

Where the X_2 is the position in x of the section centroid and l_{F2} is the distance between the trailing edge of the root chord of the wing and the end of the fuselage.

The $\overline{\left(\frac{\partial \varepsilon_u}{\partial \alpha}\right)}$ is evaluated by the following formula:

$$\frac{\partial \varepsilon}{\partial \alpha} = 4.44\left[\left(K_A K_\lambda K_h \left(cos\Lambda_{c/4}\right)^{1/2}\right)^{1.19}\right]\frac{CL_\alpha}{CL_{\alpha\, M=0}} \qquad \textbf{(3.4.8)}$$

Where the K factors are obtained from the figures in 3.48, where l_h and h_h are the distance in x and z of the back of the fuselage.

The shift of the aerodynamic center caused by the presence of the fuselage is obtained by the formula (3.4.9).

$$x_{ac}^{wb} = x_{ac}^{w} - \frac{C_{m\alpha}^{fus}}{C_{L\alpha}^{w}} \qquad \textbf{(3.4.9)}$$

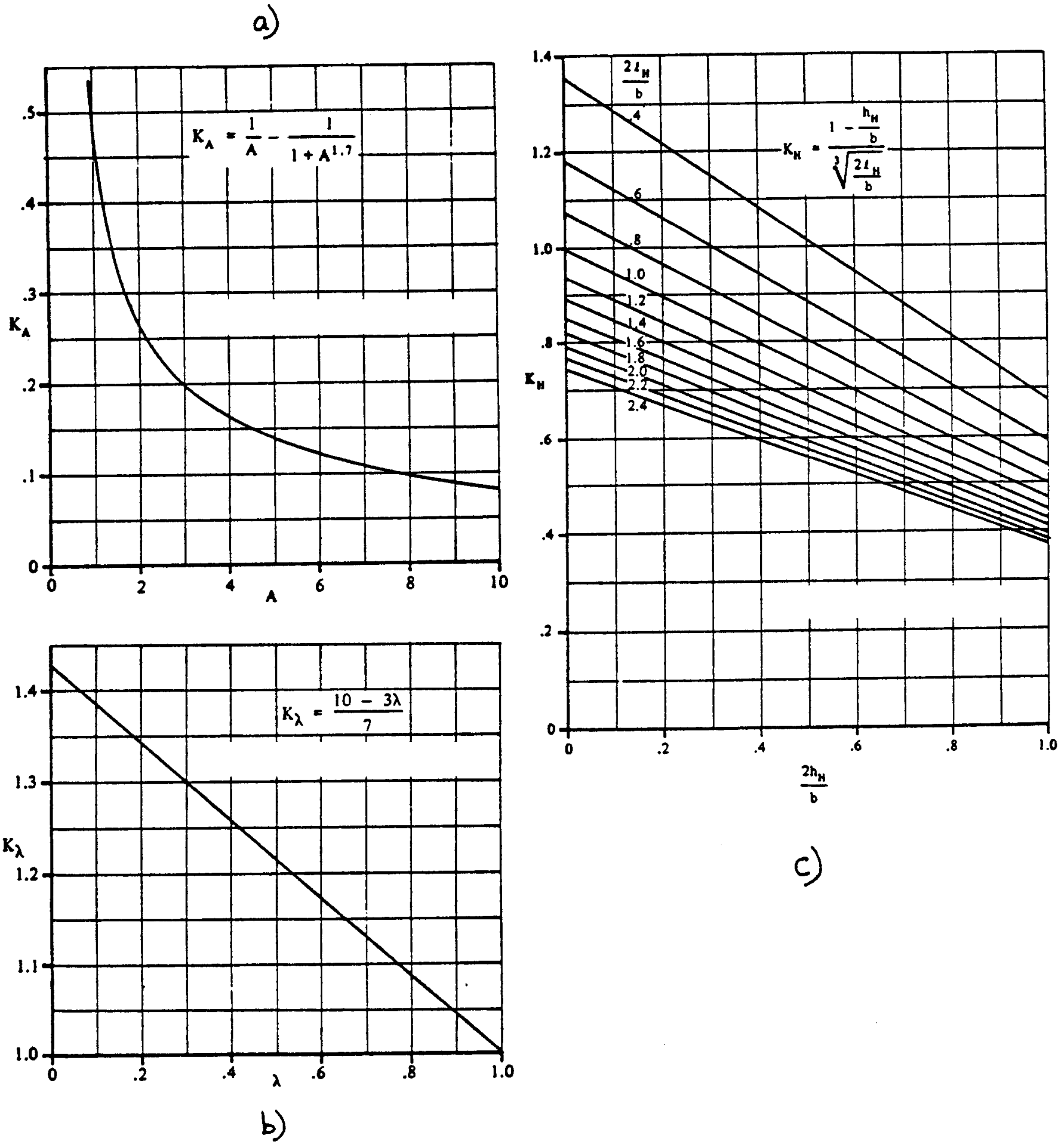

Figure 3.48 –Diagram useful for determination of the factor for the computation of downwash.

3.4.5 Fuselage Analysis – Drag coefficient

For the evaluation of the contribution on drag coefficient of the fuselage, precisely on the parasite drag,it's used the following formula valid also for any type of component of the aircraft.

$$C_{D0} = K_{ff} \cdot C_f \cdot \frac{S_{wet}}{S} \quad \textbf{(3.4.10)}$$

Where C_f is the friction coefficient of the flat plate corresponding at the fuselage,$K_{ff}$is the form factor that correct the friction coefficient for the real form of the fuselage.

S_{wet} is the surface of the component touched by the flow, S is the reference wing surface.
For the calculation of the friction coefficient C_f the first step is to calculate the Reynolds number by the classical formula.

$$Re = \frac{\rho V l_f}{\mu} \quad \textbf{(3.4.11)}$$

Then the second step is to evaluate the laminar and turbulent C_f, this is possible by the use of the moody diagram or the formula (3.4.12) and (3.4.13).

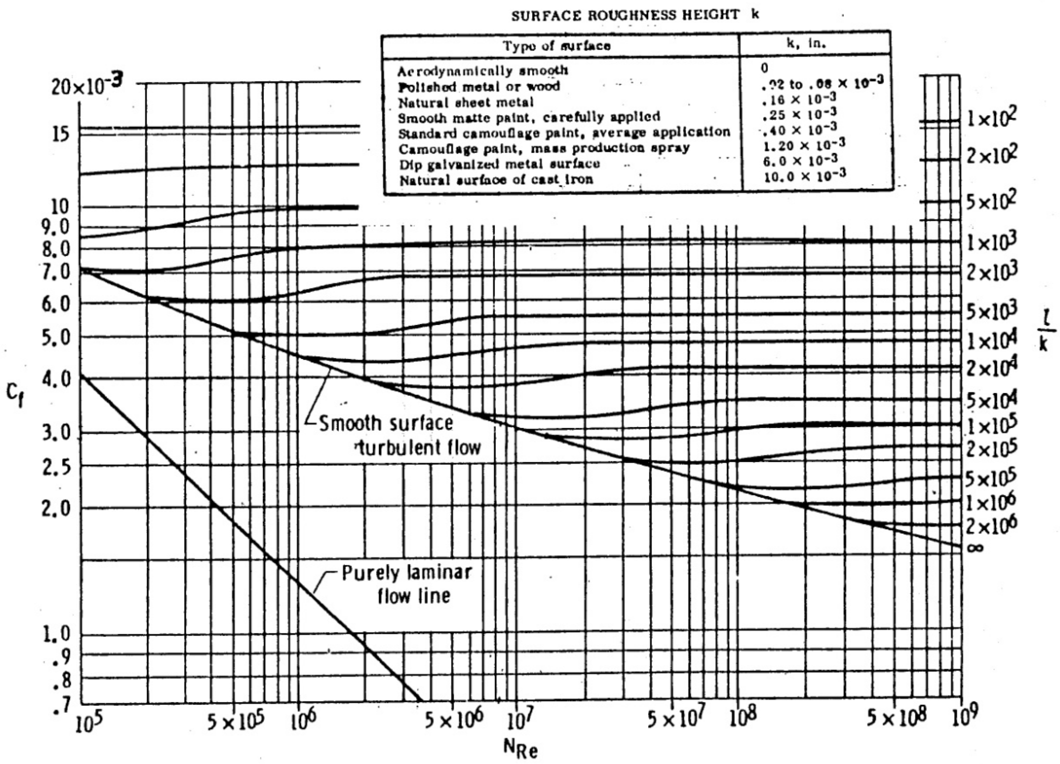

Figure 3.48 –Moody diagram.

$$C_f \text{ laminar} = \frac{1.328}{\sqrt{\text{Re}}} \quad \textbf{(3.4.12)}$$

$$C_f \text{ turbulent} = \frac{0.455}{\left(\frac{\log(\text{Re})}{\log(10)}\right)^{2.58}} \quad \textbf{(3.4.13)}$$

The value of turbulent C_f must be corrected to consider the effect of Mach number, this is possible using the following chart.

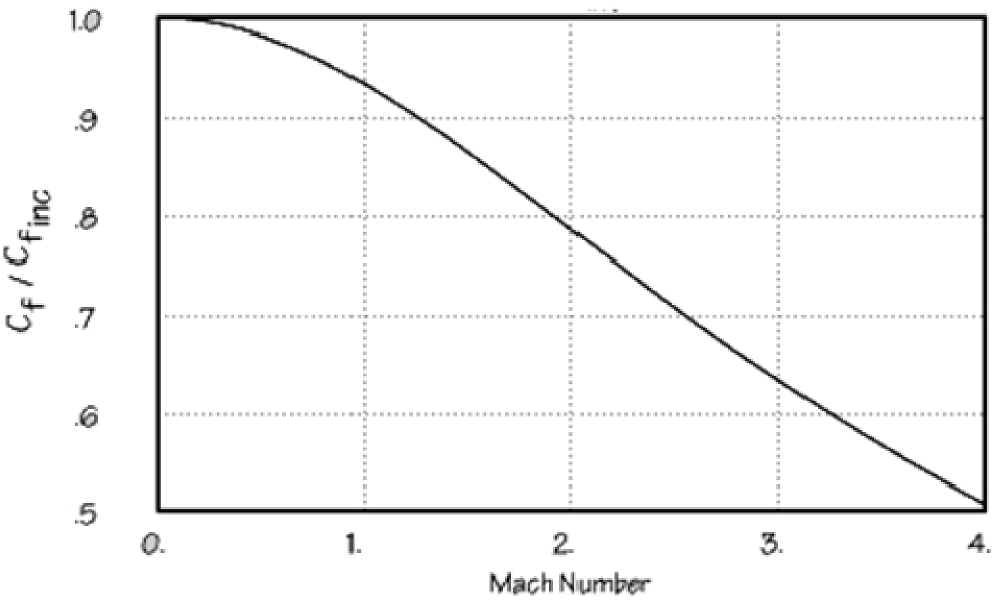

Figure 3.49 –Effect of Mach number on turbulent skin friction.

Then assuming a position in X of transition between laminar and turbulent flow, it's possible to evaluate C_f as follow.

$$C_f = C_f\ lam \cdot Xt + C_f\ turb \cdot (1 - Xt) \quad \textbf{(3.4.14)}$$

The next step is to evaluate the form factor K_{ff} from the figure 3.50, valid for a revolution surface, as a function of the fineness ratio l_f/d, or alternatively from formula (3.4.15).

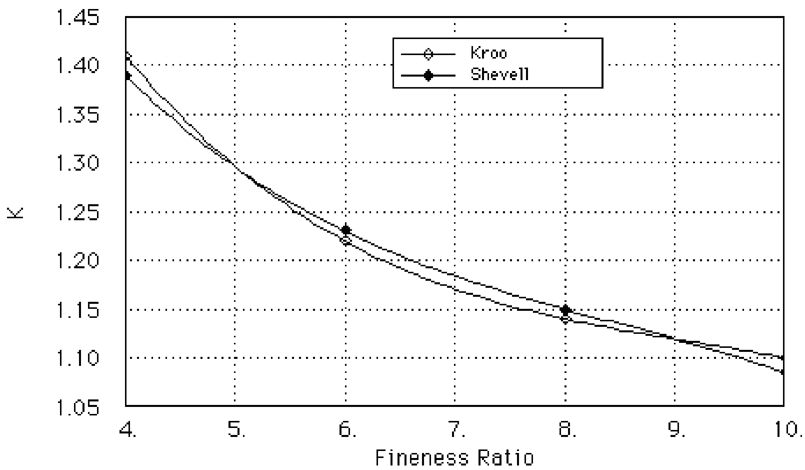

Figure 3.49 –Form Factor diagram for a revolution surface.

$$K_{ff} = 1 + \frac{60}{(l_f / d)^3} + 0.0025 \cdot l_f / d \quad \textbf{(3.4.15)}$$

The last step is to calculate the wetted area of the fuselage S_{wet}that is the sum of strip integration of the perimeter of the section in which the fuselage is divided as shown in the figure 3.50.

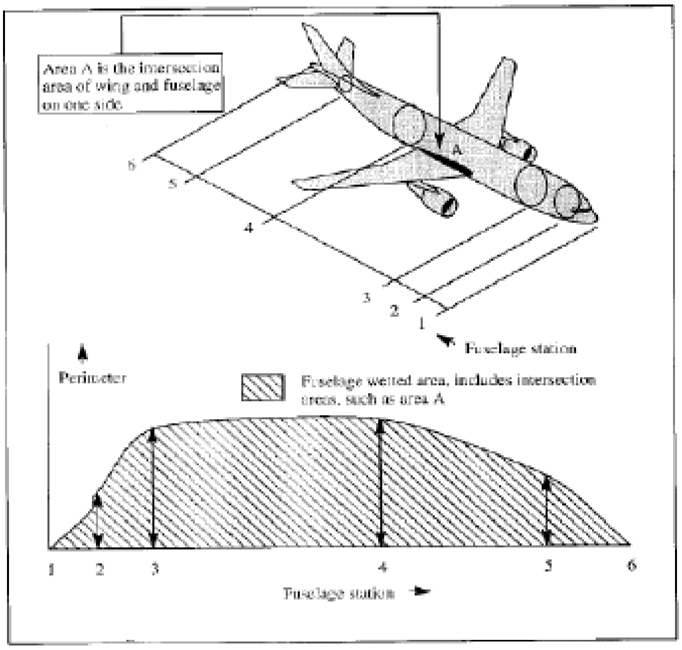

Figure 3.50 – Method of integration of the perimeter for the calculation of the wetted area.

For an approximated evaluation is possible to use the following formulas.

$$S_{wet\ \ like-body} = S_{nose} + S_{central} + S_{cone} \quad \textbf{(3.4.16)}$$

$$\begin{cases} S_{nose} = 0.75 \cdot \pi \cdot d_{nose} \cdot l_{nose} & \textbf{(3.4.17)} \\ S_{central} = \pi \cdot d_{central} \cdot l_{central} & \textbf{(3.4.18)} \\ S_{cone} = 0.72 \cdot \pi \cdot d_{cone} \cdot l_{cone} & \textbf{(3.4.19)} \end{cases}$$

Another contribution due to fuselage is the Base Drag, this can be calculated by the formula (3.4.20) and must be added to parasite drag.

$$C_{D\,base} = 0.029 \cdot \frac{S_{body}}{S} \left(\frac{d_{base}}{d_{equiv}} \right)^3 \cdot \left[C_{D0} \cdot \left(\frac{S}{S_{body}} \right) \right]^{\frac{1}{2}} \quad \textbf{(3.4.20)}$$

Also the upsweep angle generate a contribution on the drag, that will be added to parasite drag. This contribution is due to the enlargement of the boundary layer on the cone that induce an increment to the parasite drag. In the initial zone of the inclination the flow accelerate converting its pressure energy to kinetic energy, so this decrease the fuselage contribution on lift that can be recovered through an increment of inclination of the wing, which implies in return an increment of the parasite drag.

The contribution of the upsweep is calculated as follow.

$$C_{D_{upsweep}} = 0.075 \cdot \frac{S_{fuselage\ \text{costant}\ \text{sec}tion}}{S} \left(\frac{h}{l} \right)_{0.75l} \quad \textbf{(3.4.20)}$$

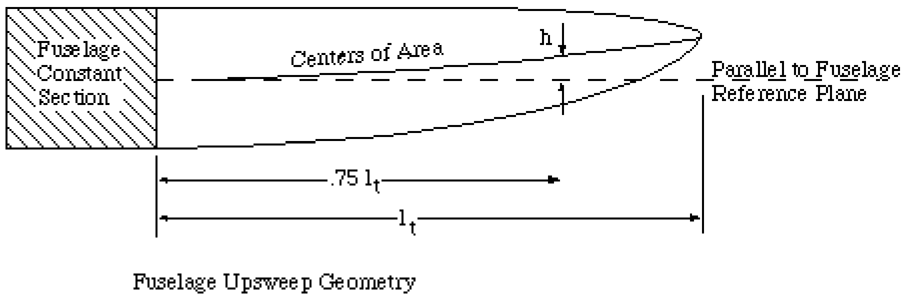

Figure 3.51 –Upsweep parameters.

3.5 - NACELLE SIZING

3.5.1 - Introduction

In the aeronautic design is very important the requirement of the engines efficiency, so to reduce the costs, consumption and noises. So is opportune a correct nacelles sizing that have a notably influence on the aerodynamic parameters of the aircraft.

3.5.2 -The statistical laws for nacelle sizing

To design properly the nacelles is a good way use statistical laws obtained by the value of weight, thrust and power of a large number of aircraft. For the jet driven aircraft the used method is taken by the procedure of Prof. Charlie Svoboda, while for the propeller driven it's used a similar method based on the same procedure type.

3.5.3 - Jet driven

Starting by the study of a number of turbofan, are the trends of the nacelle's parameters with thrust obtained. The list of turbofan have the bypass ratio "BPR" greater than 2. The dimensions of the nacelles, lengths L_n and diameters D_n, are put in a chart in function of the takeoff thrust T_{TO}, then the trendlines are obtained and so the following equations.

$$\begin{aligned} L_N[in] &= 40 + 0.59\sqrt{T_{TO}[lb]} \\ D_N[in] &= 5 + 0.39\sqrt{T_{TO}[lb]} \end{aligned} \quad \textbf{(3.5.1)}$$

Below the charts are shown.

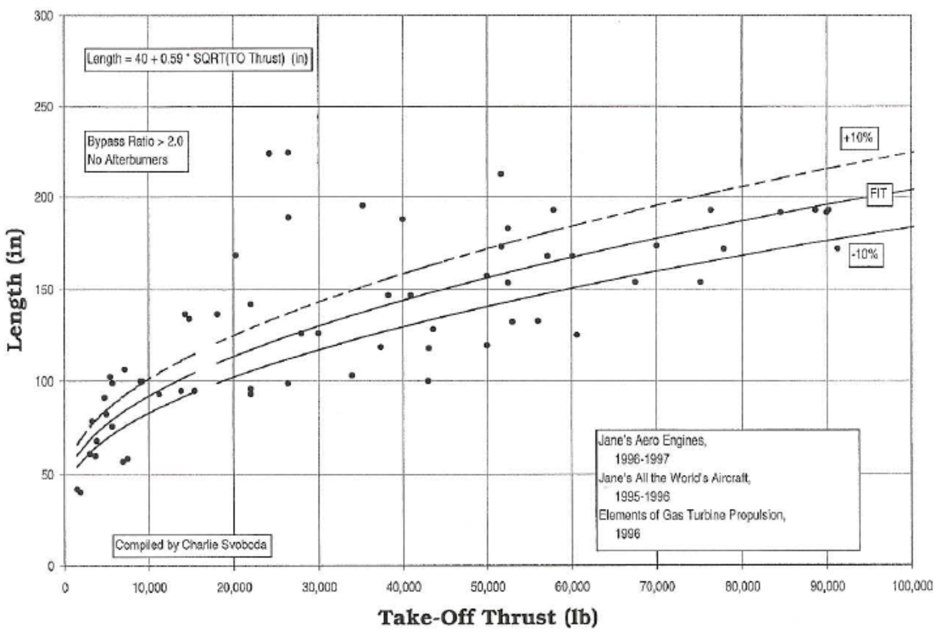

Figure 3.52 –Trends of the length with thrust.

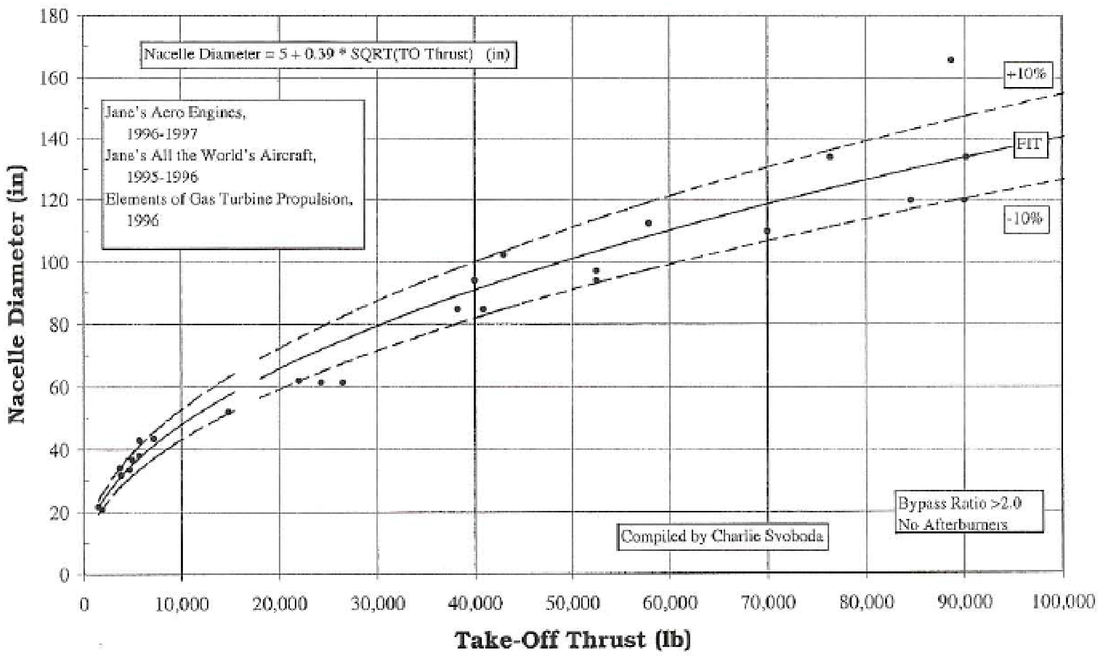

Figure 3.52 –Trends of the diameter with thrust.

3.5.4 - Propeller driven

For the propeller driven aircraft it's possible to proceed in the same way of the method described before.

Taking from a number of propeller aircraft the value of the shaft horse power "**Πa**" and the dimensions of the nacelles. So the trends of this value are obtained as shown below.

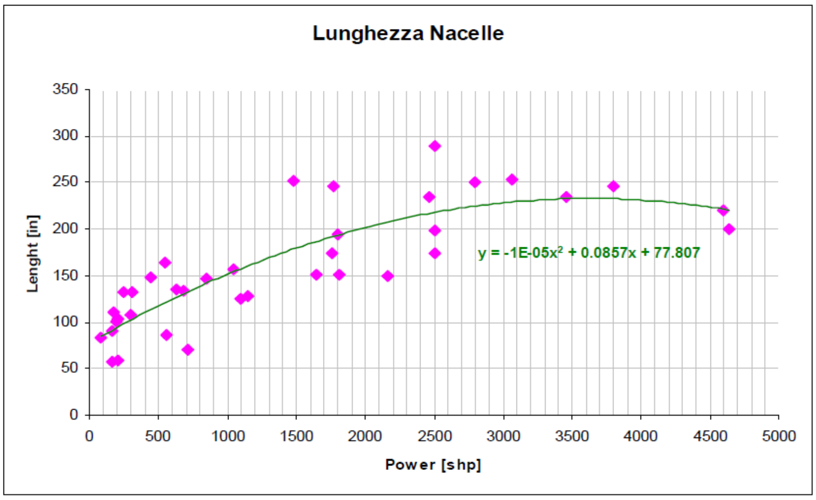

Figure 3.53 –Trends of the length with Power.

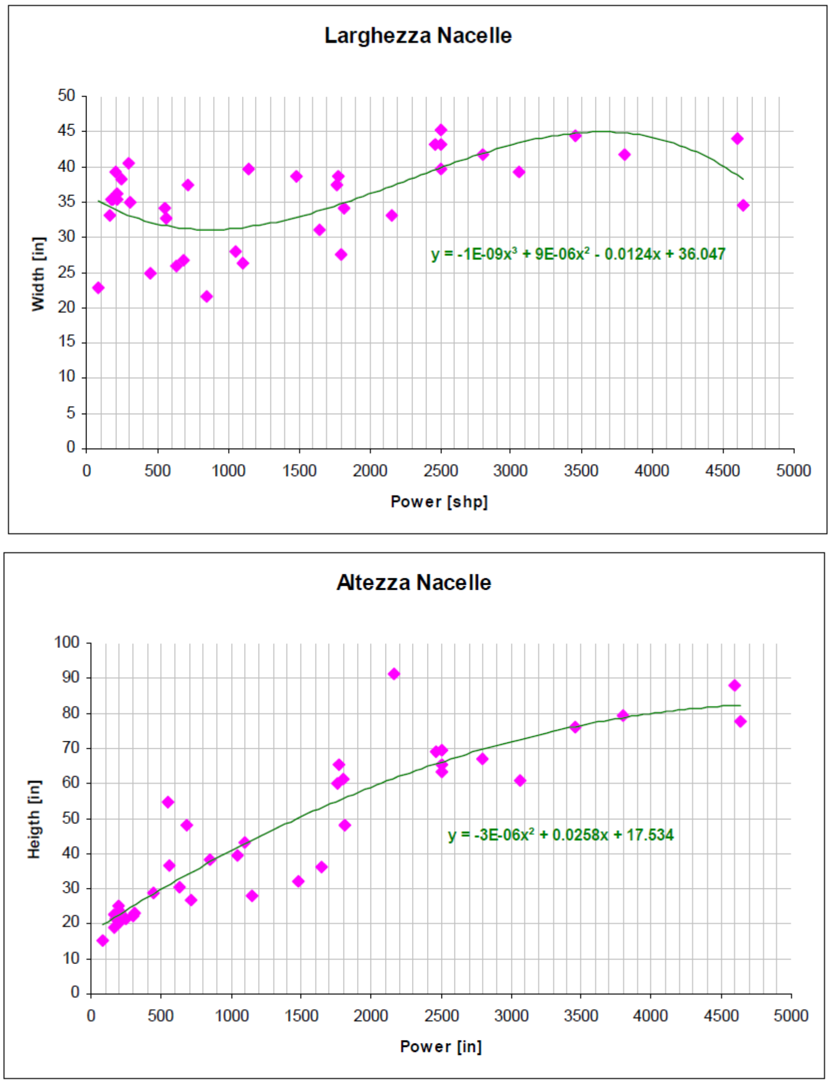

Figure 3.54 –Trends of the width and height with Power.

The trends shows as there is a strong difference between piston propeller and turbopropeller engines. This justify the use of two different trends for each one, obtaining the following curves.

- Piston Propeller

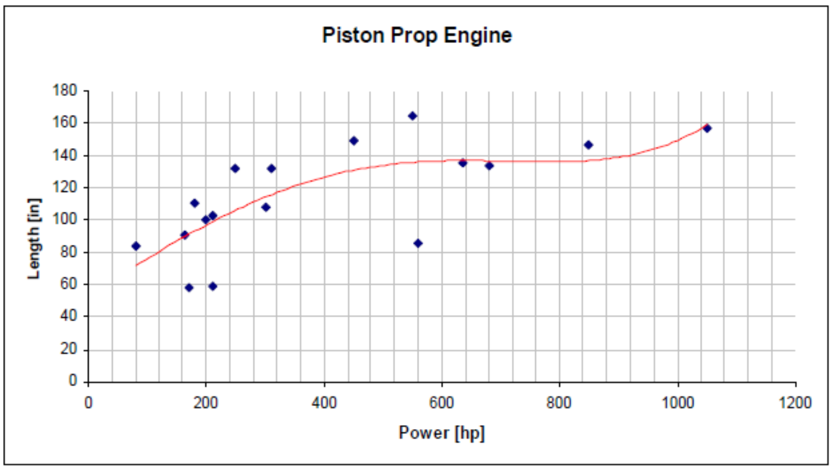

Figure 3.55 –Trends of the length with Power for piston propeller.

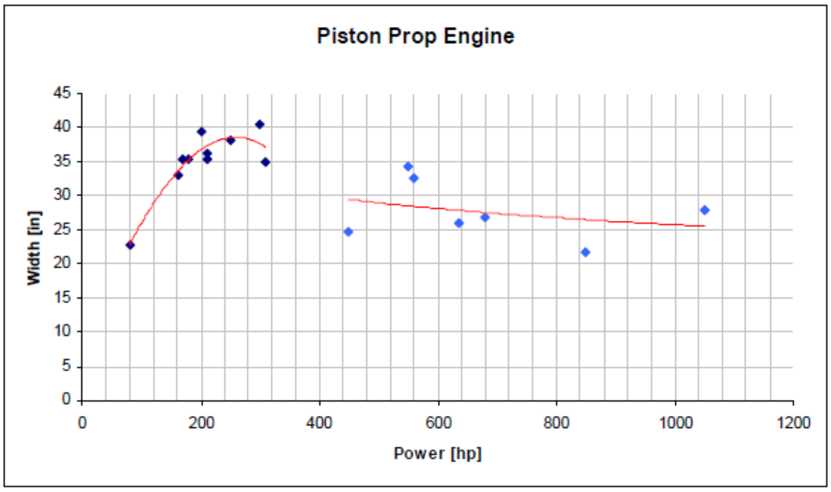

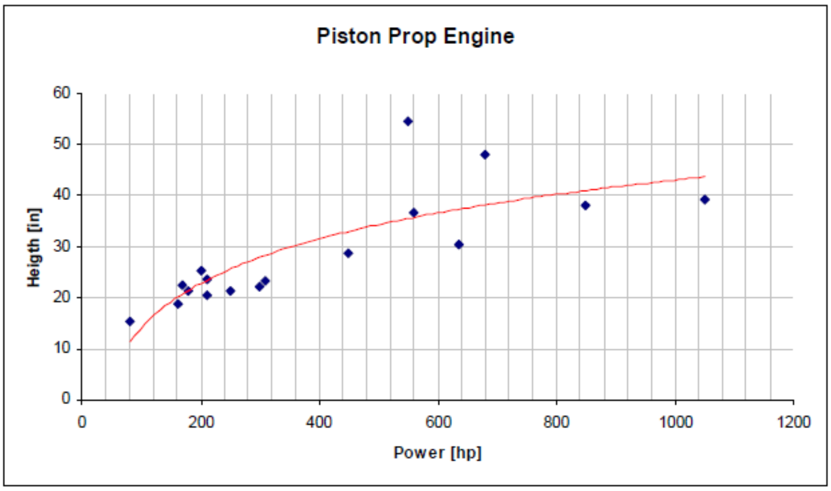

Figure 3.56 –Trends of the width and height with Power for piston propeller.

The obtained equation are the follows.

$$
\begin{aligned}
L_N &= 4 \cdot 10^{-10} \cdot \Pi_a^{\ 4} - 6 \cdot 10^{-7} \cdot \Pi_a^{\ 3} + 8 \cdot 10^{-5} \cdot \Pi_a^{\ 2} + 0.2193 \cdot \Pi_a + 54.097 \\
W_N\left(\Pi_a \le 410hp\right) &= -3 \cdot 10^{-7} \cdot \Pi_a^{\ 3} - 0.0003 \cdot \Pi_a^{\ 2} + 0.2196 \cdot \Pi_a + 7.3966 \\
W_N\left(\Pi_a > 410hp\right) &= -4.6563 \cdot \ln\left(\Pi_a\right) + 57.943 \\
H_N &= 12.595 \cdot \ln\left(\Pi_a\right) - 43.932
\end{aligned}
\qquad \textbf{(3.5.2)}
$$

- Turbopropeller

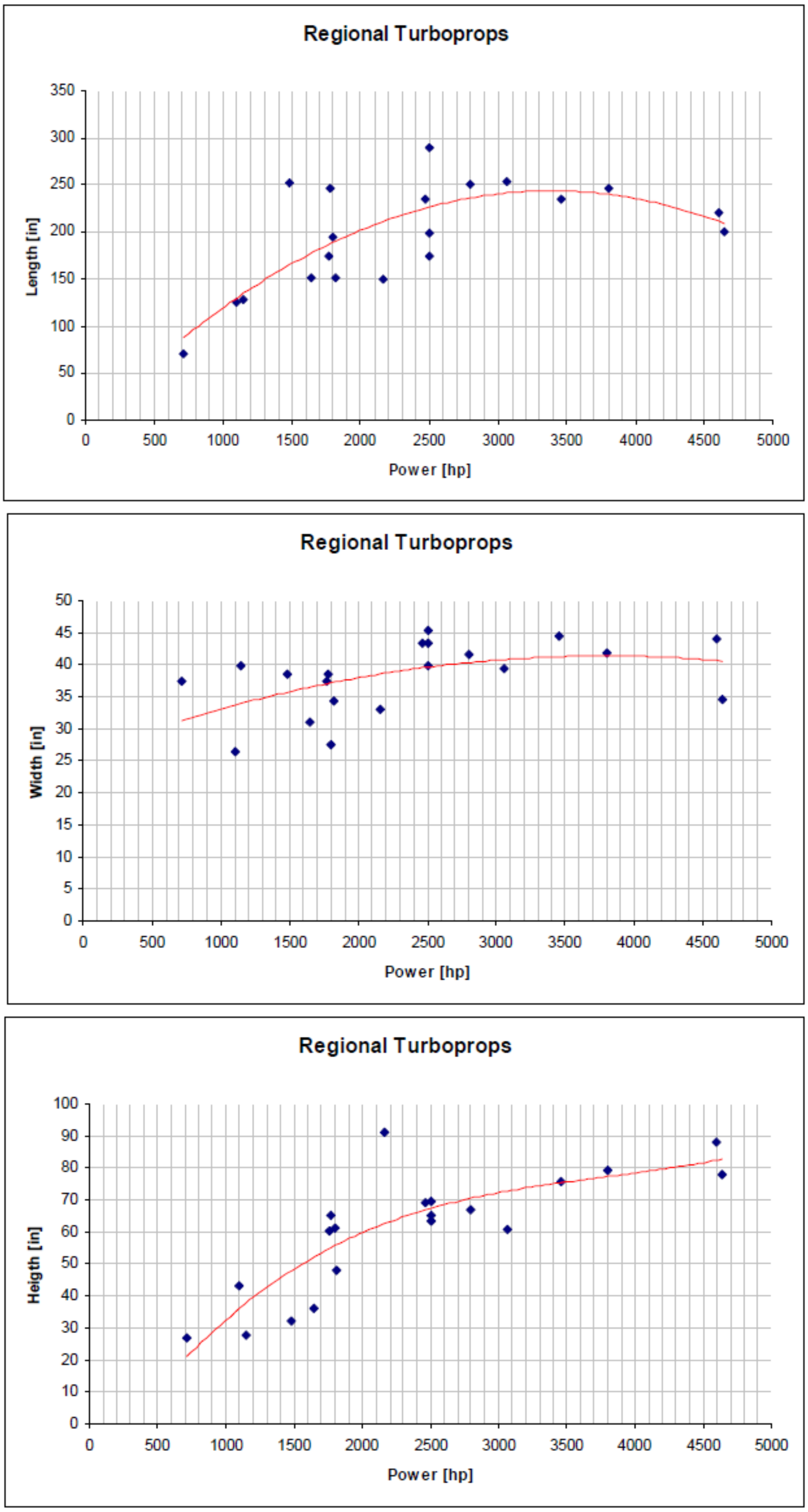

Figure 3.57 –Trends of the Length, Width and Height with Power for Turbopropeller.

The obtained equation in this case are the follows.

$$L_N = -1.28 \cdot 10^{-5} \cdot \Pi_a^{\,2} + 9.273 \cdot 10^{-2}\,\Pi_a - 8.3456$$
$$W_N = -0.95 \cdot 10^{-6} \cdot \Pi_a^{\,2} + 0.0073 \cdot \Pi_a + 25.3 \qquad \textbf{(3.5.2)}$$
$$H_N = 0.67 \cdot 10^{-11} \cdot \Pi_a^{\,3} - 3.35 \cdot 10^{-6} \cdot \Pi_a^{\,2} + 0.029 \cdot \Pi_a - 5.8425$$

The analysis of this component is done as described in paragraph 3.4.4 and 3.4.5.

3.6 - HIGH LIFT DEVICES

3.6.1 - Introduction

The aircraft's performances at low speed are very important for the their mission, in fact good high lift devices allow to land or take off on many airports, with their various runways.
So it's very important, in the preliminary design, to predict the aerodynamic characteristics, lift, drag and moment, which can be used to estimate the low speeds performances and maneuver quality, in order to have a realistic objective for the next aerodynamic development. The method shown here is inspired by Prof. Torembeekand Prof. Roskamand allow to evaluate with good accuracy the lift curve and drag and moment variations, with deflection of trailing edge and leading edge devices.

3.6.2 - Methodology for the estimation of the high lift devices effects

The traditional approach for the calculation of the lift generated by the wing with flap and/or Slat deflected is based on the assumption that the lift obtained from the two-dimensional airfoil can be considered a starting point. Later with semi empirical correction is done a conversion to the tridimensional wing. This procedure is acceptable and it show good results when spanwise flows and the interference effects are of minor importance or completely absent. The method is based on the thin airfoil theory and on experimental data.
Below is shown the methodology for the calculation of lift curve, drag and moment variations, for the trailing edge and leading edge devices.

3.6.3 -Trailing edge devices (Flap)

3.6.3.1 - Lift effects

The estimation of the lift curve is divided in the calculation of the increment of the lift coefficient at zero angle of attack ΔCL_0, the increment of the maximum lift coefficient CL_{max} and the variation of the lift curveslope $CL\alpha$.
the ΔCL_0 can be evaluated for the first step in 2D through the calculation of the efficiency factor τ,defined by the formula (3.6.1),using the figure 3.58 and one of the figures 3.59 and 3.62 depending on the type of devices.

$$\tau = \alpha_\delta \eta_\delta \quad \textbf{(3.6.1)}$$

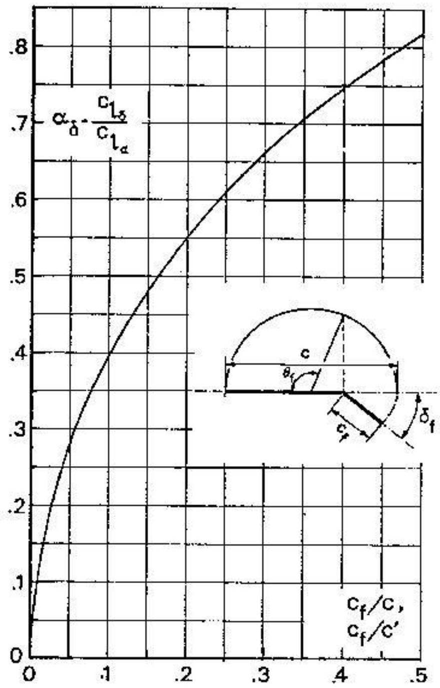

Figure 3.58 – 2D thin plate efficiency

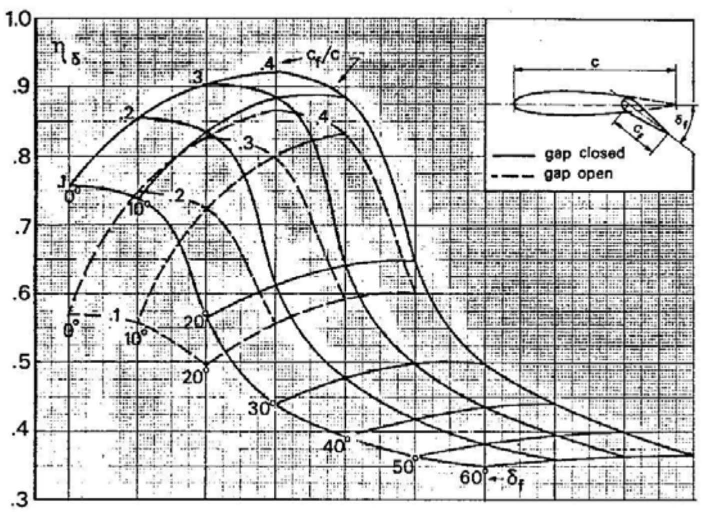

Figure 3.59 – 2D efficiency correction for a plain flap.

For the slotted, double slotted, fowler flaps that, when they are deflected, have wider chord than the retracted position.

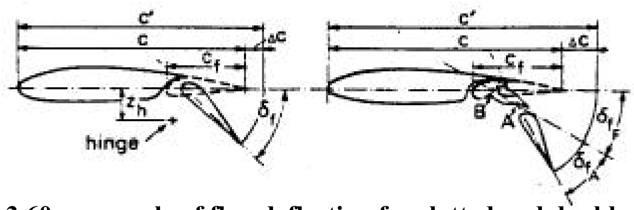

Figure 3.60 – example of flap deflection for slotted and double slotted flap.

So in the figure 3.58 the correct chord ratio must be used, this can be estimated the figure 3.61.

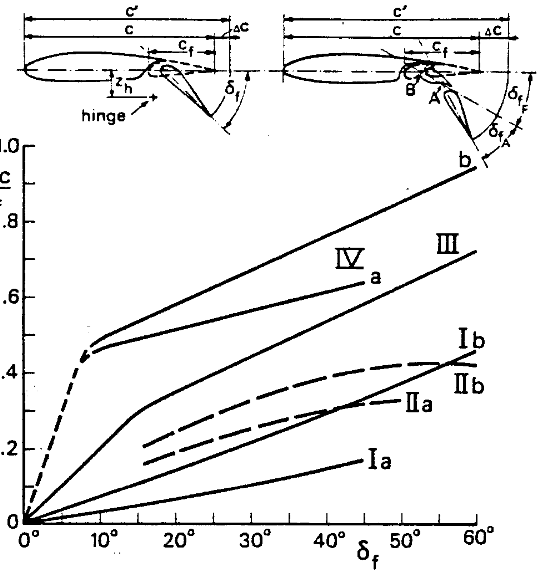

I: Fixed hinge - a: z_h/c_f = .2
b: z_h/c_f = .4
II: Typical optimum flap position
a: single slotted
b: double slotted, fixed vane
III: Double slotted, variable geometry, with flap extension
IV: Fowler - a: single slotted, double slotted with fixed vane
b: double and triple slotted, with flap extension

Figure 3.61 – Diagram useful for the evaluation of the chord ratio.

Then through the formula (3.6.2) is obtained the chord ratio to use.

$$\frac{C_f}{C'} = \frac{C_f}{C}\frac{1}{1+\dfrac{\Delta C}{C_f}\dfrac{C_f}{C}} \quad \textbf{(3.6.2)}$$

After this it's possible enter in the figure 3.62.

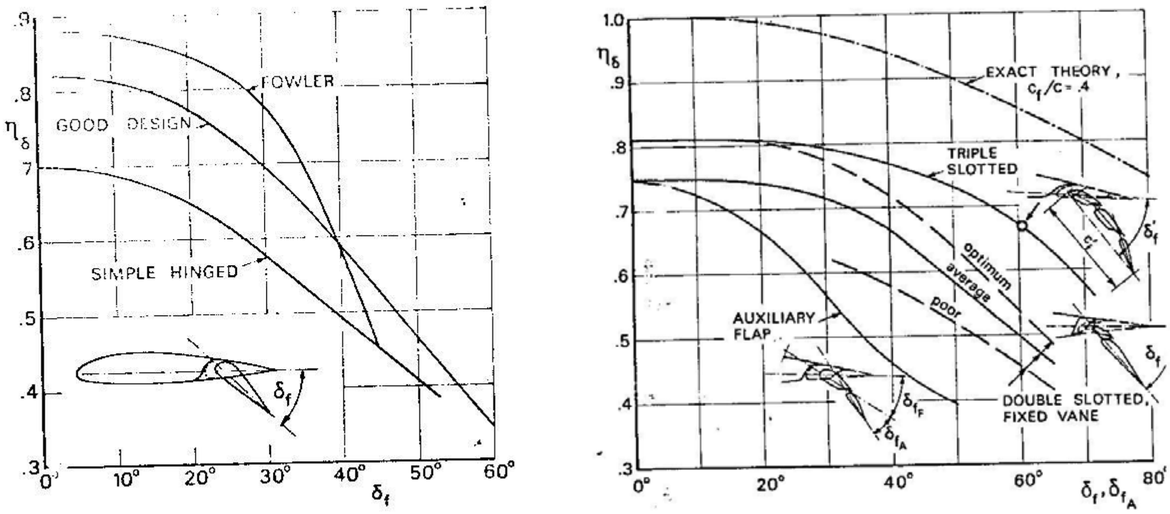

Figure 3.62 – 2D efficiency correction for slotted, double slotted, fowler flap.

So the increment of lift coefficient at zero angle of attack can be calculate as follows.

$$\Delta Cl_0 = \tau \cdot Cl\alpha \cdot \delta_f \qquad \textbf{(3.6.3)}$$

Then the increment can be converted in to 3D through the formula.

$$\Delta_f C_{L_0} = \Delta_f C_{l_0}\left(\frac{C_{L\alpha}}{C_{l\alpha}}\right)\left[\frac{(\alpha_\delta)C_L}{(\alpha_\delta)C_l}\right]K_b \qquad \textbf{(3.6.4)}$$

The factor $[(\alpha_\delta)C_L/(\alpha_\delta)C_l]$, also called K_c, that represent the ratio of the efficiency factors 2D and 3D, and K_b can be evaluated by the figure 3.63, η is the inner position of the flap first and then the outer position, then the K_b is the difference between the obtained values.

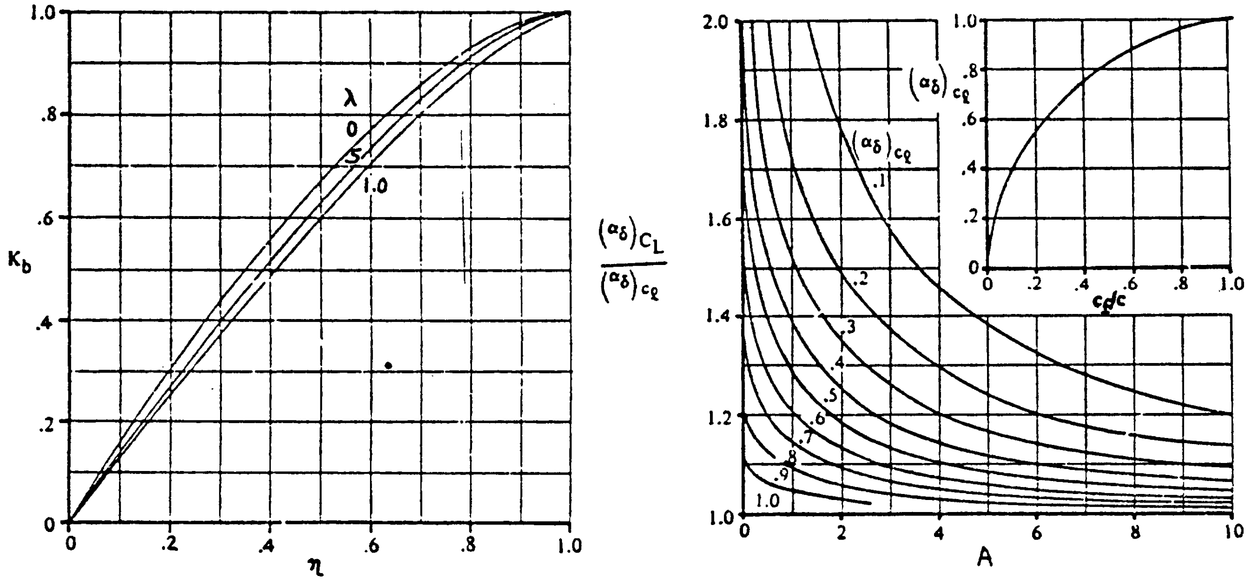

Figure 3.63 – 2D to 3D correction factor.

The increment of the maximum lift coefficient follow the same procedure just shown above, the 2D value is obtained by the following relationships.

- Approximate $$Cl_{\max} = (Cl_{\max})_{\delta=0} + \frac{2}{3}\Delta_f Cl_0 \qquad \textbf{(3.6.5)}$$

- Accurate $$Cl_{\max}' = 0.533\Delta y\left(\frac{R_C}{3\cdot 10^6}\right)^{0.08} + \frac{1}{2}\left(Cl_0 + \Delta_f Cl_0'\right)$$

The choice can be made on the lower value between approximate formula and accurate one, for safety.
The conversion in 3D is shown in formula (3.6.6).

$$\textbf{(3.6.6)} \qquad \Delta_f C_{L\max} = 0.92\Delta_f Cl_{\max} K_b \cos\Lambda_{c/4}$$

Where the K_b is the same used in the evaluation of the increment ΔCl_0.
The factor 0.92 take into account the loss of lift near the flap tips as show the following figure.

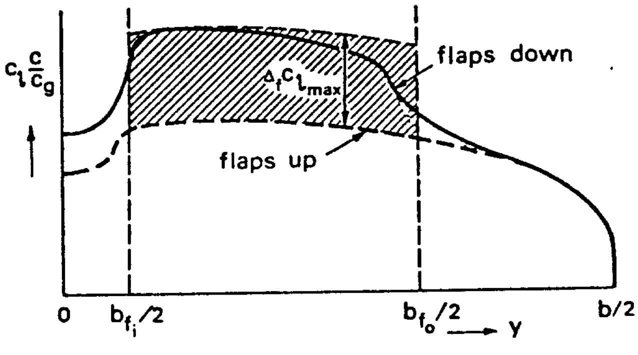

Figure 3.65 – Lift distribution with flaps deflection.

The lift curve slope is modifieddue tothe increment of the chord. So the plain flap haven't this modify, while yes for the other type of flaps. It's possible to calculate directly the 3D value of CL_α starting by the mean airfoil 2D value.

$$\frac{CL_\alpha'}{CL_\alpha} = 1 + \frac{\Delta_f C_{L_0}}{\Delta_f C_{l0}}\left[\frac{c'}{c}\left(1 - \frac{c_f}{c'}\sin^2\delta_f\right) - 1\right] \quad \textbf{(3.6.7)}$$

3.6.3.2 - Moment effects

The moment coefficient is calculated with the same methodology, first the two dimensional value is evaluated by the formula (3.6.8), then the correction is done to convert to the three dimensional value, formula (3.6.9).

$$\Delta_f C_{m_{1/4}} = -\mu_1 \Delta_f Cl \frac{c'}{c} - \frac{Cl}{8}\frac{c'}{c}\left(\frac{c'}{c} - 1\right) \quad \textbf{(3.6.8)}$$

$$\Delta_f C_{M_{1/4}} = \mu_2 \Delta_f C_{m_{1/4}} + 0.7\frac{AR}{1 + 2/AR}\mu_3 \Delta_f Cl \tan\Lambda_{1/4} \quad \textbf{(3.6.9)}$$

Where μ the coefficients are estimated by the following figures.

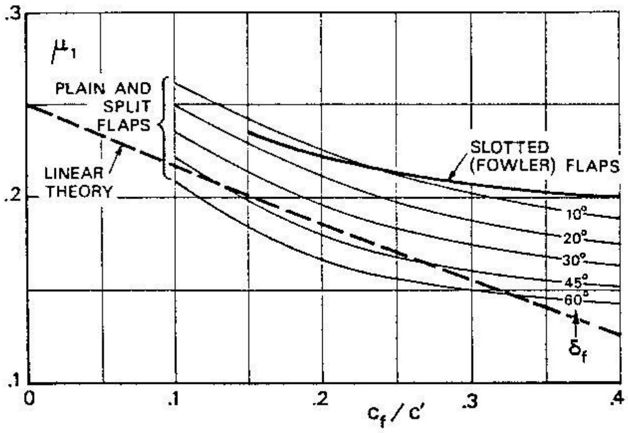

Figure 3.66 – diagram used to evaluate μ_1.

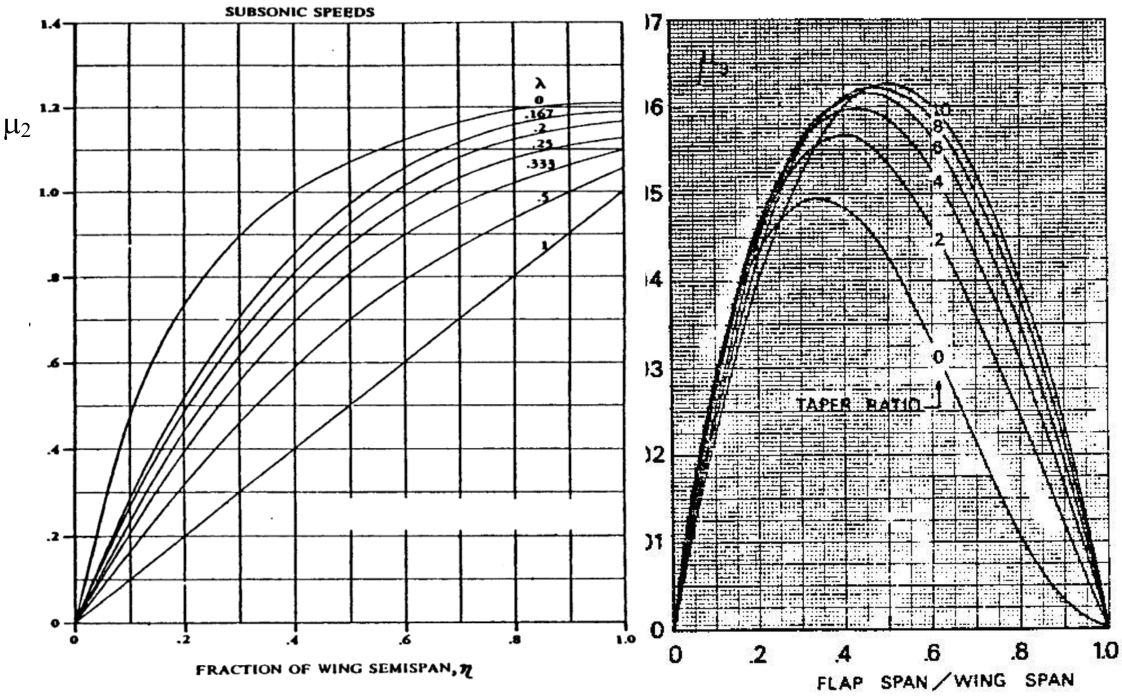

Figure 3.65 –μ_2 and μ_3 correction factors (the taper ratio in the first diagram are, from the top: 0, 0.167, 0.2, 0.25, 0.333, 0.5, 1).

3.6.3.3 - Drag effects

The drag increment due to extended flap can be evaluated by the first step with the two dimensional evaluation, $\Delta_f Cd_{p_0}$, through the follow diagrams.

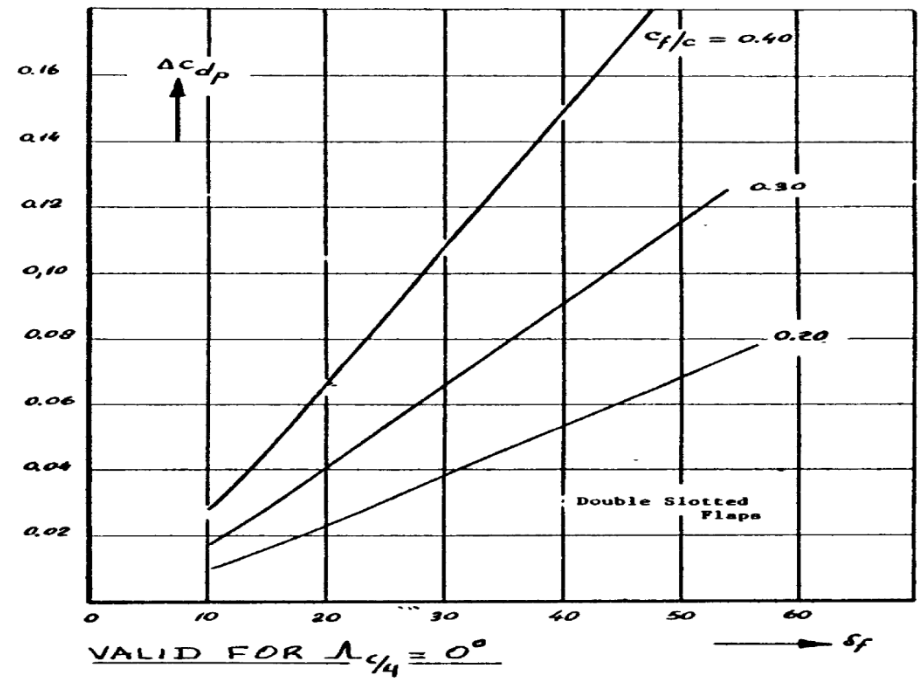

Figure 3.67 – value of two dimensional drag increment for double slotted flap

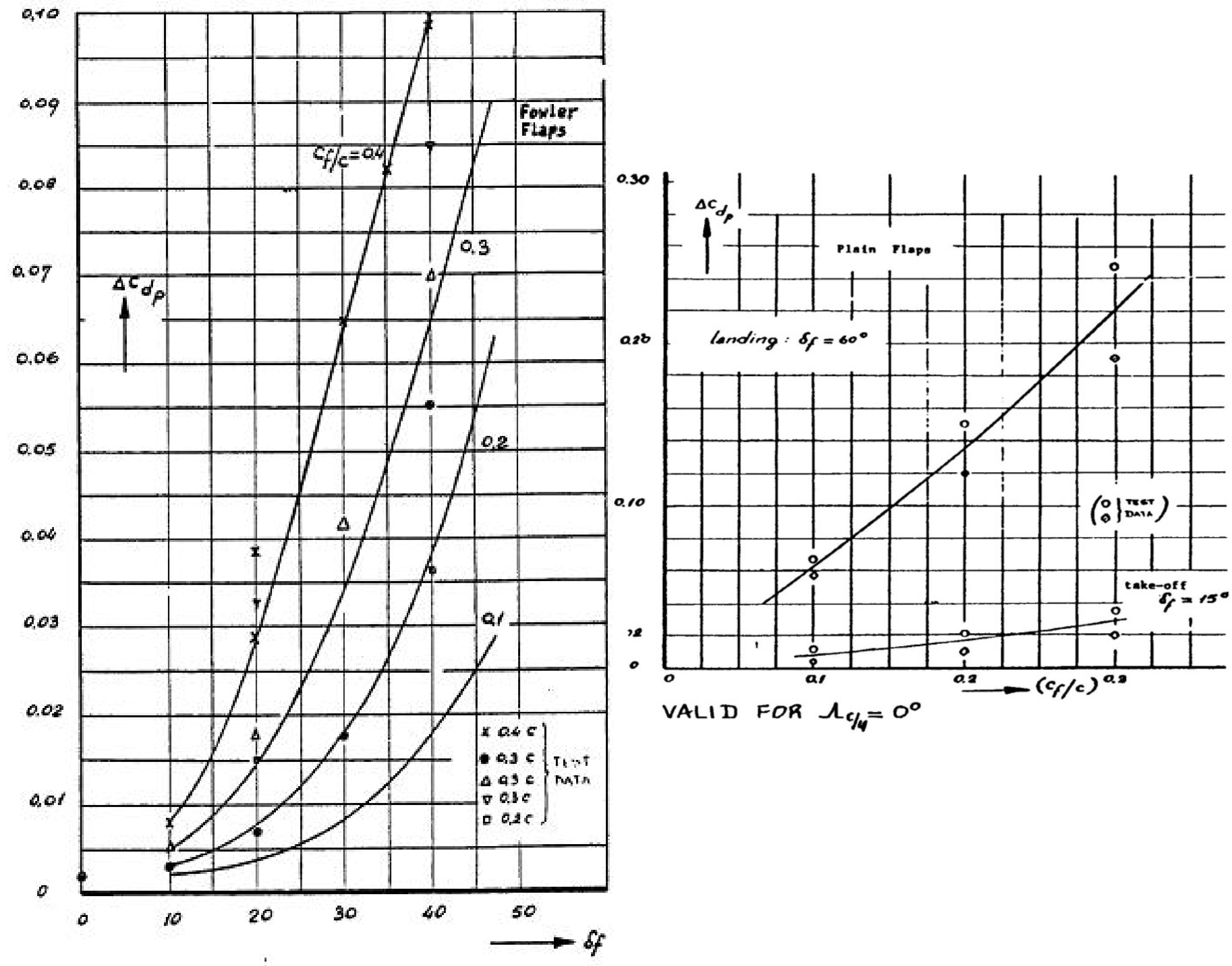

Figure 3.68 – value of two dimensional drag increment for fowler and plain flaps.

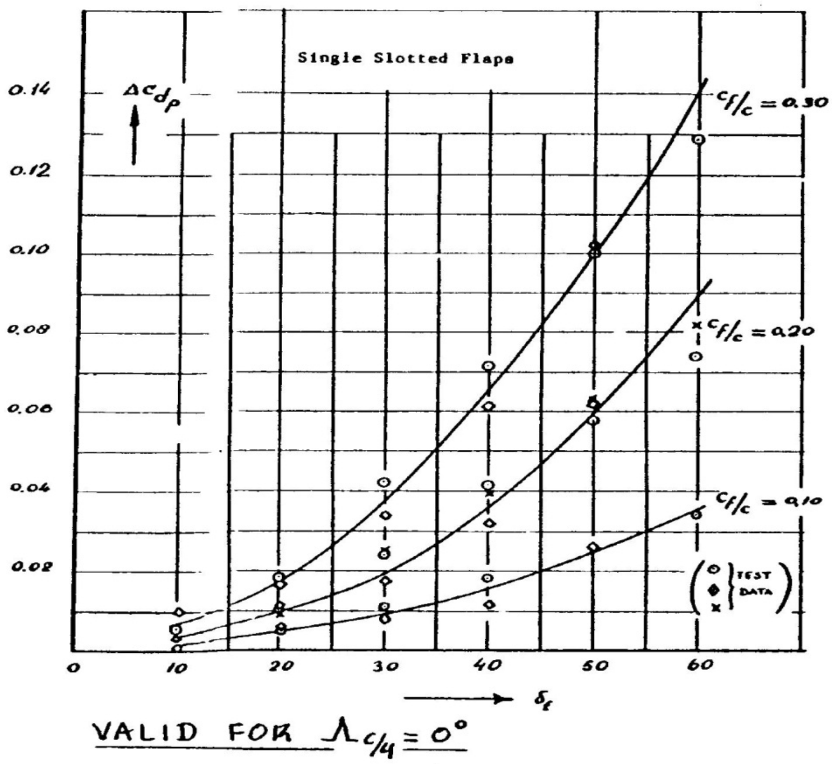

Figure 3.69 – value of two dimensional drag increment for slotted.

Then the three dimensional correction is given by the following formula.

$$\Delta_f C_{D_P} = \frac{S_{wf}}{S} \Delta_f Cd_{p0} \cos \Lambda_{1/4} \qquad \textbf{(3.6.8)}$$

Where S_{wf}/S can be substituted by K_b shown before in the figure 3.63, or can be evaluated by the following formula, valid for straight tapered wings.

$$\frac{S_{wf}}{S} = \frac{b_{fo} - b_{fi}}{b} \left[1 + \frac{1-\lambda}{1+\lambda} \left(1 - \frac{b_{fo} - b_{fi}}{b} \right) \right] \textbf{(3.6.9)}$$

3.6.4 - Leading Edge Flaps

3.6.4.1 - Lift effects

The most important leading edge flap are, “Plain leading edge flap”, “Slat” and “Krueger”the increment of C_{L0} for the first one is calculate by the following formulas.

$$\Delta_S C_{L0} = \Delta Cl_0 \cdot Cl_\alpha \cdot \frac{S_{ws}}{S} \cdot \cos^2 \Lambda_{1/4} \textbf{(3.6.10)}$$

Where : $$\Delta Cl_0 = \frac{\arccos\left(1 - 2 \cdot \frac{C_S}{C}\right) - \sin\left(\arccos\left(1 - 2 \cdot \frac{C_S}{C}\right)\right)}{\pi} Cl\alpha \cdot \delta_f \textbf{ (3.6.11)}$$

The ratio S_{ws}/S is evaluated in the same way shown in (3.6.9) or using the figure 3.63.
The Slat and Krueger flaps don’t cause a sensible variation of the C_{L0}, at least in this preliminary design, so this contribution is not evaluated.
The maximum two dimensional C_l can be obtained by the variation of the critical angle, for “Plain leading edge flap”, as shown the formula 3.6.10, or by the chord ratio of the slat with wing, for “Slat” and “Krueger”, so if the flap are retracted, it will be used the formula (3.6.11) else the (3.6.12).

$$\text{Plain Leading Edge Flap: } \Delta\alpha_{crit} = 0.58 \delta_S \sqrt{\frac{c_s}{c}} \textbf{ (3.6.12)}$$

Slat and Krueger flap:

$$\text{Flap retracted: } \Delta Cl_{\max} = 2.2 \sqrt{\frac{c_s}{c}} \textbf{ (3.6.13)}$$

$$\text{Flap extended: } \Delta Cl_{\max} = 1.9 \sqrt{\frac{c_s}{c}} \textbf{ (3.6.14)}$$

An example of use of slats is shown below.

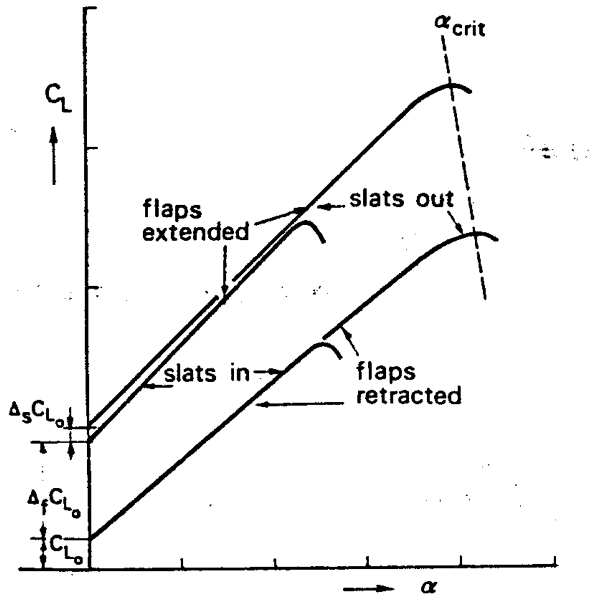

Figure 3.70 – Slat effect with retracted and extended flaps.

The conversion in the three dimensional increment is done with the following formulas, the first one valid for the Plain leading edge flap and the second one for Slat and Krueger flaps.

$$\Delta_S C_{L\max} = \Delta Cl_{\max} Cl_{\alpha} \frac{S_{ws}}{S} \cos^2 \Lambda_{1/4} \quad \textbf{(3.6.15)}$$

$$\Delta_S C_{L\max} = \Delta Cl_{\max} \frac{S_{ws}}{S} \cos^2 \Lambda_{1/4} \quad \textbf{(3.6.16)}$$

3.6.4.2 - Drag effects

The drag produced by the leading edge flaps have small influence on the parasite drag, probably due to the separation of the flow from the inferior surface of the slat. The equation is shown below.

$$\Delta_S C_{D_P} = \left(C_{D_P}\right)_{basic} \frac{S_{ws}}{S} \frac{c_s}{c} \cos \Lambda_{1/4} \quad \textbf{(3.6.17)}$$

Where the C_{Dp} basic is the profile drag with flap and slat retracted.

3.7 – AILERON DESIGN

3.7.1 – Introduction

It's very important for preliminary design to analyze the roll and turn performances of the aircraft, paying attention on its use and category. the system used for these is the aileron, that is a classical trailing edge plain flap,so it's very important, starting from its geometry, to predict the aerodynamic characteristics that allow to estimate the roll coefficient and its derivatives in function of the aileron deflectionsδ_a and rolling velocity$P$. The ailerons on each wing deflect asymmetrically, one going up and one going downnot necessarily with same deflection, this modify the spanwise loading on the wing and generate the roll moment.

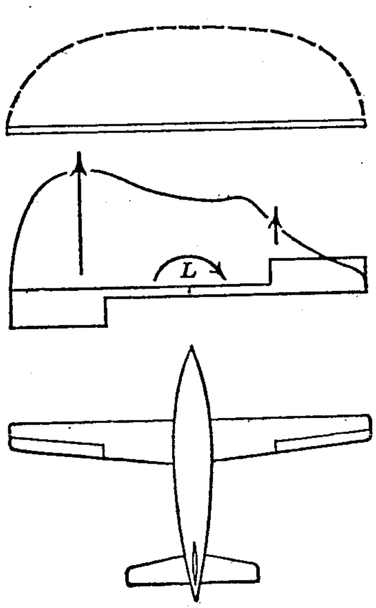

Figure 3.71 – example of spanwise loading due to aileron deflection.

As the airplane increase the rolling speed, a new spanwise loading will be created which opposes the rolling moment, this is called damping moment of the wing.
The size of the control is determined by the fulfill of two basic requirements:

- The aileron have to provide sufficient rolling moment at low speeds to counteract the effect of the vertical asymmetric gusts tending to roll the airplane.
- It have to roll the airplane at a sufficiently high rate at high speed for a given stick force.

The design criterion for the evaluating of aileron effectiveness is the non-dimensional parameter *pb/2V*, also called "Lateral Control Power".
Another step isto estimate the turn performances knowing also the characteristics of the engine system. The objective is, to satisfy the minimum maneuvering requirements, so paying attention on the bank angle, load factor, and minimum radius.

3.7.2 - Methodologies for the rolling performances

The estimation of Lateral Control Power and so the rolling performances is made by two different methodologies, one semi-empirical, based on diagram which give all the needed contribution for the calculation, and one strip integration, that can give results little higher than semi-emipirical one due to its assumptions.

3.7.2.1 Strip Integration Method

The damping moment of the wing can be calculated as follows.

$$M_d = 2\left(\frac{1}{2}\rho V^2\right) Cl_\alpha \frac{p}{V} B \qquad \textbf{(3.7.1)}$$

Where the factor B is given by: $B = \int_0^{b/2} c(y) y^2 dy$

While the aerodynamic moment due to the change of lift produced by the aileron is obtained by the following formula.

$$M_A = 2\left(\frac{1}{2}\rho V^2\right) Cl_\alpha \tau \delta_a A \qquad \textbf{(3.7.2)}$$

Where the factor A is given by: $A = \int_{y_{in}}^{y_{out}} c(y) y dy$

The y_{in} and y_{out} are the positions of aileron tips.τ is the aileron efficiency at a fixed deflection, estimated by the (3.6.1), if it is different between right and left aileron then the mean efficiency is taken. So By the equality between damping aerodynamic moment and aerodynamic moment due to the change of lift produced by aileron it's possible to obtain the value of rolling velocity *p*.

$$M_A = M_d \qquad => p = \frac{A\tau}{B}\bar{\delta} V \qquad \textbf{(3.7.3)}$$

Where $\bar{\delta}$ is the mean ailerons deflections.
It's clear that the rolling velocity grows with the airspeed linearly but this is real until the value of max couple on the wheeling steer is reached. In fact considering the hinge moments, the equilibrium of works must be kept.

$$C \cdot \Delta\psi = H \cdot \Delta\delta \qquad \textbf{(3.7.4)}$$

Where C is the couple on the steering wheel, limitated by FAR 25 at 36·Diameter and by FAR 23 at 22.5·Diameter, the and H is given as follows.

$$H = \frac{1}{2}\rho V^2 S_a \bar{c}_a C_{ha} \qquad \textbf{(3.7.5)}$$

Where the hinge moment coefficient C_{ha} can be calculated by the (3.7.6).

$$C_{ha} = 2\frac{p}{V}\left(C_{h\delta}\frac{B}{A\tau} - C_{h\alpha}\bar{y} \right) \qquad \textbf{(3.7.5)}$$

So substituting the (3.7.5) in the (3.7.4) the following formula is obtained.

$$C = \rho V p S_a \bar{c}_a K\left(C_{h\delta}\frac{B}{A\tau} - C_{h\alpha}\bar{y} \right) \qquad \textbf{(3.7.6)}$$

Where K is: $K = \dfrac{\Delta\delta}{\Delta\psi}$ (generally 1/6).$C_{h\delta}$ and $C_{h\alpha}$ are obtained from following charts.

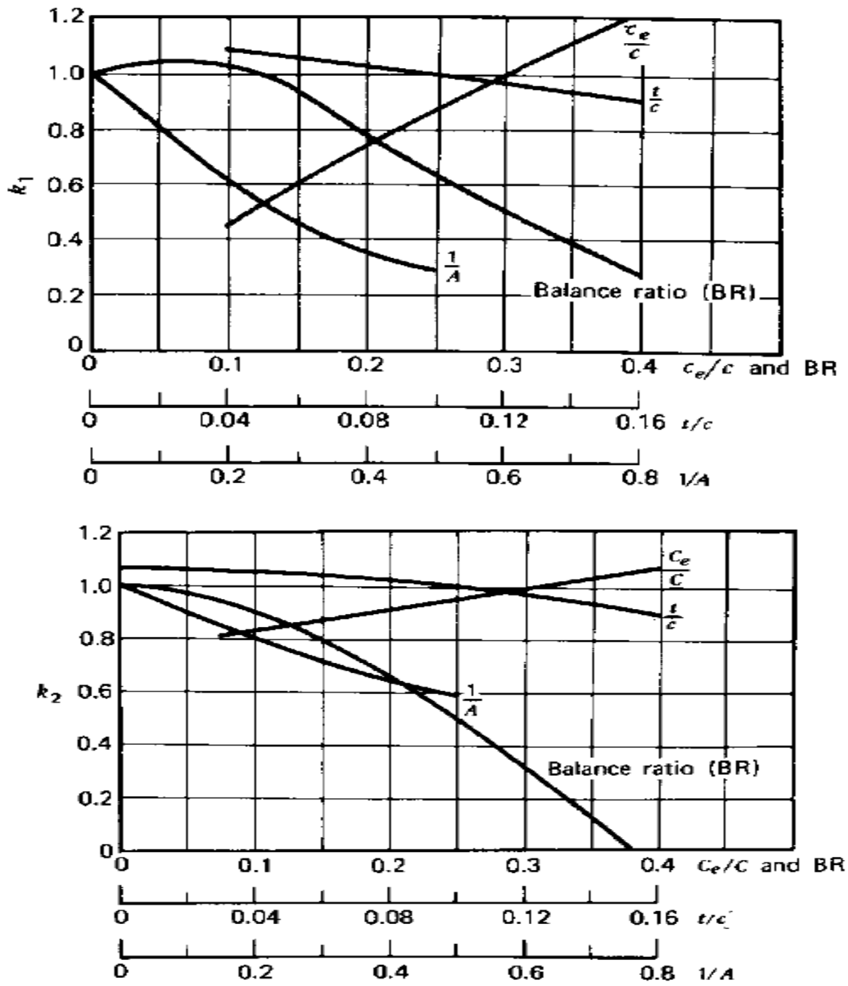

Figure 3.72 – Charts used for the estimation of $C_{h\delta}$ and $C_{h\alpha}$.

$$Ch_{\alpha} = -0.55 \cdot K1_{ce/c} \cdot K1_{t/c} \cdot K1_{1/A} \cdot K1_{BR} \qquad \textbf{(3.7.7)}$$

$$Ch_{\delta} = -0.89 \cdot K1_{ce/c} \cdot K1_{t/c} \cdot K1_{1/A} \cdot K1_{BR} \qquad \textbf{(3.7.8)}$$

These must be substituted in (3.7.6) with their absolute value.

Imposing the C=Cmax the value of *p* is obtained for any speed, so the intersection between this curve and the curve described by the (3.7.3) identifies the V at maximum *p*.

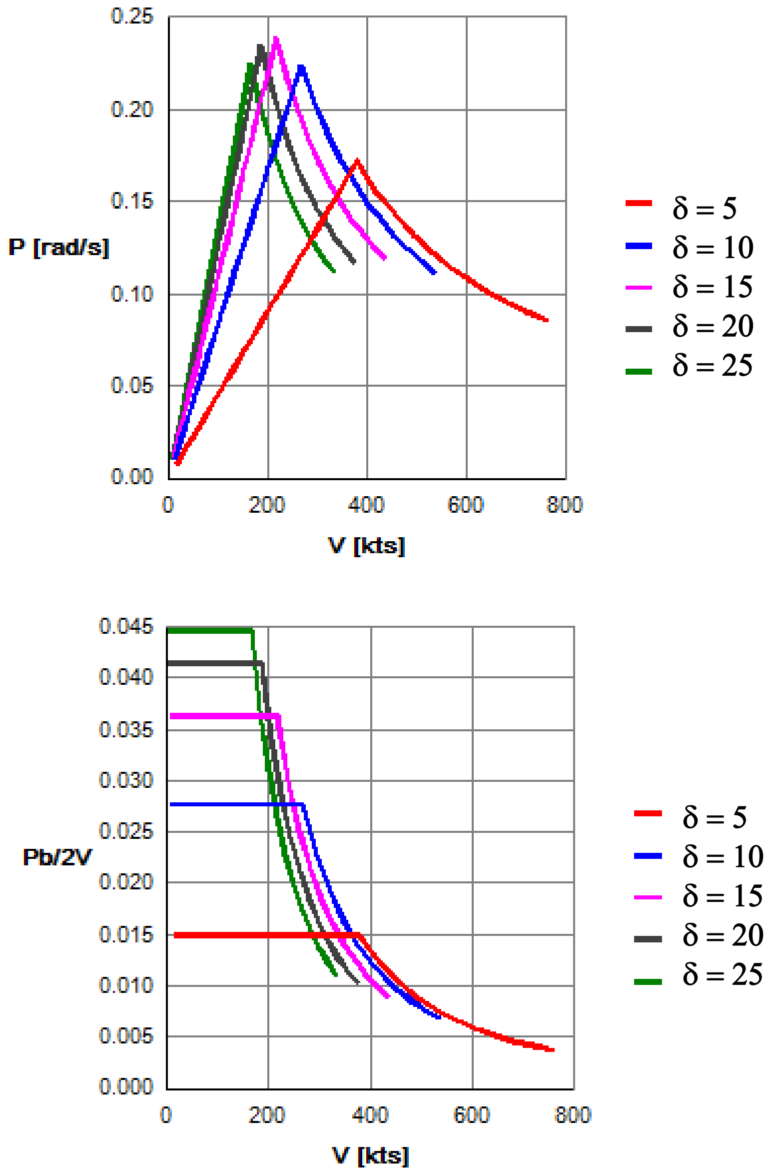

Figure 3.73 – Example of airplane rolling characteristics.

Since the rolling velocity *p*in the second part of the curve changes its trend, also the useful deflection changes, it decrease as shown by the figure 3.74.

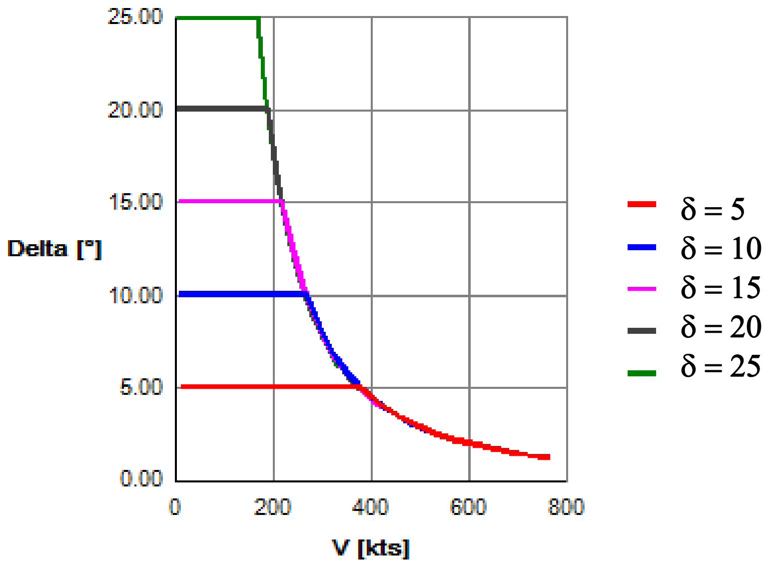

Figure 3.74 – Reduction of the required aileron deflection.

3.7.2.2 –The Semi-Empirical Method

The semi-empirical method is based on the use of various charts where it's possible to obtain directlythe value of derivative of the rolling coefficient due to aileron deflection and due to rolling velocity. From the aileron lateral coordinateη, wing sweep angle Λ, aspect ratio Aand taper ratioλ, it's possible to enter in the diagrams below to obtain the value of $Cl_{\delta a}$, the number of Mach effect can be ignored here.

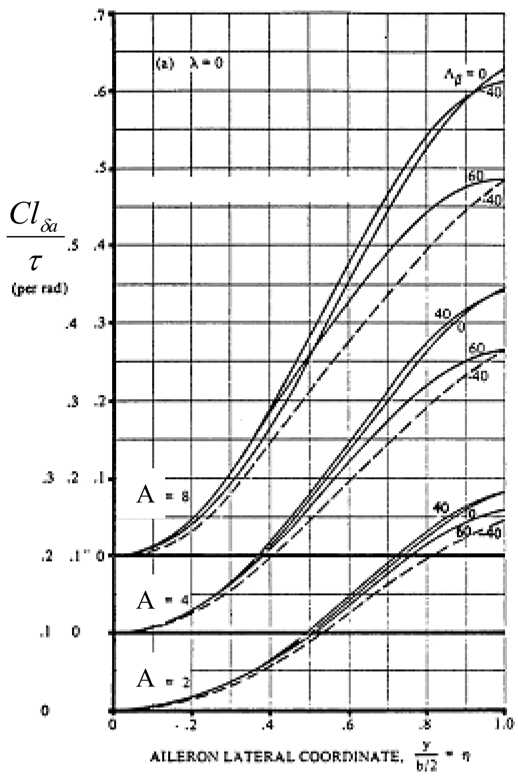

Figure 3.75 – Diagram used to estimate the $Cl_{\delta a}$.

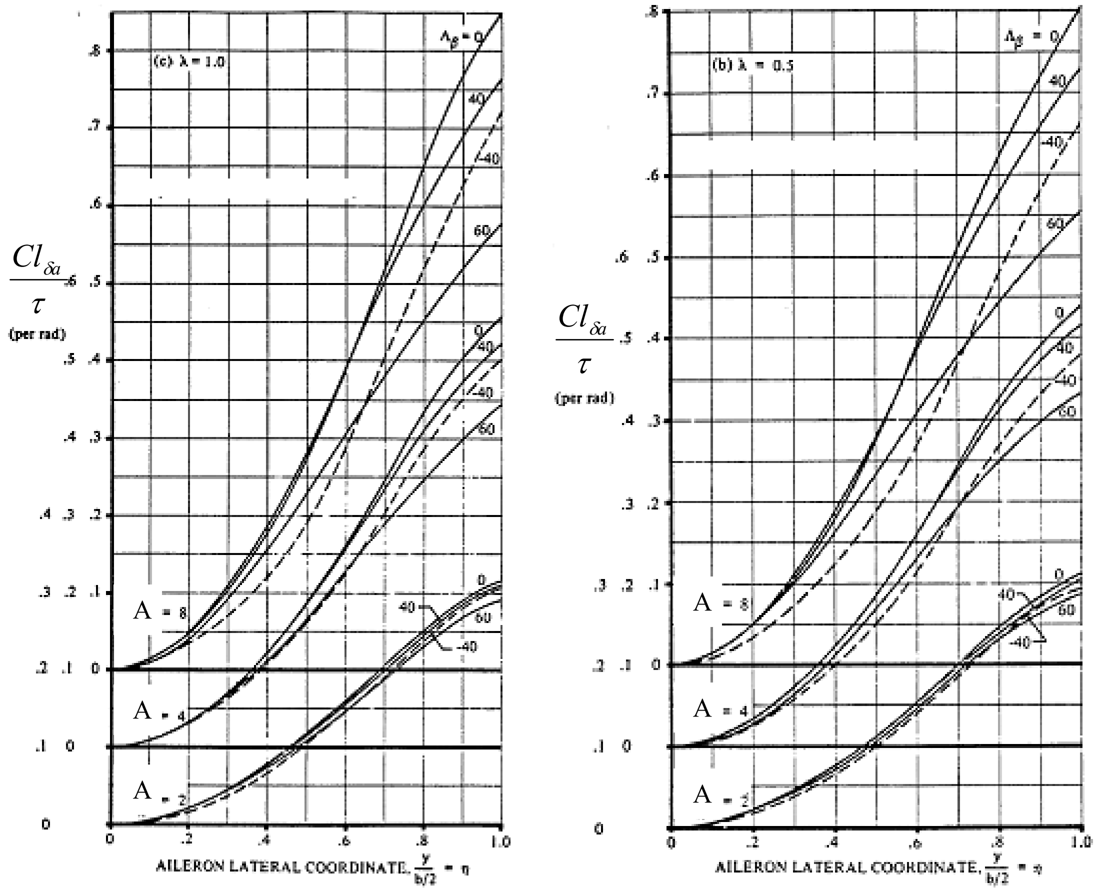

Figure 3.76 – Diagrams used to estimate the $Cl_{\delta a}$.

Then the equivalent of the factor A saw in the (3.7.2) is calculated by the following formula.

$$A = \frac{Cl_{\delta a} \cdot b}{CL_{\alpha} \cdot Sw} \qquad \textbf{(3.7.7)}$$

The contribution of the wing on Cl_{pw} is obtained by the following figure.

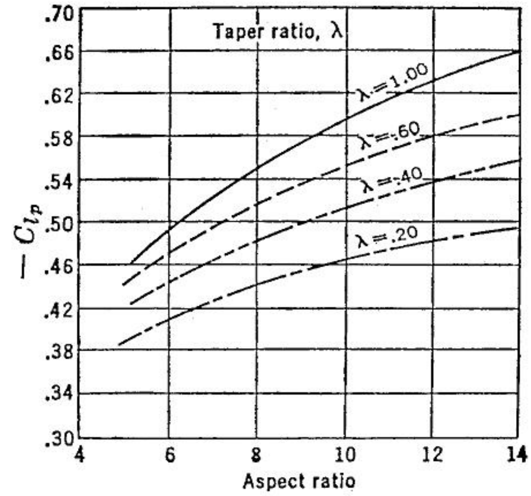

Figure 3.77 – Diagram used to estimate the Cl_{pw}.

The contribution of the presence of the dihedral angle is obtained by the formula (3.7.8).

$$K_{\Gamma} = 1 - 4 \cdot \frac{Zw}{b} \cdot \sin(\Gamma_w) + 12 \cdot \left(\frac{Zw}{b}\right)^2 \cdot \sin^2(\Gamma_w) \qquad \textbf{(3.7.8)}$$

The contribution due to the wing sweep angle is evaluated taking for reference the figure 3.78 and building the equation (3.7.9) or (3.7.10).

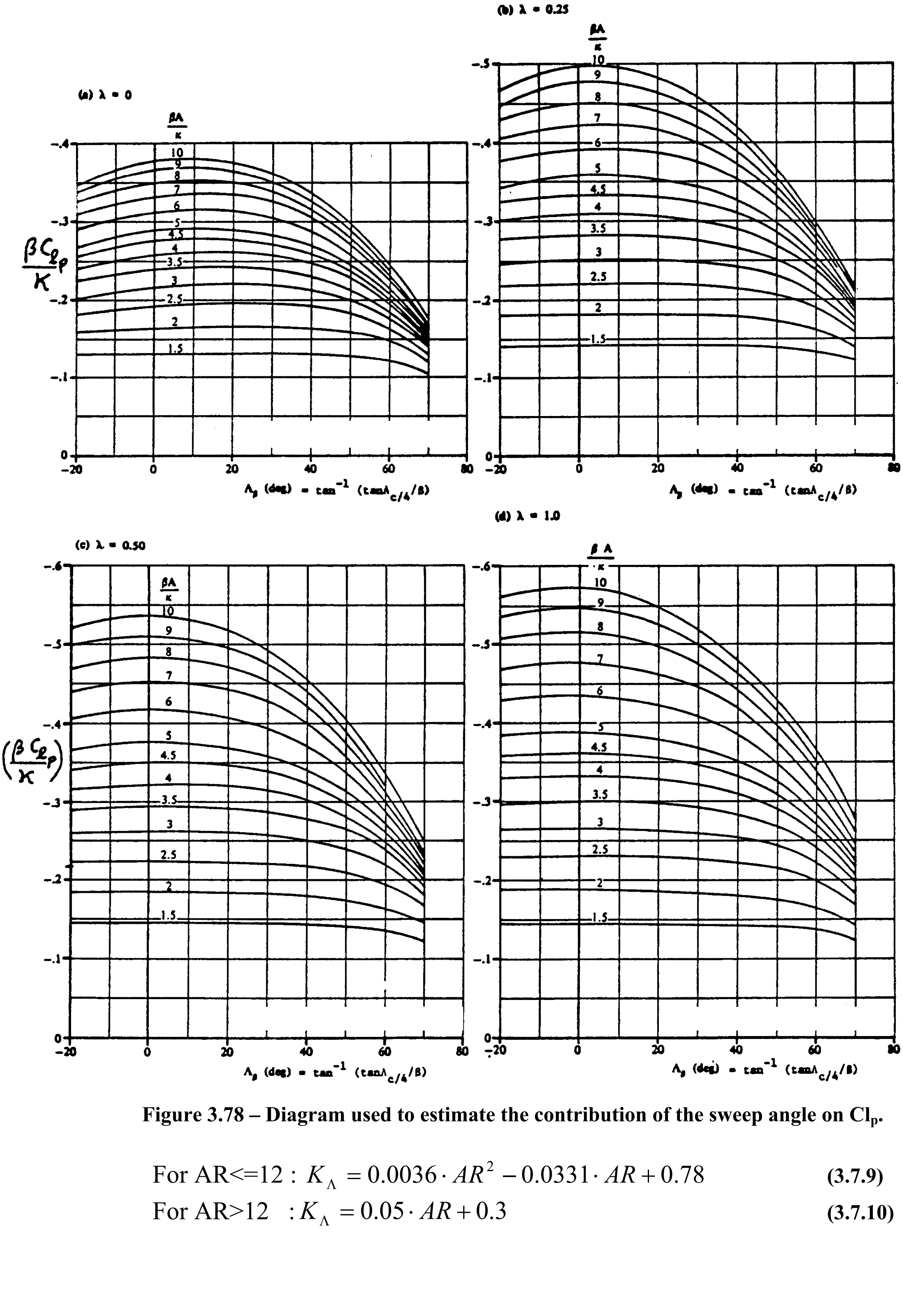

Figure 3.78 – Diagram used to estimate the contribution of the sweep angle on Cl_p.

$$\text{For AR<=12}: K_{\Lambda} = 0.0036 \cdot AR^2 - 0.0331 \cdot AR + 0.78 \qquad \textbf{(3.7.9)}$$

$$\text{For AR>12}: K_{\Lambda} = 0.05 \cdot AR + 0.3 \qquad \textbf{(3.7.10)}$$

So the value of rolling coefficient derivative due to *p* is given by the following equation.

$$Cl_p = Cl_{pw} \cdot K_\Gamma \cdot \cos(\Lambda \cdot K_\Lambda) \qquad \textbf{(3.7.11)}$$

At this value can be added the contribution of vertical tail and horizontal tail, which have minor effect.
The horizontal Tail is evaluated in the same way of the wing, described above, for the contribution $(Cl_p)_h$ which is used in the following formula.

$$Cl_{ph} = 0.5(Cl_p)_h \frac{S_h}{S}\left(\frac{b_h}{b}\right)^2 \qquad \textbf{(3.7.12)}$$

The vertical Tail instead is calculated as follows.

$$Cl_{pv} = 2 \cdot \left(\frac{Z_v}{b}\right) C_{Y\beta v} \qquad \textbf{(3.7.13)}$$

Where Z_v is defined by the following figure.

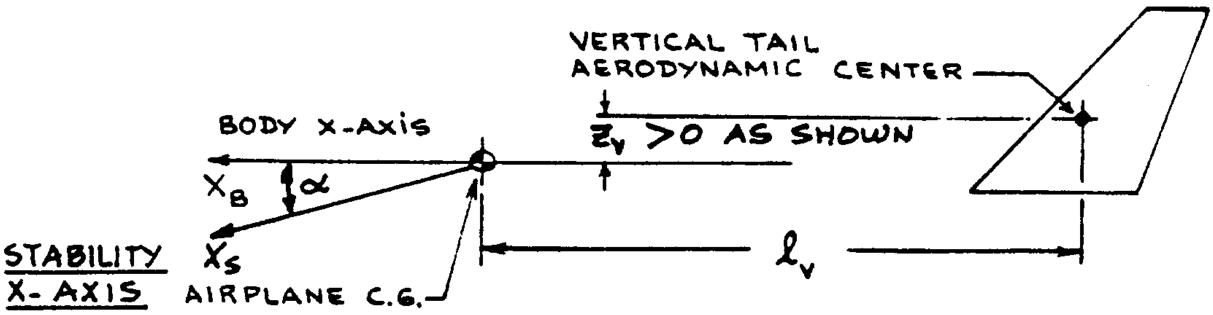

Figure 3.79 – Diagram used to estimate the contribution of the sweep angle on Cl_p.

The $C_{Y\beta v}$ is given by following formula.

$$C_{Y\beta v} = -K_v \cdot Cl_{\alpha v} \cdot \eta_v \left(1 + \frac{\partial\sigma}{\partial\beta}\right) \frac{S_v}{S} \qquad \textbf{(3.7.14)}$$

Where K_v is obtained by the following chart.

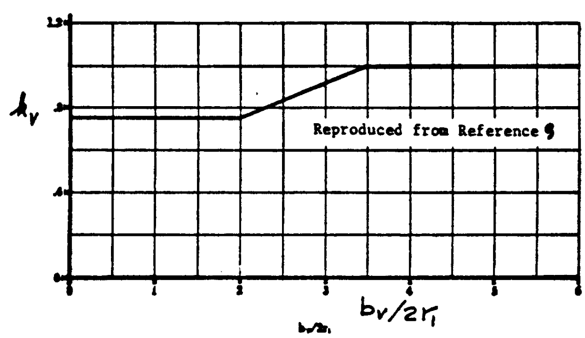

Figure 3.79 – Chart used to obtain the value of Kv.

r_l is the local equivalent radius of the fuselage at the vertical tail position and b_v is the span.

While the sidewash is estimated as follows.

$$\left(1+\frac{\partial\sigma}{\partial\beta}\right)\eta_v = 0.724+3.06\left[\frac{\left(\frac{S_v}{S}\right)}{\left(1+\cos\left(\Lambda_{c/4w}\right)\right)}\right]+0.4\frac{Z_W}{Z_f}+0.009AR_w \qquad \textbf{(3.7.15)}$$

Where Z_w is taken as shown by the figure 3.80.

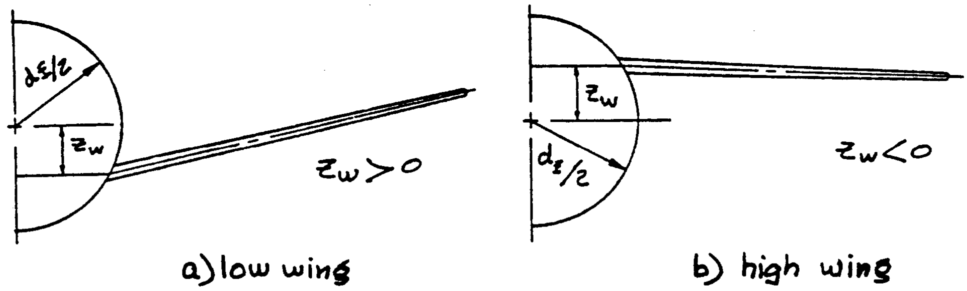

Figure 3.80 – Definition of Wing-Fuselage parameter Z_w.

$S_v$is the effective vertical tail area, defined by the following figure.

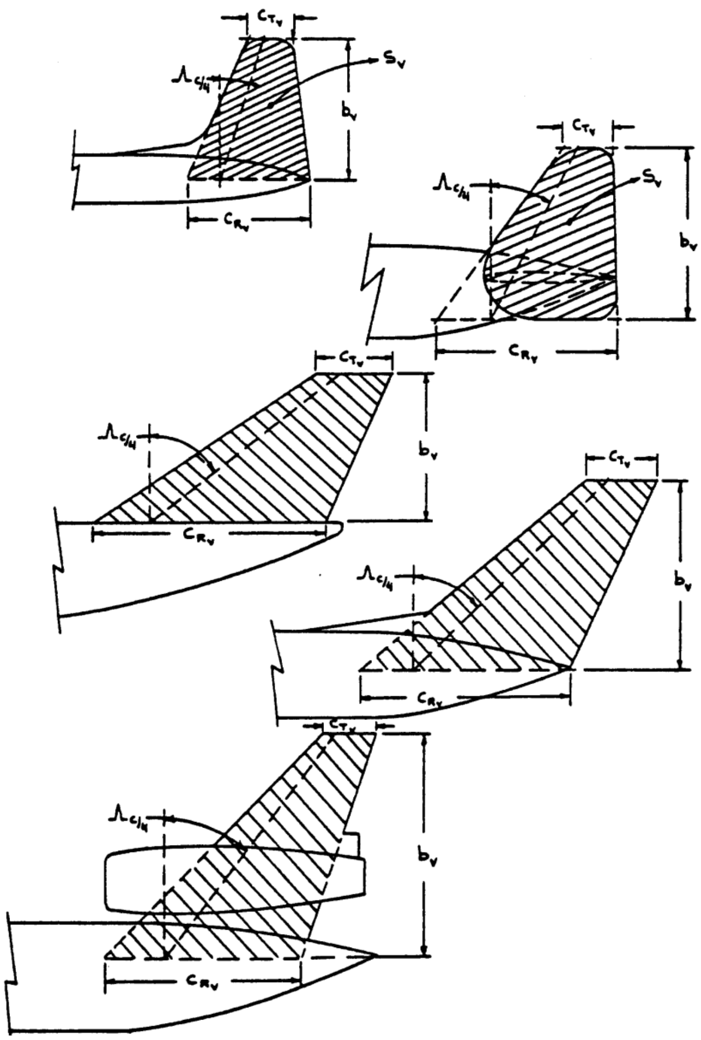

Figure 3.81 – Definition of effectivevertical tail area.

Finally the total $Cl_p$is obtain by the sum of all the contribution.

$$Cl_p = Cl_{pw} + Cl_{ph} + Cl_{pv} \quad \textbf{(3.7.15)}$$

The factor B shown in (3.7.1) can be obtained now from the following formula.

$$B = -\frac{Cl_p S_w b^2}{2Cl_\alpha} \quad \textbf{(3.7.16)}$$

Then the methodology is the same shown for the strip integration method.

3.7.2.3 - Turn Performances

To evaluate the turn performances is necessary know some engine data and Polar curve data. During a constant altitude turn it's possible to divide the calculation in two region, since the available power is greater than the required power at CL_{max}that is the "First Region". If the available power is lesser then required power at CL_{max} that is the "Second Region".
The required power is given by the (3.7.17) while the available power is given by the engine model for the chosen aircraft.

$$\Pi_r = D \cdot V \quad \textbf{(3.7.17)}$$

In the First Region it's possible to use the following formulas.

$$CD = CD(CL_{max}) \ (= CD_0 + \frac{CL^2}{e\pi AR} \text{ if parabolic}) \quad \textbf{(3.7.18)}$$

$$D = \frac{1}{2}\rho V^2 S \cdot CD \quad \textbf{(3.7.19)}$$

$$L = \frac{1}{2}\rho V^2 S \cdot CL_{\max} \quad \textbf{(3.7.20)}$$

Then is possible evaluate the load factor.

$$n = \frac{L}{D} \quad \textbf{(3.7.21)}$$

The most important value for the turn performances studies are the angle of bank Φ, the turn radius *R*and Time to turn *T*.

$$\Phi = \arctan(1/n) \quad \textbf{(3.7.22)}$$

$$R = \frac{V^2}{g\sqrt{n^2 - 1}} \quad \textbf{(3.7.23)}$$

$$T = \pi \frac{R}{V} \quad \textbf{(3.7.24)}$$

In the second region the Power is equal to Power available, so the CD is the following.

$$CD = \frac{\Pi_a}{\frac{1}{2}\rho V^3 S} \qquad \textbf{(3.7.25)}$$

The value of CL is obtained from the drag polar, for example from the parabolic form, then the other value is calculated by the equations (3.7.33) (3.7.23) (3.7.24).
So it's possible to draw the following charts.

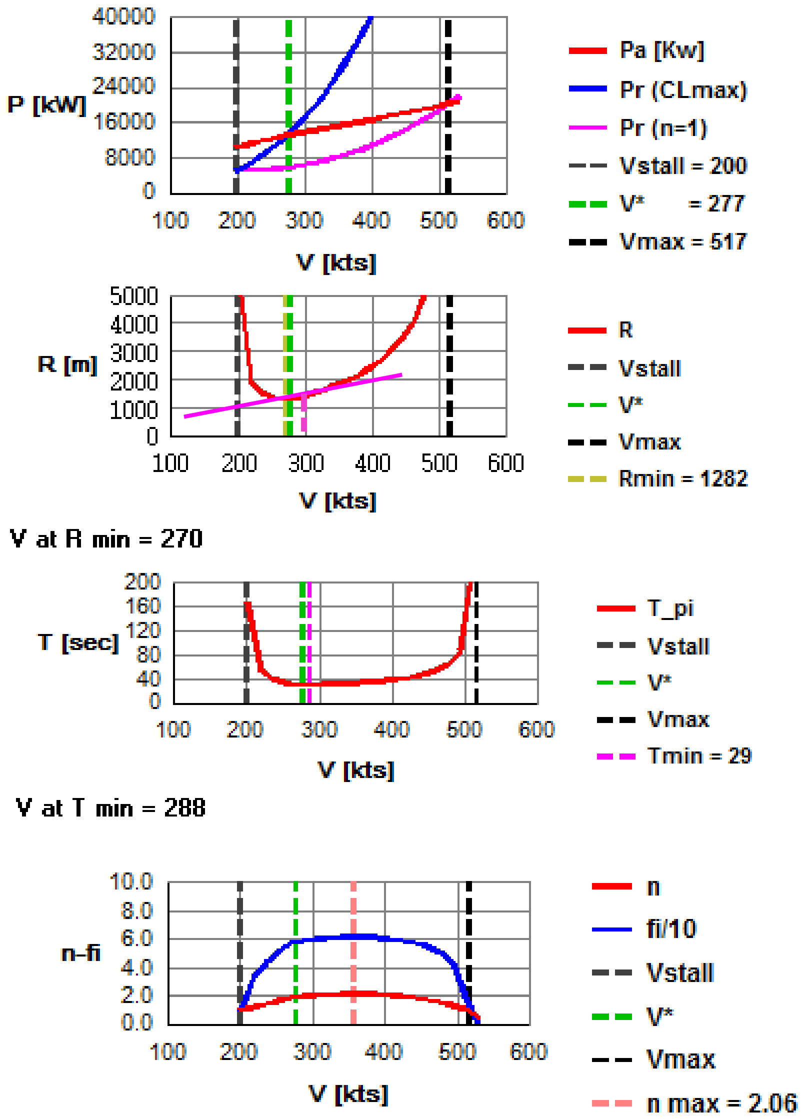

Figure 3.82 – Turn Performances plots.

To note that the minimum T is located at the point of contact between the curve of R and the tangent starting by the origin of the axis.

With increasing the load factor the curve of the required power shift over as shown in the figure 3.83.

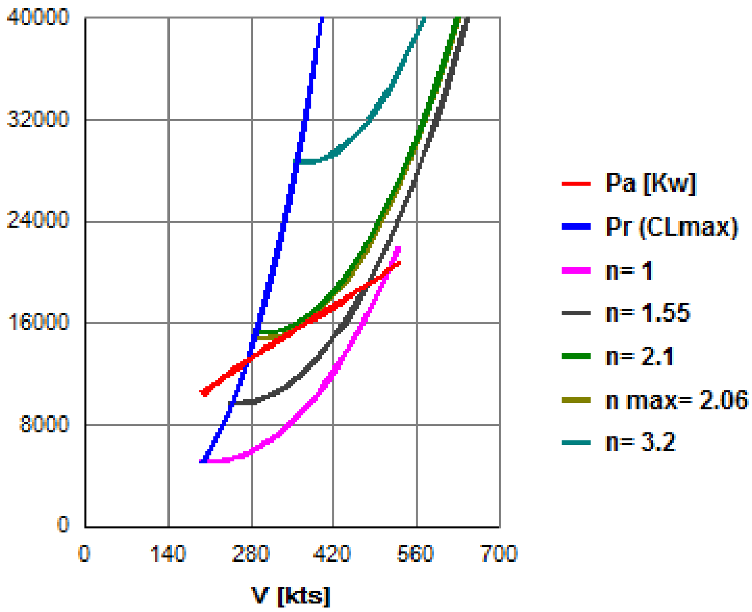

Figure 3.82 – Power vs speed with varying of load factor *n*.

The radius obtained by the 3.7.23 with stall speeds and maximum speeds give the follows plot.

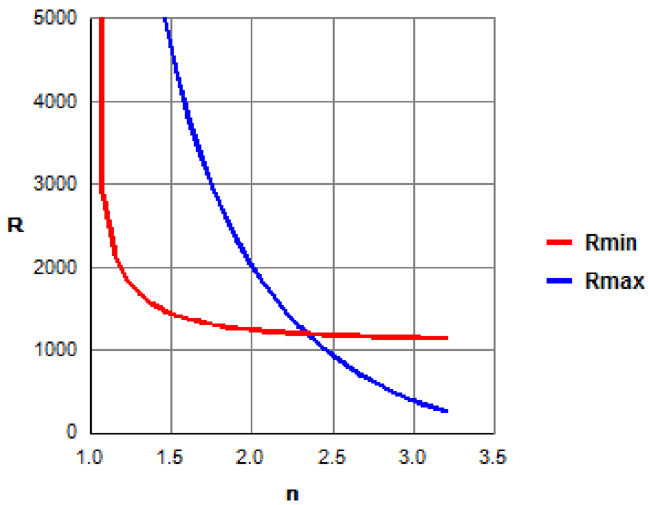

Figure 3.82 – Minimum and maximum radius obtained by the stall speeds and maximum speeds.

3.8 – *AIRPLANE DRAG POLAR*

3.8.1 – Introduction

The aerodynamic behavior of the airplane is influenced by many part that constitute it, through the lift and drag contributions that each component give at the calculation of the drag polar. The drag given by the aircraft is identifiable through the drag coefficient C_D, this is given by the superposition of the effects of parasite drag, induced drag, viscous lift dependent drag, trim drag and compressibility drag.

$$C_D = C_{Dp} + C_{Di} + C_{Dv} + C_{Dtrim} + C_{Dcompr} \qquad \textbf{(3.8.1)}$$

At the same time the lift used to support the airplane in the air can be considered, with good approximation, as the sum of the wing and horizontal tail contributions. So the coefficient is given as follows.

$$C_L = C_L^w + C_L^h \cdot \frac{S_h}{S} \qquad \textbf{(3.8.2)}$$

This evaluation needs the knowing of many geometrics data, someone unknown in the first analysis, as the geometries of horizontal and vertical tail that can be estimated for the first time by statistical data, seeing the similar existent aircraft, then when they are sized it's possible recalculate the drag polar to obtain the definitive one.
It's important to observe that in this part the result of the calculation are expressed in function of the angle of attack α_{body}, given by the direction of the asymptotic flow with the reference line of the fuselage. The α_{body} doesn't coincide with the angle of attack α_w which is the angle that the root chord have with the asymptotic flow direction, because it is keyed with an angle i_w, so it is the sum of the two angles.

$$\alpha_{body} = \alpha_w - i_w \qquad \textbf{(3.8.3)}$$

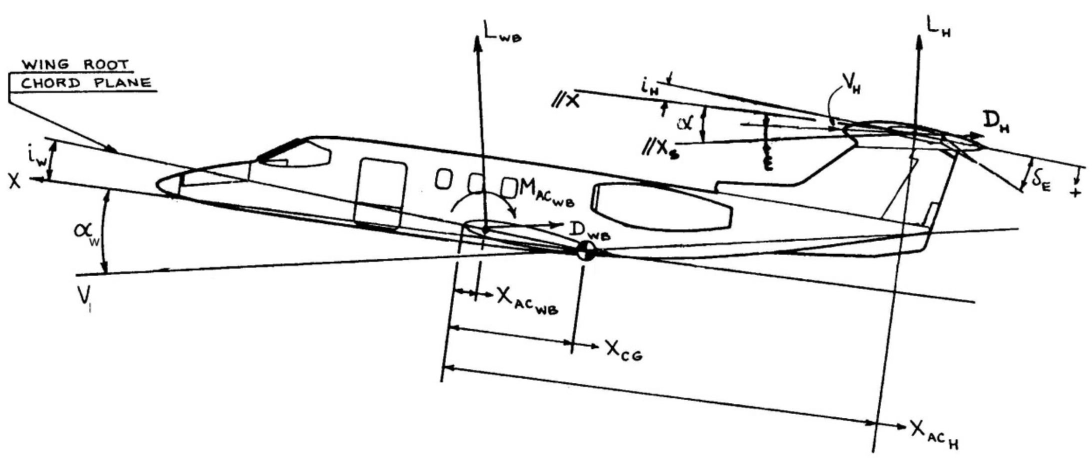

Figura 3.83 – Definition of the angle α_{body}.

3.8.2 – Parasite Drag

The parasite drag can be estimated, with good approximation, by the sum of the following contribution:

1. WingParasite Drag
2. Fuselage skin friction Drag + Fuselage Base Drag + Upsweep Drag
3. HorizontaltailParasite Drag
4. Vertical tailParasite Drag
5. Nacelle skin friction Drag + Nacelle Base Drag + Upsweep Drag
6. Control Surface Gap
7. Excrescence
8. Landing gear (if it is fix or if the analysisis about takeoff or landing condition)
9. Wing structure, for braced high-wing.
10. Windshield
11. Other elements

The parasite drag for some component of the aircraft, from point 1 to 5, can be evaluated by the following formula.

$$C_{D0} = K_{ff} \cdot C_f \cdot \frac{S_{wet}}{S} \quad \textbf{(3.8.4)}$$

Where C_f is the friction coefficient of the plain plate, K_{ff} is the form factor that correct the friction coefficient.
$S_{wet}$is the surface of the component touched by the flow, S is the reference wing surface.
For the calculation of the friction coefficient C_f the first step is to calculate the Reynolds number by the classical formula.

$$Re = \frac{\rho V l_f}{\mu} \qquad \textbf{(3.8.5)}$$

Then the second step is to calculate the Cut-off Reynolds number as follow.

SUBSONIC

$$Re_{cut-off} = 38.21 \cdot \left(l/k \right)^{1.053}$$

(3.8.6)

TRANSONIC or **SUPERSONIC**

$$Re_{cut-off} = 44.62 \cdot \left(l/k \right)^{1.053} \cdot M^{1.16}$$

Where k is the skin roughness depending on the type of surface, below is shown a table with the most used surface.

Skin roughness value (k)

Surface	k (ft)
Camouflage paint on aluminum	3.33×10^{-5}
Smooth paint	2.08×10^{-5}
Production sheet metal	1.33×10^{-5}
Polished sheet metal	0.50×10^{-5}
Smooth molded composite	0.17×10^{-5}

Figure 3.84 –Skin roughness value (k).

Then is possible to evaluate the laminar and turbulent C_f through the use of the moody diagram or the formula (3.4.12) and (3.4.13), choosing the minimum value between the Reynolds numbers evaluated with (3.8.5) and (3.8.6) .

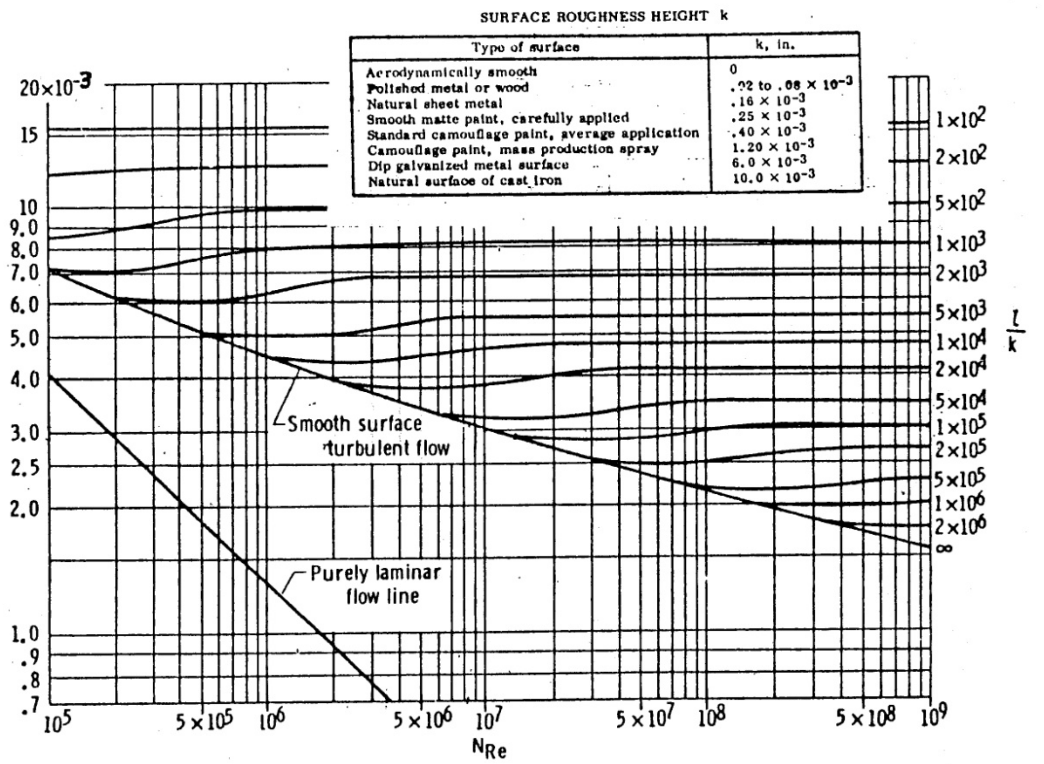

Figure 3.85 –Moody diagram.

$$C_f \text{ laminar} = \frac{1.328}{\sqrt{\text{Re}}} \quad \textbf{(3.8.7)}$$

$$C_f \text{ turbulent} = \frac{0.455}{\left(\frac{\log(\text{Re})}{\log(10)}\right)^{2.58}} \quad \textbf{(3.8.8)}$$

The value of turbulent C_f must be corrected to consider the effect of Mach number, this is possible using the following chart.

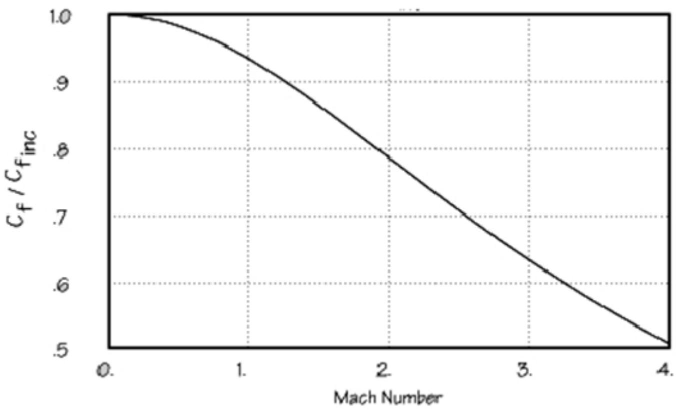

Figure 3.86 –Effect of Mach number on turbulent skin friction.

Then assuming a position in X of transition between laminar and turbulent flow, it's possible to evaluate C_f as follow.

$$C_f = C_f\ lam \cdot Xt + C_f\ turb \cdot (1 - Xt) \quad \textbf{(3.8.9)}$$

The wet surface S_{wet} can be evaluated for lifting surface as a function of the exposed surface and maximum thickness ratio of the mean airfoil t/c .

$$S_{wet\ \text{like-wing}} = 2 \cdot \left(1 + 0.2 \cdot \frac{t}{c}\right) \cdot S_{\exp} \quad \textbf{(3.8.10)}$$

In the case of fuselage and nacelle see the paragraph 3.4.5.
The friction coefficient calculated in 3.8.9 is referred to a flat plate so it take not in account the effect of the acceleration due to the thickness. So is introduced the form factor k_{ff} obtained by semi-empirical diagrams, for lifting surface it used the following diagram.

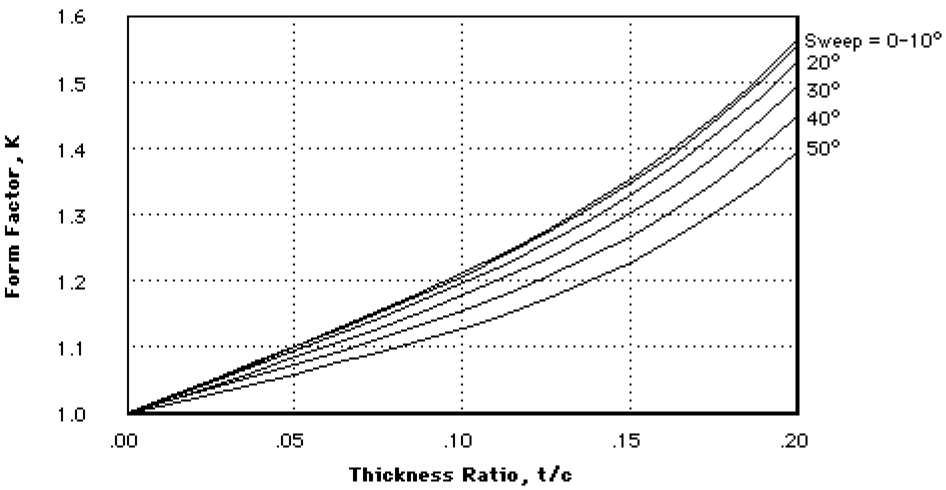

Figure 3.87 –Form factor as a function of thickness ratio and sweep at ¼ of the chord.

In the case of revolution surfaces the form factor depend on the fineness ratio given by the fraction between the body length and its maximum diameter, that for non-circular sections is considered as follows.

$$d_{equiv} = \sqrt{\frac{4 \cdot S_{\max}}{\pi}} \quad \textbf{(3.8.11)}$$

Where $S_{\max}$ is the maximum section area.

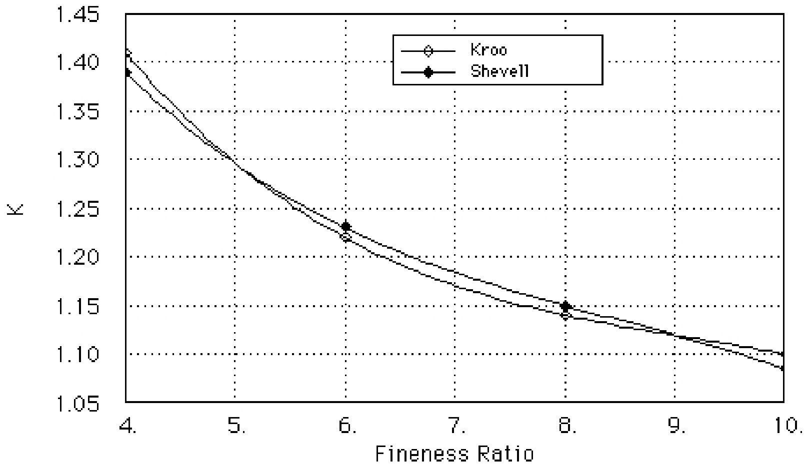

Figure 3.88 –Form factor as a function of fineness ratio.

Alternatively at figure 3.88 is possible use the following formula.

$$K_{ff} = 1 + \frac{60}{\left(l_f / d\right)^3} + 0.0025 \cdot l_f / d \quad \textbf{(3.8.12)}$$

The base drag of fuselage and nacelle is given by the following relationship.

$$C_{D\,base} = 0.029 \cdot \frac{S_{body}}{S}\left(\frac{d_{base}}{d_{equiv}}\right)^3 \cdot \left[C_{D0} \cdot \left(\frac{S}{S_{body}}\right)\right]^{\frac{1}{2}} \quad \textbf{(3.8.13)}$$

Also the upsweep angle produce a contribution on the drag, that will be added to parasite drag. This contribution is due to the enlargement of the boundary layer on the cone that induce an increment to the parasite drag. In the initial zone of the inclination the flow accelerate converting its pressure energy to kinetic energy, so this decrease the fuselage contribution on lift that can be recovered through an increment of inclination of the wing, which implies in return an increment of the parasite drag.
The contribution of the upsweep is calculated as follow.

$$C_{D\,upsweep} = 0.075 \cdot \frac{S_{fuselage\ \text{costant section}}}{S} \left(\frac{h}{l} \right)_{0.75l} \tag{3.8.14}$$

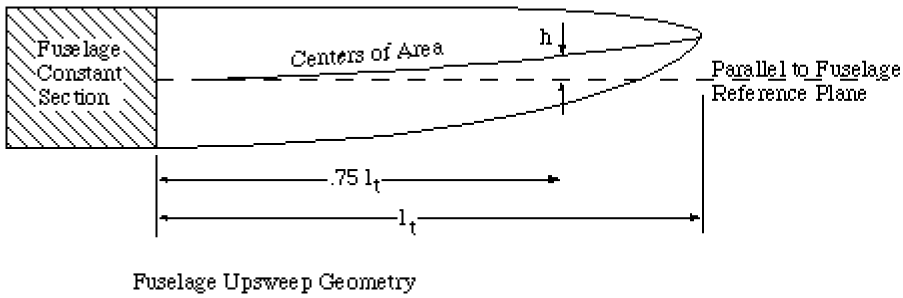

Figure 3.89 –Upsweepparameters.

The parasite drag due to gap that have the control surfaces can be estimated by the following relationship, based on experimental data.

$$C_{D\,gap} = 0.0002 \cdot \cos^2(\Lambda) \cdot \frac{S_{affected}}{S} \tag{3.8.15}$$

Where Λ is the sweep angle of the control surface and $S_{affected}$ is the "affected" surface or the portion of the surface involved by the control.

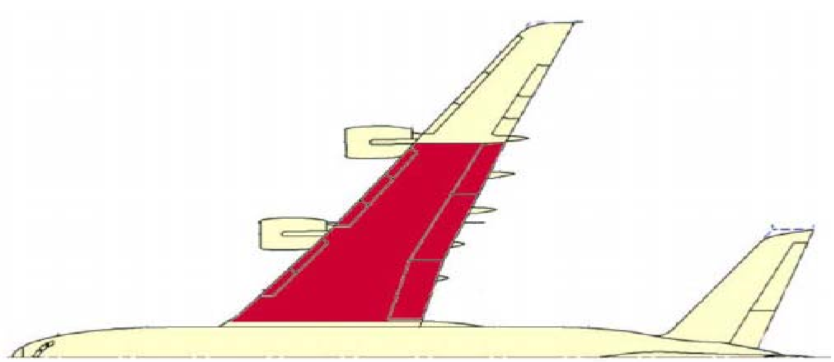

Figure 3.90 –Example of affected surface.

The real aircraft is very different from the ideal aircraft that is the model of the aircraft tested in the wind tunnel that allows a preliminary estimation of the aerodynamic coefficients. The drag coefficient due to excrescences is generated by all those particulars such as antennas, pitot tubes, surface imperfections and not perfect closures that characterize the real aircraft. The estimation of such contribute cannot be precisely afforded in the phase of design since the aircraft has not been realized yet so that a statistical approach is generally used. Several estimations on transport aircrafts fixed that the contribute of the excrescences amounts to 10% of the total drag coefficient in cruise condition. A deep refinement of the structures of the aircraft allows to reduce this percentage to 5% of the total drag coefficient in cruise condition. The statistical approach links the total wetted area to the drag coefficient due to the excrescences through a 4th order curve whose expression is the following.

$$K_{ex} = 4 \cdot 10^{-19} \cdot S_{wet}{}^4 - 2 \cdot 10^{-14} \cdot S_{wet}{}^3 + 5 \cdot 10^{-10} \cdot S_{wet}{}^2 - 7 \cdot 10^{-6} \cdot S_{wet} + 0.0825 \quad (3.8.16)$$

The corrective factor K_{ex} has to be included in the computation of the total skin friction drag coefficient of the aircraft previously obtained.

$$C_{D0} = C_{Dsf}(1 + K_{ex}) \quad (3.8.17)$$

For transport and light aircraft windshields that smoothly fair into the fuselage, an additional D/q of about 0.07 times the windshields frontal area is suggested.

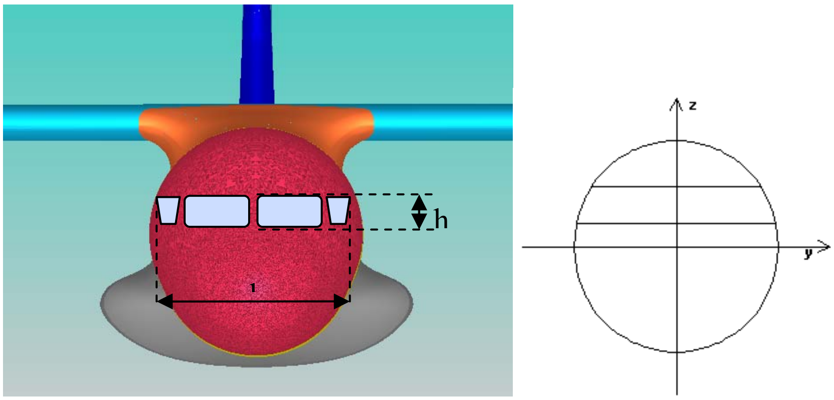

Figure 1 – Windshield on ATR 72-500 and its schematization.

$$C_{DWS} = \frac{0.07 \cdot A_{WS}}{S_{ref}} \quad (3.8.18)$$

Where the A_{WS} is the frontal windshield area.

A different approach is presented in Figure by Roskam – "Method for estimating drag polar of subsonic aircraft".

Considering the skin friction drag coefficient of the fuselage previously estimated, the effect of the windshield can be estimated as follows :

$$C_{DWS} = \frac{\Delta C_{DWS}}{C_{DFUS}} \cdot C_{DsfFUS} \quad (3.8.19)$$

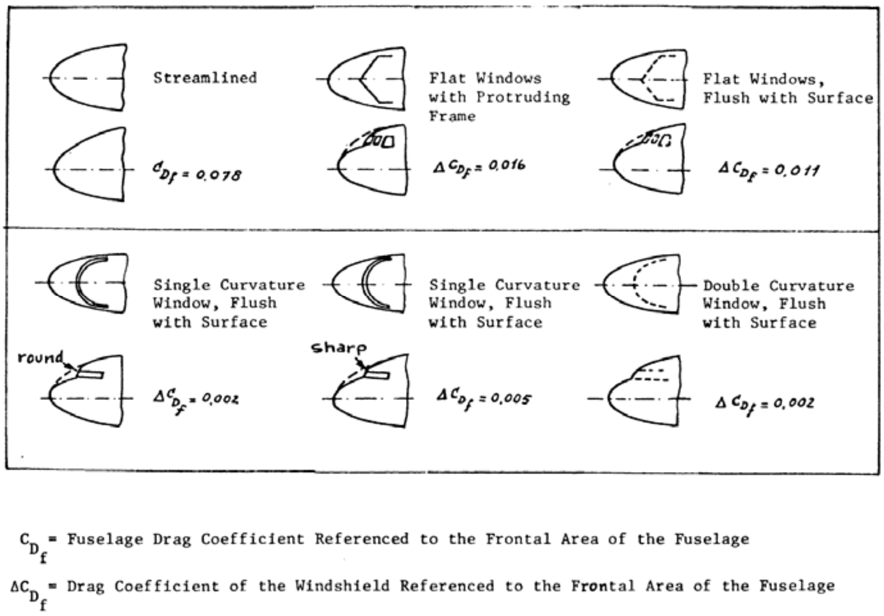

Figure 3.92 – Roskam procedure for estimation of windshield drag coefficient

The contribution at the parasite drag due to landing gear can be calculated as the sum of two terms, one about the wheels and the other about the legs.

$$CD_0^{gear} = CD_0^{wheels} + CD_0^{legs} \qquad \textbf{(3.8.20)}$$

The first term is evaluable as follows.

$$CD_0^{Wheels} = 0.24 \cdot n_{wheels} \frac{S_{wheel}}{S} \qquad \textbf{(3.8.21)}$$

Where n is the number of wheels and S_{wheel} is the frontal surface of one wheel, that can be approximated as a rectangle.
The second term is evaluable as follows.

$$CD_0^{legs} = 0.82 \cdot n_{legs} \frac{d_{leg} \cdot l_{leg}}{S} \qquad \textbf{(3.8.22)}$$

Where n is the number of the legs, d_{leg} is the diameter of the leg and $l_{leg}$is its length.
In case of a non-retractable tricycle type, is possible evaluate the CD_0 of the legs as follows.

$$CD_0^{legs} = C_f \frac{S_{wet}}{S} \qquad \textbf{(3.8.23)}$$

Where the C_f is the friction coefficient estimated with Reynolds number referred at mean chord of the leg.

For airplane with braced high-wings the addictive contribution on the parasite drag is not negligible and it can be evaluated as follows.

$$CD_0^{struct} = Cd_{struct} \frac{d_{struct} \cdot l_{struct}}{S} \qquad \textbf{(3.8.24)}$$

Where the coefficient Cd_{struct} is contained between 0.15 and 0.25, d_{struct} the maximum thickness of the support structure and l_{struct} is its length.
In the end, the air conditioning system and other miscellaneous components give a final contribution on the parasite drag as a percentage of the total.

Airplane	DC-8-62	DC-8-63	DC-9-10	DC-9-20	DC-9-30
Flap Hinge Covers	0.12	0.12	0.69	0.97	0.69
Air Conditioning System (incl. thrust recovery)	0.84	0.82	0.25	0.24	0.24
Vortilon	-	-	0.30	0.29	0.29
Fence and Stall Strip	-	-	0.99	-	-
Miscellaneous	0.25	0.25	-	-	-
Total	1.21%	1.19%	2.23%	1.50%	1.22%

Figure 3.93 – Statistical choice of the drag percentage due to other secondary factors.

3.8.3 - Induced Drag

The induced drag is depending on the induced vorticity of the wing. The coefficient C_{Di} can be calculated through the same method shown in paragraph 3.3.3.

3.8.4 - Viscous Lift dependent Drag

The viscous lift dependent drag can be estimated as follows.

$$C_{Dv} = K \cdot C_{Dp} \cdot C_L^{\,2} \qquad \textbf{(3.8.24)}$$

Where the value of the factor *K* is obtained statistically and is about 0.38 for old aircraft type and 0.15 for advanced aircraft. C_{Dp} is the parasite drag coefficient estimated before.
Another method is to estimate the C_{Dv} for each component, wing, fuselage and nacelle, that must be multiplied with C_L^2.
For the wing the equation is the following.

$$C_{DviscW} = K_w \left(C_L - C_{L\,C_D\min}\right)^2 \qquad \textbf{(3.8.25)}$$

For the fuselage and nacelle is given as follows.

$$C_{DviscForN} = 2\alpha^2 \frac{S_b}{S} + \eta c_{d_c} \alpha^3 \frac{S_{plf}}{S} \qquad \textbf{(3.8.26)}$$

Where:

$$\alpha = \frac{\left[\left(\frac{W}{qS}\right) - C_{L0}\right]}{C_{L\alpha}} \quad \textbf{(3.8.27)}$$

S_b is the fuselage or nacelle base area, Cd_c is the experimental steady state cross-flow drag coefficient of circular cylinder, η is the ratio of drag of a finite cylinder to the drag of an infinite cylinder and $S_{plf}$is the fuselage or nacelle planform area.
Then the C_{Dv} is given by the sum of all the contributions.

3.8.5 - Trim Drag

To calculate the trim drag is necessary to evaluate the lift contribution given by the horizontal tail with various incidence. This can be calculated by the resolution of the equilibrium equation system through the normal axis at the aircraft and at the rotation around at the pitching axis.

$$\begin{cases} C_{Lw} + C_{Lh} \cdot \dfrac{S_h}{S} = C_L \\ C_{Lw} \cdot \dfrac{x_w}{c_w} - C_{Lh} \cdot \dfrac{(l_t - x_w)}{c_w} \cdot \dfrac{S_h}{S} + C^{wb}_{m.ac} = 0 \end{cases} \quad \textbf{(3.8.24)}$$

Where:

1. C_{Lw} - Lift coefficient of the wing;

2. S_h -Horizontaltail area;
3. $C^{wb}_{m.ac}$ - Moment coefficient respect the aerodynamic centre of the partial aircraft. It can be calculated by the following formula.

   $$\left(C_m^{wb}\right)_{a.c.}^{wb} = \left(C_m^{w}\right)_{a.c.}^{w} + C_{L\alpha}^{w} \cdot \alpha_{body} \cdot (x_{a.c}^{wb} - x_{a.c.}^{w}) + C_{m0}^{fus} + C_{m\alpha}^{fus} \cdot \alpha_{body} + C_{m0}^{nac} + C_{m\alpha}^{nac} \cdot \alpha_{body} \textbf{(3.8.25)}$$

   Where are considered the contributions of the wing, fuselage and nacelles, and in which are present the wing moment coefficient $\left(C_m^{w}\right)_{a.c.}^{w}$, the lift curve slope $C_{L\alpha}^{w}$, the position of the aerodynamic centre of the wing and the partial airplane, the fuselage moment coefficient C_{m0}^{f}, the nacelle moment coefficient C_{m0}^{nac} and the derivative of the moment coefficients of the fuselage and nacelles respect to the angle of attack α_{body}.
4. x_w - distance from the aerodynamic centre and the centre of gravity.
5. l_t -distance from the aerodynamic centre of the partial airplane and aerodynamic centre of the horizontal tail.

All the quantity here introduced have been described before in the par. 3.3.3, 3.4.4.

After the calculation of all contributions in the equations 3.8.24, is possible to calculate the value of C_L^h and C_L for any α_{body} and so starting by the values of $C_L^h = f(\alpha_{body})$ to evaluate the trim drag coefficient from the following relationship.

$$C_{Di}^h = \frac{(C_L^h)^2}{\pi \cdot AR_h \cdot u} \cdot \frac{S_h}{S} \qquad \textbf{(3.8.26)}$$

Where AR_h is the horizontal tail aspect ratio and u is obtained by the first chart in the figure 3.31 for the horizontal tail.

3.8.6 - Compressibility Drag

The contribution to the drag of the complete airplane due to compressibility effects can be considered, for a first approximation, as the compressibility drag of the wing so using the same figures shown in the chapter 3.2, from the wing geometry is possible evaluate the crest critical mach number Mcc, the first diagram is valid for peaky airfoil so for supercritical and aggressive supercritical airfoil it have to consider an additive factor of 0.035 for the first one, and 0.06 for the second one.Then from the second chart is possible to estimate the ΔC_D.

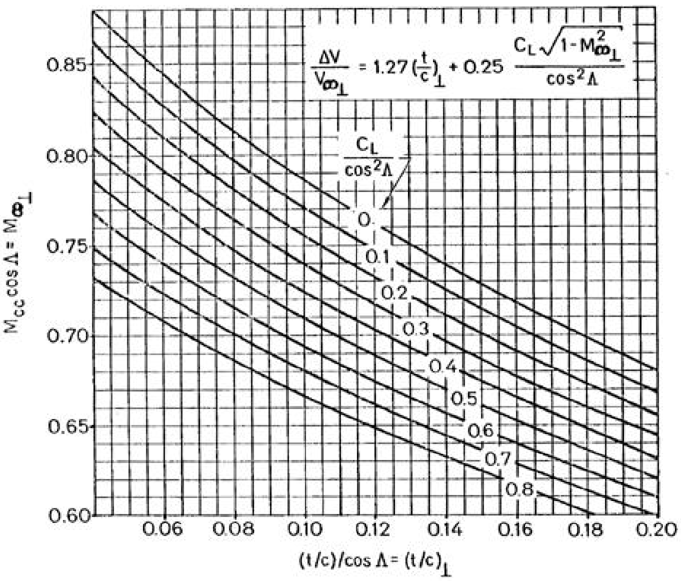

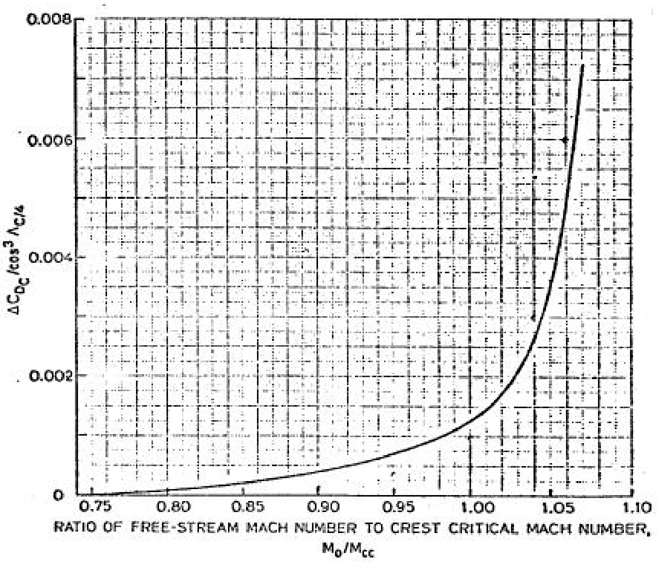

Figure 3. 94 – Compressiblity effect.

Where t/c is the maximum thickness of the mean airfoil and Λ is the sweep angle at ¼ of the chord.

3.8.7 - Total Airplane Polar Drag

The knowing of all principal contribution for the lift and drag of the complete airplane, at a fixed position of the barycenter and at a fixed flight condition, allow to draw the complete airplane polar.

$$C_D = C_{Dp} + C_{Di} + C_{Dtrim} + C_{Dcompr} \quad C_L = C_L^w + C_L^h \cdot \frac{S_h}{S} \quad \textbf{(3.8.27)}$$

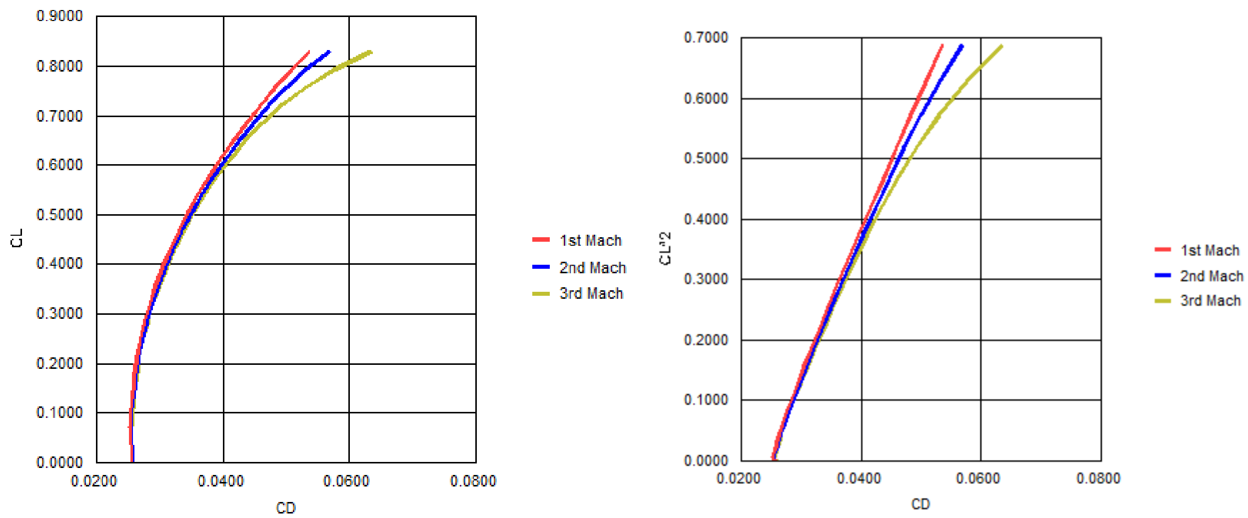

Figure 3. 95 – example of Drag polars.

3.8.8 - The Osvald Factor

After the calculation of the two contributes of the drag, the Induced drag and Viscous Drag, it's possible to obtain the canonic relation of the parabolic polar.

$$C_{Di} = \frac{C_L{}^2}{\pi \cdot AR \cdot e} \qquad \textbf{(3.8.28)}$$

Where the factor *e* is called “Osvald factor”, often defined as an indicator of the shift from the elliptic load (obtained for a wing plunged by ideal flow) to wing load, due to the particular wing geometry, wing-fuselage inference and to the variation of the profile drag of many part of the airplane with the incidence.
Statistical studies have confirmed that for many airplane this value is about 0.80, with a little reduction for propeller driven aircraft by 3 - 4%.
A possible comparison with what has been done in this chapter is to use the following semi-empirical relations.

Straight-wing Aircraft: $e = 1.78\left(1 - 0.045A^{0.68}\right) - 0.64$ **(3.8.29)**

Swept-wing Aircraft: $e = 4.61\left(1 - 0.045A^{0.68}\right)\cos\left(\Lambda_{LE}\right)^{0.15} - 3.1$ (for $\Lambda_{LE} > 30\deg$)

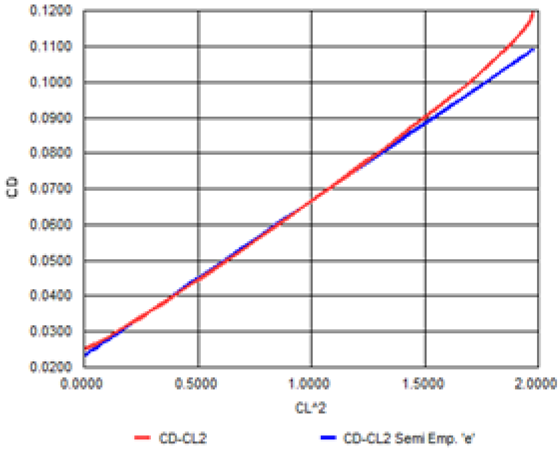

Figure 3. 95 – example of comparison between semi-empirical methods.